Velocity–Difference Induced Focusing in Capillary Electrophoresis and Preparative Capillary Electrophoresis

by

Wuyi Zha

B.Sc., Tsinghua University, 1995
M.Sc., Tsinghua University, 1998

A THESIS SUBMITTED IN PARTIAL FULFILMENT OF
THE REQUIREMENTS FOR THE DEGREE OF

DOCTOR OF PHILOSOPHY

in

THE FACULTY OF GRADUATE STUDIES

(Chemistry)

THE UNIVERSITY OF BRITISH COLUMBIA

November 2007

ABSTRACT

Velocity – difference induced focusing (V-DIF) with a dynamic pH junction in capillary electrophoresis (CE) using a sample with a pH different from that of the background electrolyte (BGE) was developed in our group, but the mechanism was not well understood. In this work, the mechanism of this focusing technique was first studied using an appropriate dye to monitor the pH of the BGE and the sample during the focusing process. A mechanism was proposed based on the experimental results. This technique was then applied to serotonin to improve the detection limit when CE was used with a UV absorption detector. It was also applied to focus amino acids, peptides, and proteins to improve the concentration sensitivity. It is found that the pKa rather than the pI of the analytes is the key criterion for selecting the pH for the sample and for the BGE to obtain the optimum focusing for these molecules. Since UV detection only provides migration time information, more structure information is obtained by using a photodiode array (PDA) and mass spectrometer (MS) for peak identification. Comparisons were made between the PDA detection and MS detection for aromatic amino acids with V-DIF using a dynamic pH junction. This V-DIF technique was then applied to non-aromatic amino acids with MS detection. It was used at low pH with positive ESI-MS detection and at high pH with negative ESI-MS ionization. The results of the two methods were compared and discussed. Finally, the preparative operation of continuous flow counterbalanced CE (FCCE) was studied. The effects of larger sample volumes and multiple capillary systems on improving the purification yield were investigated.

TABLE OF CONTENTS

LIST OF TABLES

LIST OF FIGURES

LIST OF SYMBOLS AND ABBREVIATIONS

BGE	Background Electrolyte
CE	Capillary Electrophoresis
CFFE	Continuous Free Flow Electrophoresis
CHES	2-(N-Cyclohexylamino)-ethanesulfonic acid
CIEF	Capillary Isoelectric Focussing
CITP	Capillary Isotachophoresis
ε	Dielectric Constant
E	Electric Field Strength
EDTA	Ethylenediaminetetraacetic acid
EOF	Electroosmotic Flow
ESI-MS	Electrospray Ionization – Mass Spectrometry
FCCE	Flow Counterbalanced Capillary Electrophoresis
η	Viscosity
HPLC	High Performance Liquid Chromatography
i.d.	Internal Diameter
L_d	Length to Detector
LIF	Laser Induced Fluorescence
LOD	Limit of Detection
μ_{ep}	Electrophoretic Mobility
μ_{eo}	Electroosmotic Mobility
MEKC	Micellar Electrokinetic Chromatography
MS	Mass Spectrometry
N	Number of Theoretical Plates
o.d.	Outer Diameter
PDA	Photodiode Array
pI	Isoelectric Point
pKa	Acid dissociation constant
Q_{eff}	Effective Charge
q	Electric charge
r	Radius
σ	Standard Deviation
σ^2	Variance
SDS	Sodium Dodecyl Sulfate
UV	Ultraviolet
V	Voltage
V-DIF	Velocity – Difference Induced Focusing
V_{eo}	Velocity of EOF
Vis	Visible
ζ	Zeta Potential

ACKNOWLEDGEMENTS

I want to thank the Natural Sciences and Engineering Research Council of Canada (NSERC) for funding this research.

I would like to thank Dr. David Chen for providing an environment that encouraged a successful research program. I also want to thank other members of our research group. Their suggestions and friendship are very important to my success in this research. In no particular order, they are: Brad and Cindy Schneider, Angela Duso, Jennifer Chu, David McLaren, Gwen Bebault, Ning Fang, Irina Manisali, and Rong Yi. Here I want to give my special thanks to Dr. David McLaren for giving me invaluable help and great support in my research and everyday life.

CO-AUTHORSHIP STATEMENT

For all the chapters, I designed and performed the experiments, analyzed the data, and prepared the manuscripts. All the results were discussed with my supervisor, and all the manuscripts were read and revised by my supervisor. For Chapter 7, Jingyan Zheng also involved in the experiments and David Mclaren involved the discussion.

CHAPTER 1

Introduction

1.1 Separation Science

Separation science plays a key role in many areas including chemistry, biochemistry, pharmaceutical science, food science, forensic investigation, and the petroleum industry. Most natural and synthesized substances are mixtures containing different components. In order to analyze the components of interest, a chemical separation process is needed.

The majority of chemical separation techniques for chemical analysis can be classified into three categories: ultracentrifugation, which is dependent on the different densities of the analytes; chromatography, which is based on a distribution equilibrium of analytes between stationary phase and mobile phase; and capillary electrophoresis (CE) which can employ both a distribution equilibrium and the differential migration of ions in an electric field. [1] Although these separation techniques are based on different principles, it is possible to use a unified theory to describe them. [1] Bowser *et al.* derived a unified equation to describe all column separation techniques, showing that the migration rate of an analyte in the separation process is a weighted average of the migration rates of its different species. [1]

These techniques are widely used in current academic research and industry. In biological science, CE is becoming more popular due to its high separation efficiency, short analysis time, and minimum sample and buffer consumption.

1.2 Introduction to Capillary Electrophoresis (CE)

CE is being used in DNA sequencing, [2] clinical chemistry, [3] forensic analysis, [4] pharmaceutical assay, [5] and chiral separations. [6] Because CE is easier to operate, more cost-effective, and has high separation efficiencies, it is used more frequently as an alternative or supplemental technique to high performance liquid chromatography (HPLC) in different applications.

Electrophoresis refers to the migration of ions in a medium in an electric field. Anions and cations migrate to different poles (anions migrate towards the anode and cations migrate towards the cathode) and separate from each other with a rate of migration related to their charge to size ratios. The CE technique was developed in the early 1980s. [7] Earlier electrophoresis separations were carried out on paper or gel, but detection could only be accomplished by visualisation after the electrophoretic separation was finished. Due to the inefficient dissipation of Joule heating in these separations, only low voltages could be applied which resulted in long analysis times. Electrophoresis performed in capillaries has many benefits. Heat dissipation is very efficient in CE due to the large surface-to-volume ratios of capillaries, so by employing high voltages, separation in CE can be very fast. Various modes of CE have been developed, including capillary zone electrophoresis (CZE), micellar electrokinetic capillary chromatography (MEKC), [8] capillary gel electrophoresis (CGE), [9] and capillary electrochromatography (CEC). [10] CZE is used to separate ions in free solutions, while MEKC is mainly used to separate neutral compounds with surfactants. CGE separates analytes based on their sizes using a sieving mechanism, and CEC is a hybrid technology between CE and HPLC.

The migration rate of an ion in CE is the sum of its electrophoretic velocity and the electroosmotic flow (EOF). The electrophoretic velocity is given by:

$$v = \mu_{ep} \cdot E \qquad (1.1)$$

where μ_{ep} is the electrophoretic mobility of the ion and E is the electric field strength.

μ_{ep} is expressed as:

$$\mu_{ep} = \frac{Q_{eff}}{6\pi\eta r} \qquad (1.2)$$

Where Q_{eff} is the effective charge of the ion, η is the viscosity of the medium, and r is the hydrated radius of the ion.

It can be seen from equation 1.2 that ions will migrate at different velocities if they have different charge to size ratios.

EOF results from the electric double layer established due to the charged capillary wall. Because most capillaries in CE are made of silica, the surface of the capillary wall hydrolyzes to form silanol groups in aqueous solutions. The deprotonation of these silanol groups causes the capillary wall to be negatively charged. An electric double layer of cations consisting of a Stern layer and a diffuse layer as described by Stern's model is built to neutralize the negative charges on the capillary wall surface. [11] Under an electric field, cations in the diffuse layer and their solvating water molecules will move towards the cathode, dragging the rest of the solution in the capillary with them. The flow profile of EOF is flat because the driving force originates at the capillary wall. The flat flow profile is advantageous because it minimizes the band broadening caused by longitudinal

diffusion, resulting in high separation efficiencies in CE. The velocity of EOF (V_{eo}) and electroosmotic mobility (μ_{eo}) are given by:

$$v_{eo} = \mu_{eo} \cdot E \tag{1.3}$$

and

$$\mu_{eo} = \frac{\varepsilon \cdot \zeta}{4\pi \cdot \eta} \tag{1.4}$$

Where E is the electric field strength, ζ is the zeta potential which is the potential across the diffuse layer, ε is the dielectric constant of the buffer solution, and η is the viscosity of the buffer solution.

The EOF is affected by the dielectric constant, viscosity of the buffer, and the zeta potential as seen from equation 1.4. The dielectric constant and the viscosity of the buffer are mainly dependent on the buffer composition, but other factors such as temperature also influence the viscosity. The zeta potential is mainly influenced by the pH, ionic strength, and the temperature. If the pH is increased, the capillary wall becomes more negatively charged, leading to a greater zeta potential. The zeta potential will not increase significantly when the pH is higher than 9 because most of the silanol groups on the capillary wall surface are dissociated. A solution with higher ionic strength can provide more cations to neutralize the negative charges on the capillary wall, leading to a smaller zeta potential. Higher temperatures usually increase the zeta potential because more silanol groups are deprotonated. So usually at higher pH, lower ionic strength, and higher temperature, a larger EOF will be generated.

The instrumentation for CE is straightforward. Figure 1.1 shows a typical CE system.

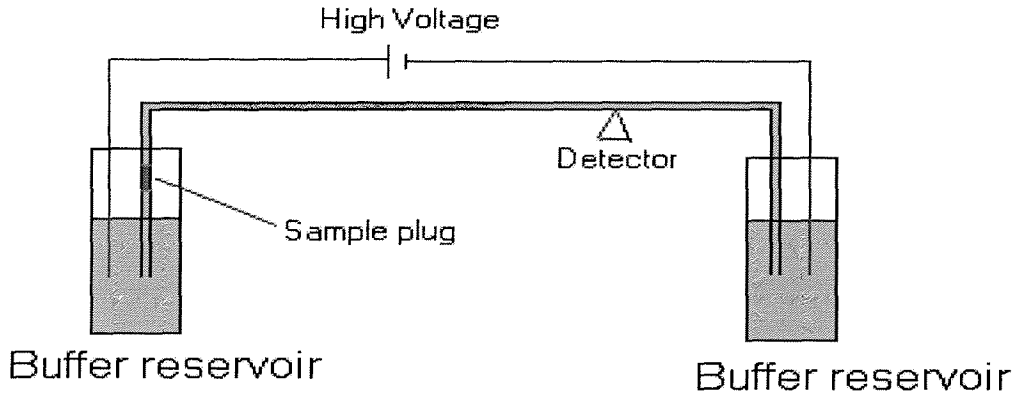

Figure 1.1 Schematic of a typical CE system.

The capillary ends are placed in two separate vials holding buffer and the electrodes. The electrodes are used to conduct the electricity. After the sample injection with a voltage or a low pressure, the separation is carried out with an applied voltage between the two vials.

1.3 Introduction to CE-MS

The most common method to detect analytes in CE is to monitor UV absorption, but UV is often not sufficient for peak identification. UV detection mainly provides the migration times of the analytes, but variations in the migration times often occur in CE, leading to great difficulty in identifying unknown peaks. For analytes without UV absorbance, precolumn or postcolumn derivatization using a UV chromophore is often needed. A mass spectrometer is a highly sensitive and selective detector, which is applicable in many fields. It gives unambiguous molecular weights of analytes and also provides structural information, helping with the identification of unknowns. MS also can directly

detect analytes that have no UV absorbance, without derivatization. CE and MS coupling greatly expands the application of CE.

Electrospray ionization (ESI)-MS is most widely used to couple MS with CE. In CE-ESI-MS, analytes from the separation capillary are directly transferred to the MS via an interface. Large molecules such as peptides and proteins are often multiply-charged in ESI-MS, which makes it possible for them to be detected within the limited mass to charge (m/z) range of most mass spectrometers. [12]

Different interfaces are used for CE-ESI-MS, but the coaxial sheath-flow interface is the most commonly used. The normal design of a coaxial sheath-flow interface is that two additional tubes surround the separation capillary. [13] The inner tube transfers a sheath liquid to maintain the continuity of the electric circuit and offers the necessary flow rate for a stable electrospray. The outer tube carries a nebulizing gas, which is used to help droplet formation and evaporation in ESI. [13]

MS has several scan modes including full scan mode and selected ion monitoring (SIM) mode. The signal to noise ratio is improved in SIM mode due to the decreased noise, and the size of the data file is also reduced significantly.

1.4 Band broadening effects in CE

The band broadening effects in CE are reflected by the separation efficiency which is often described by the number of theoretical plates (N). A large theoretical plate number means the tendency of a particular column to produce band broadening is small.

N can be defined as:

$$N = \frac{L_d^{\ 2}}{\sigma^2} \tag{1.5}$$

Where L_d is the capillary length to the detector and σ^2 is the peak variance.

In CE, band broadening or peak dispersion is caused by many factors including diffusion, electrophoretic dispersion, Joule heating, injection volume, and adsorption. [14]

The band broadening effects can be minimized significantly through proper design and optimization of separation conditions. Under the optimum conditions, the major contribution to peak dispersion in CE is longitudinal diffusion and injection related broadening. Due to the flat profile of EOF in CE rather than the laminar flow profile in HPLC, the band broadening caused by longitudinal diffusion is minimized in CE. The main band broadening factor remaining in CE is the length of the injection. [15] Peng and Chen [15] demonstrated that the band broadening was mainly contributed by the injection volume when the injection time was more than 2 seconds in CE. The length of the sample injection can be reduced by the utilization of stacking which reduces the breadth of the sample zone while maintaining the injected analyte mass, resulting in improved separation efficiency and thus better concentration sensitivity.

1.5 Concentration sensitivity improvement in CE

1.5.1 Introduction

CE is currently one of the most important techniques for separation of analytes. The main advantages of CE are high separation efficiency, high speed, and minimal sample and solvent consumption. However, the concentration sensitivity in CE with UV absorption detection is not sufficient for some practical analysis due to the short light path. In order to increase the concentration sensitivity, two strategies are used. The first strategy is to improve the sensitivity of the detectors. Alternative detectors to UV detectors such as laser-induced fluorescence detectors (LIF) can be used. However, direct LIF detection is only applicable for fluorescent analytes. An alternative to direct detection is to derivatize the analytes with fluorescent regents, but derivatization costs much more labour and time. Though MS is generally far more sensitive than UV detection, the current CE-MS interfaces employing sheath liquid dilute the CE eluent, resulting in much lower concentration sensitivity. The light path for UV detection can be increased by using capillaries with a bubble-cell or a Z-shaped cell, but this may deteriorate the separation efficiency. [16] A second strategy is to use stacking or focusing techniques, which are most commonly used in real applications.

1.5.2 Sample stacking

Sample stacking is a well-known phenomenon in capillary electrophoresis. [17] The factors and mechanism of this method in CE were investigated in detail by Burgi and Chien. [18] A sample plug prepared in a buffer with lower concentration than that of the separation buffer is injected into the capillary, resulting in a significant improvement for

the concentration sensitivity. In this technique, the field strength is higher in the sample zone because of the lower ion concentrations in the sample plug. Thus the analytes have higher migration rates in the sample zone. When the analytes enter the separation buffer, they slow down because they encounter the lower field strength in the separation buffer. The analytes then stack at the boundary between the sample zone and the separation buffer. Because the major requirement for this method is that the analytes are prepared in a lower conductivity solution relative to the separation buffer, biological or environmental samples often need desalting before analysis. [14] Sample stacking methods have also been modified by Quirino and Terabe [19] to focus neutral analytes with charged additives. Palmer *et al.* [20] used micellar CE to focus neutral analytes where the sample matrix had higher salt contents than the BGE (background electrolyte), which allowed the efficient stacking of micelles in the BGE zone prior to interacting with the neutral analytes in the sample zone. The analytes in the sample zone were then picked up and concentrated by the focused micelles when the micelles entered the sample zone.

1.5.3 Transient ITP

Transient isotachophoresis [21, 22] is another on-line preconcentration technique for focusing analytes. In this technique, a leading ion and a terminating ion are used. A leading ion has a higher mobility than sample analytes, while a terminating ion has a lower mobility than the sample analytes. Once a voltage is applied, the leading ion will move ahead and the terminating ion will fall back. The sample analytes will search for their mobility positions to keep pace with the leading ion. Then all the separated bands move at the same speed. A steady-state stacking is obtained. Because the electric field

strength is inversely proportional to the ion mobility, the field strength is higher in the terminating ion area and lower in the leading ion region. If any analytes move into the leading zone, they encounter lower field strength and slow down, moving back to their own segment. If some analytes fall back into the terminating ion region, they are exposed to a higher field strength, speeding up to return to their own segment. This method can concentrate the sample 50-1000 fold. [23] Since many factors such as the charge and pH influence the velocity of the ions, it is necessary to pay attention to every detail when designing the conditions.

1.5.4 CIEF

Capillary isoelectric focusing (CIEF) [24, 25] is a powerful tool in separating amphoretic compounds such as proteins, peptides, and amino acids. Here the analytes are separated based on their different isoelectric points in a pH gradient formed by carrier ampholytes when an electric field is applied. In the gradient, analytes move to a position where their net charge is zero and focus. After the focusing, if an analyte diffuses towards the anode, it will gain positive charges, resulting in migration back to its focused zone. If an analyte diffuses towards the cathode, it will acquire negative charges and move back to the focused zone. Very high resolution can be achieved by this technique. However, this technique also has several drawbacks, such as absorption interferences caused by ampholytes and the need for the focused zones to be transported to the detection window. A two-step process is usually performed for focusing and mobilization. After the completion of focusing, mobilization of the focused zones out of the capillary is accomplished by changing the chemical composition of anolyte or catholyte solution by

adding acid or base. The change in anolyte or catholyte will cause a shift in the pH gradient and the focused zones will move across the detection window. The focused zones can also be moved by using pressure to displace the capillary contents while leaving the voltage on to maintain resolution of the focused zones. [26]

1.5.5 Velocity-difference induced focusing (V-DIF)

Velocity-difference induced focusing (V-DIF) using a dynamic pH junction is a unique focusing technique developed in our group. [14] In this method, the sample and the BGE are prepared at different pH values to obtain the focusing. It allows the injection of a large sample volume and a separation efficiency greater than a million theoretical plates is achieved. [14] This method does not depend on the conductivity of the sample matrix, and is applicable for weakly acidic species and zwitterionic analytes that have different migration rates in the sample and BGE with different pH values.

1.6 Preparative operation of CE

Despite the rapid advance of CE as a powerful analytical tool with broad applications in research and industry, its application as a preparative technique has been limited. This is due to the limitation of sample loading capacity in CE with small diameter capillaries. Another disadvantage of CE is that CE competes with other preparative techniques such as HPLC which is applicable for most preparative purposes. However, because CE has high separation efficiency, it has the ability to separate complex samples that cannot be isolated by other separation methods. It leads to even more interest for purifying individual components in complex samples.

Most preparative CE methods have been based on fraction collection [27, 28] techniques. The fractions are collected into a microvial or other apparatus at the exit of the separation capillary. The separation voltage needs to be interrupted and the capillary end or the collection vials need to be relocated for each fraction collection. However, this technique requires very accurate and reproducible migration times for analytes. Other disadvantages include solution losses and diffusion of separated bands, which often occur during the collection step.

Techniques without interruption of the electrical circuit [29, 30] have also been developed such as using a porous glass frit that keeps the continuity of applied voltage for collection. [30] Though many efforts have been made to improve the recovery of separated components, the mass purified from a single run is still minute. [31] A general approach to increase the purification amount is to repeat the separations and combine the same fractions from each run in one vial. [32] This approach also needs very high reproducibility for consecutive separations, and a programmable instrument is usually necessary for routine operations. Another attempt has been made by Chankvetadze *et al.* using the technique of flow counterbalanced capillary electrophoresis (FCCE) [33] for the continuously preparative operation of CE. They purified the α-isomer of a dipeptide, aspartame, from a binary mixture with this technique.

The principles underlying FCCE were first described by Dovichi *et al.* in their study on the interaction of CE with a sheath flow cuvette fluorescence detector. [34] The technique was then employed by Culbertson and Jorgenson for the analytical – scale separation of

closely migrating species, [35] in which a hydrodynamic counter pressure was used to keep the analytes in the electric field longer and give them greater separation time.

Recently, McLaren and Chen published a quantitative study of FCCE describing the system and methods developed for CE preparative purification. [31] To purify a single analyte from the mixture, a counter pressure should be used that only allows the fastest analyte to traverse the capillary to the outlet collection vial. [31] The appropriate counter pressure is determined by constructing a curve of linear velocity of each analyte versus counter pressure, and the value is set between the x-intercepts of the fastest analyte and the second fastest one. [31] Then, with the counter pressure, only the fastest analyte can enter the capillary for purification. [31] Various methods to improve the purification rate and yield for the technique, including increasing the i.d. of the capillary and manipulating the BGE to increase the amount of analyte introduced into the capillary per unit time, were also studied. [31] The final percent recovery of analyte was calculated using the following equation: [31]

$$\%\text{Recovery} = \frac{[\text{analyte}]_{\text{outlet}} \cdot f_{\text{dil}}}{[\text{analyte}]_{\text{sample}}} \cdot 100 \qquad (1.6)$$

Where $[\text{analyte}]_{\text{outlet}}$ is the analyte concentration in the outlet collection vial, $[\text{analyte}]_{\text{sample}}$ is the concentration of the original sample and f_{dil} is a correction factor. Because of EOF, some solution from the inlet vial moved to the outlet vial, which diluted the solution of the collected analyte. The increased volume of solution in the outlet vial was determined through dividing the weight difference of the outlet vial before and after the operation by the known density of the buffer solution. The correction factor was then calculated using the increased volume. [31]

1.7 Recent developments in capillary electrophoresis

CE applications have increased significantly in the traditional fields such as environmental [36], pharmaceutical [37] and forensic analysis [38], as well as in new areas including systems-level analysis of cell signaling molecules [39], identification of biomarkers [40], analysis of virus [41] and explosives [42], and determination of enzymatic activity [43]. New types of detection methods including high resolution sector field inductively coupled plasma MS [44], electrochemiluminescence [45], and multiphoton excitation fluorescence [46] have also been used in CE.

1.8 Research Objective

Although V-DIF using a dynamic pH junction has been successfully applied to weakly acidic species and zwitterionic analytes, [14, 47] the mechanism of this technique is not well understood. In this research, the mechanism of this focusing technique was first studied using an appropriate dye to monitor the pH of the BGE and the sample during the focusing process as described in Chapter 2. This technique was then applied to focus serotonin, a well-known neurotransmitter in a variety of physiological processes, to attempt to simplify serotonin analysis in human plasma. This is the focus of Chapter 3. Chapter 4 presents the application of this technique to separation of amino acids, peptides, and proteins to improve the concentration sensitivity. The pI and pK_a of an amino acid were both used as criteria for the selection of the pH of the sample and the BGE, in an attempt to identify the key factor for focusing. As mentioned previously, the sensitivity in CE-ESI-MS with a sheath-flow interface is lowered due to the dilution of the CE eluent by the sheath liquid. The focusing technique was then used in CE-ESI-MS

to improve the concentration sensitivity. Since UV detection usually only provides migration time information, photodiode array (PDA) and MS are often used for peak identification to provide more structure information. Comparisons were made between the method with PDA detection and the method with MS detection for aromatic amino acids using V-DIF. These studies are described in Chapter 5. Chapter 6 is concerned with the improvement of concentration sensitivity for non-aromatic amino acids in CE-ESI-MS with positive ESI-MS at low pH and negative ESI-MS at high pH with the focusing method. The different conditions for the focusing in the two MS modes were investigated.

In order to improve the purification efficiency for the preparative operation of CE, the effect of more than one capillary in a continuous electrophoretic purification system was then studied with results in Chapter 7. In general, these research goals are intended to expand the utility of CE in current fields and explore applications of CE in new areas.

1.9 References

1. Bowser, M. T.; Bebault, G. M.; Peng, X.; Chen, D. D. Y. *Electrophoresis* 1997, *18*, 2928-2934
2. Slater, G. W.; Kist, T. B. L.; Ren, H. J.; Drouin, G. *Electrophoresis* 1998, *19*, 1525-1541
3. Lehmann, R.; Voelter, W.; Liebich, H. M. *J. Chromatogr., B* 1997, *697*, 3-35
4. Tagliaro, F.; Turrina, S.; Pisi, P.; Smith, F. P.; Marigo, M. *J. Chromatogr., B* 1998, *713*, 27-49
5. Lin, C. E.; Lin, W. C.; Chen, Y. C.; Wang, S. W. *J. Chromatogr., A* 1997, *792*, 37-47
6. Gubitz, G.; Schmid, M. G. *Electrophoresis* 2000, *18*, 4112-4135
7. Jorgenson, J. W.; Lukacs, K. D. *Anal. Chem.* 1981, *53*, 1298-1302
8. Watzig, H.; Degenhardt, M.; Kunkel, A. *Electrophoresis* 1998, *19*, 2695-2752
9. Tsuji, K. *J. Chromatogr., A* 1993, *652*, 139-147
10. Dadoo, R.; Zare, R. N.; Yan, C.; Anex, D. S. *Anal. Chem.* 1998, *70*, 4787-4792
11. Brown, P. R. *Advances in Chromatography* 1994, *Vol. 34*, page 3
12. Loo, J. A.; Edmonds, C. G.; Smith, R. D. *Anal. Chem.* 1991, *63*, 2488-2499
13. Smith, R. D.; Barinaga, C. J.; Udseth, H. R. *Anal. Chem.* 1988, *60*, 1948-1952
14. Britz-McKibbin, P.; Chen, D. D. Y. *Anal. Chem.* 2000, *72*, 1242-1252
15. Peng, X. J.; Chen, D. D. Y. *J. Chromatogr., A* 1997, *767*, 205-216
16. Albin, M.; Grossman, P. D.; Moring, S. E. *Anal. Chem.* 1993, *65*, 489A-497A
17. Shihabi, Z. K. *J. Chromatogr., A* 2000, *902*, 107-117
18. Burgi, D. S.; Chien, R. *Anal. Chem.* 1991, *63*, 2042-2047

19. Quirino, J. P.; Terabe, S. *Science* 1998, *282*, 465-468

20. Palmer, J.; Munro, N. J.; Landers, J. P. *Anal. Chem.* 1999, *71*, 1679-1687

21. Gebauer, P.; Thormann, W.; Bocek, P. *J. Chromatogr., A* 1992, *608*, 47-57

22. Beckers, J. L. *J. Chromatogr., A* 1993, *641*, 363-373

23. Foret, F.; Szoko, E.; Karger, B. L. *J. Chromatogr., A* 1992, *608*, 3-12

24. Watzig, H.; Gunter, S. *Clin. Chem. Lab Med.* 2003, *41*, 724-738

25. Yang, C.; Zhang, L.; Liu, H.; Zhang, W.; Zhang, Y. *J. Chromatogr., A* 2003, *1018*, 97-103

26. Nolan, J. *Application Information Bulletin A-1750*, Beckman Instruments Inc. 1993

27. Rose, D. J.; Jorgenson, J. W. *J. Chromatogr., A* 1988, *438*, 23-34

28. Yin, H. F.; Keelytemplin, C.; McManigill, D. *J. Chromatogr., A* 1996, *744*, 45-54

29. Muller, O.; Foret, F.; Karger, B. *Anal. Chem.* 1995, *67*, 2974-2980

30. Huang, X.; Zare, R. N. *Anal. Chem.* 1990, *62*, 443-446

31. McLaren, D. G.; Chen, D. D. Y. *Electrophoresis* 2003, *24*, 2887-2895

32. Heegaard, N. H. H.; Roepstorff, P.; Melberg, S. G.; Nissen, M. H. *J. Biol. Chem.* 2002, *277*, 11184-11189

33. Chankvetadze, B.; Burjanadze, N.; Bergenthal, D.; Blaschke, G. *Electrophoresis* 1999, *20*, 2680-2685

34. Cheng, F. Y.; Wu, S.; Chen, D. D. Y.; Dovichi, N. J. *Anal. Chem.* 1990, *62*, 496-503

35. Culbertson, C. T.; Jorgenson, J. W. *Anal. Chem.* 1994, *66*, 955-962

36. Ravelo-Perez, L. M.; Hernandez-Borges, J.; Rodriguez, M. A. *Journal of Separation Science* 2006, *29*, 2557-2577

37. Suntornsuk, L. *Journal of Chromatographic Science* 2007, *45*, 559-577

38. Cruces-Blanco, C.; Gamiz-Gracia, L.; Garcia-Campana, A. M. *TRAC-Trends in Analytical Chemistry* 2007, *26*, 215-226

39. Suresh Babu, C. V.; Song, E. J.; Babar, S. M. E.; Yoo, Y. S. *Biomedical Chromatography* 2007, *21*, 890-897

40. Bakry, R.; Huck, C. W.; Najam-ul-Haq, M.; Rainer, M.; Bonn, G. K. *Journal of Separation Science* 2007, *30*, 192-201

41. Kremser, L.; Bilek, G.; Blaas, D.; Kenndler, E. *Journal of Separation Science* 2007, *30*, 1704-1713

42. Pumera, M. *Electrophoresis* 2006, *27,* 244-256

43. Glatz, Z. *J. Chromatogr., B* 2006, *841*, 23-37

44. Sonke, J. E.; Salters, V. J. M.; *J. Chromatogr., A* 2007, *1159*, 63-74

45. Du, Y.; Wang, E. K. *Journal of Separation Science* 2007, *30*, 875-890

46. Du, W.; Chen, S.; Chen, Y. Z.; Chen, Z.; Luo, Q. M.; Liu, B. F. *Journal of Separation Science* 2007, *30*, 906-915

47. Britz-McKibbin, P.; Bebault, G. M.; Chen, D.D.Y. *Anal. Chem.* 2000, *72*, 1729-1735

CHAPTER 2

Mechanistic investigation of velocity-difference induced focusing (V-DIF) in capillary electrophoresis with a dynamic pH junction

2.1 Introduction

Due to the short light path through the capillaries, capillary electrophoresis (CE) has lower concentration sensitivity than high-performance liquid chromatography (HPLC). This is a major shortcoming of CE in practical applications. Z-cells and bubble-cells have been used to improve the concentration sensitivity, but these may reduce the separation efficiency. [1] Improving concentration sensitivity becomes crucial for the use of CE in industrial and research applications.

Sample stacking is one of the most effective ways to improve the concentration sensitivity in CE. [2, 3] Stacking in CE does not need special devices such as solid phase extraction (SPE) or precolumns which are usually necessary for preconcentration in HPLC. Large volume samples can be injected in sample stacking and more than a 100-fold increase in concentration sensitivity [4, 5] can be obtained. Field–amplified stacking [6-9] is based on the conductivity difference between the sample zone and the BGE. The lower conductivity sample zone has higher electric field strength, so the analyte ions move faster in the sample zone than in the BGE. Upon reaching the boundary between the sample zone and the BGE, they slow down and stack at the boundary. However, this technique requires that the analytes reside in a lower conductivity environment than that of the BGE. Biological or environmental samples often need desalting for this technique. [10] Isoelectric focusing [11] has been used to separate amphoretic compounds such as proteins in a pH gradient based on their isoelectric points. The pH gradient is formed by carrier ampholytes when an electric field is applied. Huang *et al.* developed a novel method for isoelectric focusing of proteins in pure water, creating the pH gradient by the

movement of protons and hydroxide ions produced by the electrolysis of water. [12] Wei *et al.* used another strategy to create the pH gradient for focusing analytes by inserting a short platinum wire into the capillary [13] using histidine as buffer. Quirino and Terabe [14, 15] introduced a sweeping concept for sample stacking in micellar electrokinetic chromatography (MEKC) where the analyte molecules were accumulated when the micelles penetrated the sample zone during the separation.

A special sample stacking method has been previously reported by our group for analysis of epinephrine in dental anesthetic solutions by CE. [16, 17] Using a dynamic pH junction, large volume samples were directly injected into the capillary and significant focusing was achieved, even though the samples contained high salt contents. This technique was also applied to zwitterionic analytes and weakly acidic species that possess different velocities in the sample and the BGE. [10] A limit of detection (LOD) and separation efficiencies better than 4.0×10^{-8} M and 1.0×10^{6} theoretical plates were achieved, respectively, with UV detection. As well, the method was applied to improve the concentration sensitivity for nucleotides extracted from mouse lymphoma cells. [18]

Though this technique worked effectively for many applications, its focusing mechanism was still not clear. It is different from field-amplified stacking methods because the conductivity of the sample matrix is not necessarily less than that of the BGE. [10] A mechanistic study of this focusing technique has been carried out by Kim [19] *et al.* using computer simulation (program SIMUL). In the simulation, a short sample plug of 1-3 mm was injected into a short capillary of 15 cm. Only the normal pH junction (sample

pH is lower than that of BGE) condition was studied, and no reverse pH junction (sample pH is higher than that of BGE) condition was investigated. The simulation suggested that the focusing was caused by a moving pH boundary, and the depth and lifetime of the pH boundary was a function of analyte pK_a, sample pH and injection length. However, a pH boundary was not observed during the experiments. They attributed this to mixing at the sample and BGE interface which was perturbed by the laminar flow because a low pressure was applied to deliver the sample zone to the different positions in the capillary. In a real situation, it is the EOF and not the pressure that transfers the sample zone through the capillary. In the simulation, however, the EOF was assumed to be zero. Furthermore, since BGE pH change was not investigated, the pH change was not accurately evaluated in the study.

Another similar approach has been done by Breadmore *et al.* for the stacking of weak bases using high-resolution computer simulations with an emphasis placed on the impact of sample ionic strength. [20] A 10 mm sample plug was injected into a capillary of 5 cm in the simulations and the EOF was also assumed to be zero. The focusing discussed was limited to the weak bases with pK_a not larger than 7.5. The analysis of the focusing mechanism was still based on a moving pH boundary with special consideration of impact of salts. No real experiments were performed to verify the simulation results in the study.

In this research, we have attempted to clarify the mechanism by studying how the pH of the sample and the BGE change during the focusing process with both normal and

reverse pH junction condition and by investigating the influence of the pH of both the BGE and the sample on analyte focusing under real experimental conditions. The general conditions affecting focusing, such as pH difference between the sample and BGE, different buffer systems and the ionic strength of BGE, are investigated in the following chapters.

2.2 Experimental Section

2.2.1 Chemicals.

Phenolphthalein (ACS reagent, Aldrich Chemical Company, Inc., Milwaukee WI, USA) was used as the pH indicator dye. The aqueous BGE consisted of 160 mM borate [10] (Sodium tetraborate, 99.5-105.0%, Sigma Chemical Co., St. Louis, MO) and 1 mM ethylenediaminetetraacetic acid (EDTA, ACS reagent, BDH Chemicals, Toronto, Ont., Canada). The pH of the BGE and the sample was adjusted by using 1 M HCl (Certified, Fisher Scientific, Nepean, Ont., Canada) or 1 M NaOH (Certified, BDH Chemicals, Toronto, Ont., Canada). Ethanol (95%) was purchased from BDH Chemicals. HPLC-grade acetone was purchased from Fisher Scientific. The 1.5×10^{-5} M phenolphthalein solution was prepared from a 3 mM phenolphthalein stock solution (0.0010 g phenolphthalein dissolved in 1.0 mL 95% ethanol) by diluting the stock solution 200 times with BGE. Water was purified using a Milli-Q Elix system (Millipore, Milford, MA, USA).

2.2.2 Apparatus and Procedure

Separations were performed on a P/ACE^{TM} MDQ automated CE system (Beckman-Coulter Inc., Mississauga, Ont., Canada). An uncoated fused silica capillary (Polymicro Technologies, Phoenix, AZ) with an inner diameter of 75 μm and a length of 60 cm was used. The new capillary was first rinsed with 1.0 M NaOH (20 psi for 10 min) and then rinsed with BGE (20 psi for 10 min), and finally a voltage of 15 kV was applied for 10 min. Each separation was preceded by a 1.5-min, 20 psi rinse with 1 M NaOH, followed by a 4-min rinse with the BGE. The samples were then injected using a pressure of 0.5 psi and the separation was performed with normal polarity at 15 kV and a temperature of 20 ^{0}C. The term "sample" in this chapter refers to phenolphthalein if it is dissolved in sample matrix. A Beckman MDQ PDA adsorption detector with a wavelength range of 190-600 nm was used. The average speed of the low-pressure (0.5 psi) injection was 6.83 cm / min with a 60 cm capillary, which was determined by measuring the time required to flush the indicator dye to the detection window under the pressure of 0.5 psi within a known length of capillary. The UV spectra of phenolphthalein were obtained with an HP 8451 A UV/VIS spectrometer (Hewlett-Packard, Palo Alto, CA, USA).

2.3 Results and Discussion

2.3.1 pH Investigation with a dye

Because the focusing is generated by the pH difference between the sample and the BGE, it is obvious that the pH is very important in V-DIF with a dynamic pH junction. In order to understand the mechanism of focusing, we must first determine whether the pH of the sample and BGE remain the same or change during the focusing process. However, it is

not feasible to test the pH of the solution within the capillary with a pH probe, which makes it very difficult to determine the pH inside the capillary. [21] Although we can measure the pH of bulk BGE and sample solutions before putting them into the capillary, the reading may not represent the actual pH inside the capillary when a voltage is applied because the movement of hydroxide ions and protons may result in a pH change in the capillary. [21] A pH indicator dye is useful for visualizing the pH in the capillary. This makes it possible to make an approximate estimate of the pH within the capillary from the dye color or spectra. [21]

Dyes are often used for on-column pH monitoring because their spectra and color show the pH of the solution where they reside. Timperman *et al.* used the dye carboxyseminaphthorhodafluor to study the pH changes within a capillary resulting from electrolysis at a low volume capillary outlet [22] by monitoring the dye spectra. Macka *et al.* investigated the impact of electrolysis at the anode and cathode on the pH of the electrolyte inside the capillary [23] using the dyes xylenol blue and bromocresol green. The existence of a pH gradient created from the electrolysis of water was detected by Huang *et al.* [12] using the indicator dye methyl red and whole-column imaging detection. For our investigation, we have to select a proper dye that will be used to monitor the pH of the sample plug and BGE. The dye should not move out of the plug when a voltage is applied. Otherwise, it cannot represent the true pH of the plug. If the dye is neutral, it will remain in the plug under an electric field. The requirement is the same for monitoring the pH of the BGE. Phenolphthalein is an appropriate dye because it has a high pK_a value of 9.5 and is neutral at pH 7.3. Its UV spectrum also changes with pH and can be used to

monitor the pH change within a capillary. The structure of phenolphthalein [24] is shown in Figure 2.1.

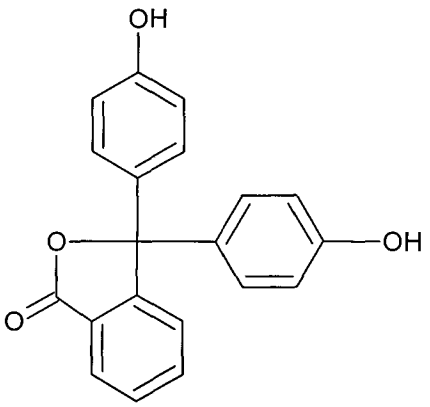

Figure 2.1 Phenolphthalein structure.

The spectra of phenolphthalein at various pH values in buffer solutions and the ratio of its absorption at 552 nm to absorption at 230 nm versus pH are shown in Figure 2.2.

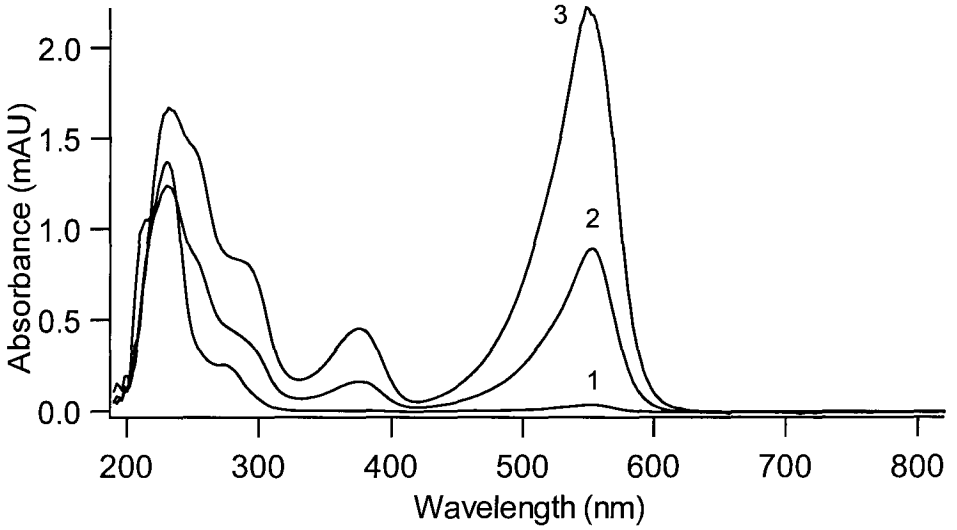

(a)

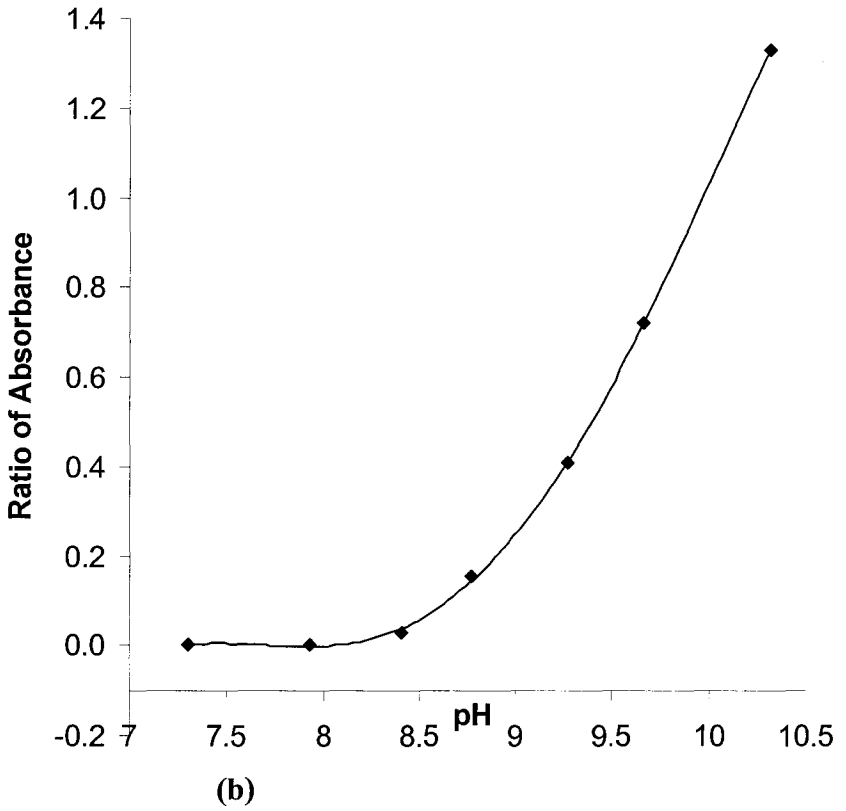

(b)

Figure 2.2 (a) Spectra of phenolphthalein at various pH values in buffer solutions obtained with an HP 8451 A UV/VIS spectrometer. 1- pH 7.3. 2 - pH 9.7. 3 - pH 10.3. The concentration of phenolphthalein was 1.5 x 10^{-5} M. The maximum in the spectra occur at 230 nm and 552 nm at pH 7.3 and 10.3, respectively. (b) Ratio of absorbance at 552 nm to absorbance at 230 nm versus pH.

2.3.2 Sample and BGE pH change during the process

Experiments were conducted to evaluate the nature of the pH junction in a multi-section electrolyte system. A series of control experiments were performed, in which both the BGE and the sample were prepared at either pH 7.3 (at which phenolphthalein is neutral) or 10.3. The sample was injected for 60 s, 120 s, and 200 s at 0.5 psi. The dye is used to probe the pH of the sample and the BGE during the focusing process.

The dye was first added to the sample during the focusing process, and then added to the BGE to monitor the pH of the BGE. The control experiments are described in Figure 2.3.

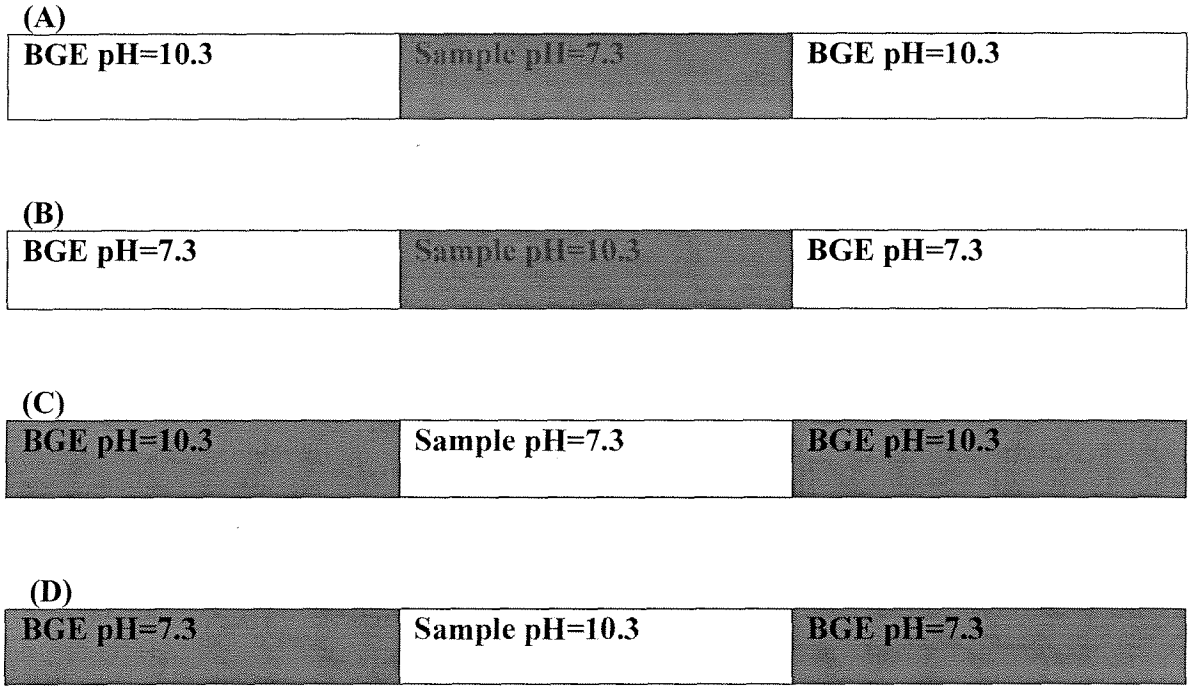

Figure 2.3 Control experiments using a multi-section electrolyte system. For (A) and (B), only the sample contained phenolphthalein. For (C) & (D), only the BGE contained phenolphthalein. Shading represents the presence of phenolphthalein. The BGE and sample matrix consisted of 160 mM borate with 1 mM EDTA. (A) The BGE pH was 10.3 and the sample pH was 7.3. (B) The sample pH was 10.3 and the BGE pH was 7.3. (C) The sample pH was 7.3 and the BGE pH was 10.3. (D) The BGE pH was 7.3 and the sample pH was 10.3.

The injection times of 60 s, 120 s, and 200 s at 0.5 psi correspond to approximately 6.83 cm, 13.66 cm, and 22.77 cm plug lengths that are equivalent to 12%, 24%, and 40% of the total capillary. The corresponding injection volumes are about 300 nL, 600 nL, and 1000 nL, respectively.

For condition (A), which is called a normal pH junction (the pH of the sample is lower than that of the BGE), the electropherograms for 60 s, 120 s, and 200 s injections are shown in Figure 2.4.

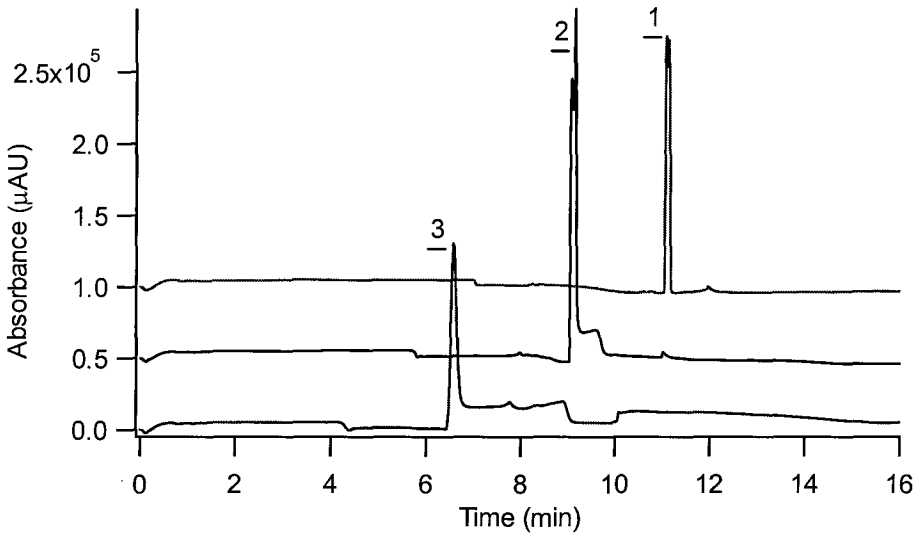

Figure 2.4 Electropherograms for different injection times in the normal pH junction condition (the pH of the sample is lower than that of the BGE), which is shown as condition A in Figure 2.3 where the sample contained dye. 1-60 s (300 nL); 2- 120 s (600 nL); 3 - 200 s (1000 nL). Conditions: BGE and sample matrix, 160 mM borate with 1 mM EDTA; phenolphthalein concentration, 1.5 x 10^{-5} M; BGE pH, 10.3; sample pH, 7.3; detection wavelength, 230 nm; voltage, 15 kV.

Phenolphthalein focused for all the injections. However, if there was no pH difference between the sample and the BGE, phenolphthalein migrated as a broad band as shown in Figure 2.5.

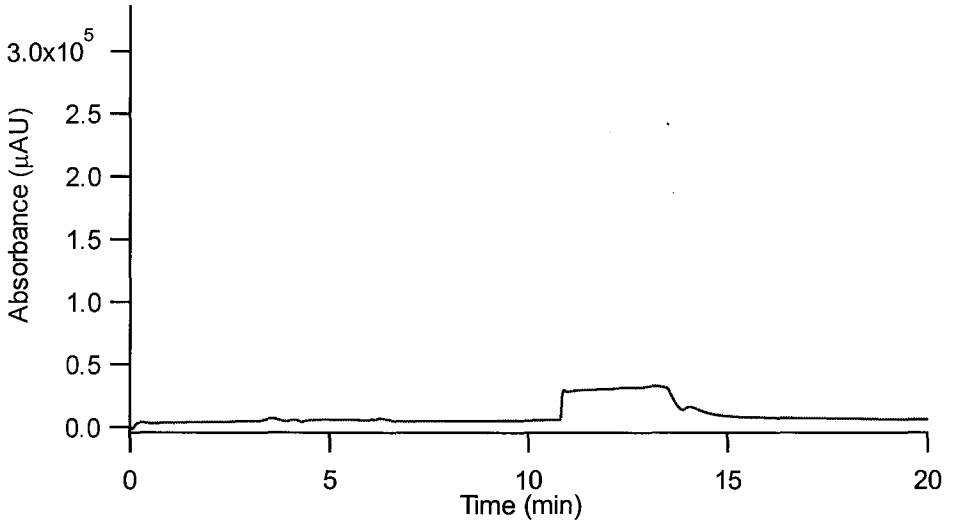

Figure 2.5 Electropherogram of phenolphthalein where both the pH values of the sample and the BGE were 10.3. Conditions: BGE and sample matrix, 160 mM borate with 1 mM EDTA; phenolphthalein concentration, 1.5 x 10^{-5} M; injection time, 99 s (500 nL); detection wavelength, 230 nm; voltage, 15 kV.

The pH values at which phenolphthalein passed the detection window for 60 s, 120 s and 200 s injections can be estimated from the corresponding UV spectra by calculating the ratio of absorbance at 552 nm to absorbance at 230 nm. The pH values were estimated to be about 9.4, 9.3, and 8.8 for 60 s, 120 s and 200 s injection times, respectively. From these values, the sample pH was found to have changed during the process, and the longer the injection plug, the less the sample pH was found to change. The migration time was also different for different injection volumes. This is because the migration time is related to the charge state of the dye and the charge state of the dye differs at different pH. The higher the pH, the more negatively charged phenolphthalein (q = -2, where the q is the electric charge) becomes. The apparent mobility of the dye is an average of the mobility fractions of the neutral and the negatively charged species. [25] The negative ions move towards the anode, which is opposite to the direction of electroosmotic flow (EOF),

so the more the dye is negatively charged, the longer the migration time will be. Therefore, the peak in the 60 s injection case appeared later than that of the 200 s injection case. It is apparent that the hydroxide ions in the BGE positioned ahead of the sample plug (front BGE) in the capillary move backwards to the anode and invade the sample zone when the voltage is applied. This leads to the sample pH change.

For condition (B), which is called a reverse pH junction (the pH of the sample is higher than that of the BGE), the electropherograms for 60 s, 120 s, and 200 s injections are shown in Figure 2.6.

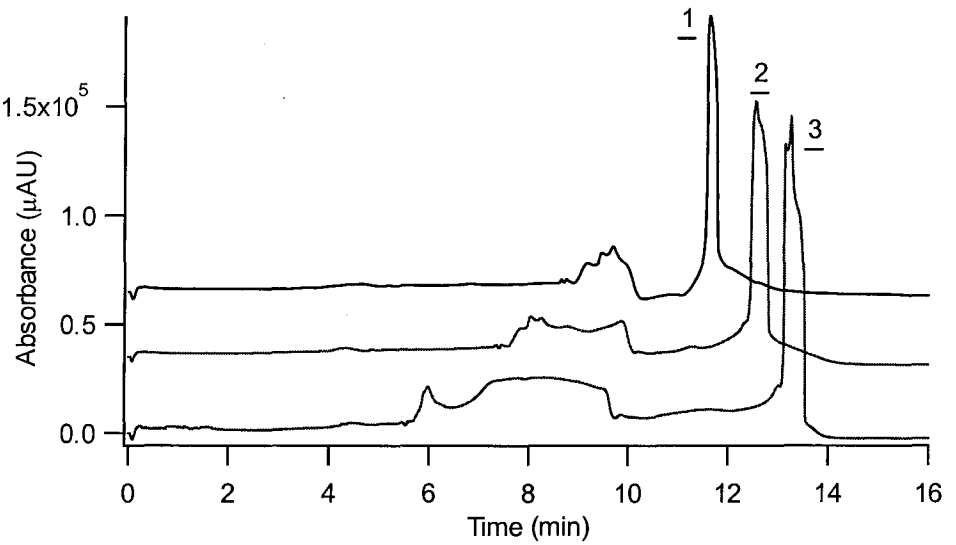

Figure 2.6 Electropherograms for different injection times with a reverse pH junction (the pH of the sample is higher than that of the BGE), condition B in Figure 2.3. 1- 60 s (300 nL); 2- 120 s (600 nL); 3 - 200 s (1000 nL). Conditions: BGE and sample matrix, 160 mM borate with 1 mM EDTA; phenolphthalein concentration, 1.5 x 10^{-5} M; BGE pH, 7.3; sample pH, 10.3; detection wavelength, 230 nm; voltage, 15 kV.

The pH of the sample changed. The pH values at which phenolphthalein crossed the detection window were estimated to be about 8.3, 8.4, and 8.7 for 60 s, 120 s and 200 s injection times, respectively. The injection volume again had a significant influence on

the resultant sample pH after the sample zone interacted with the BGE. Because the sample pH was higher than that of the BGE, a larger injection volume of sample led to a higher resultant sample pH after the interaction between the sample zone and the BGE. The higher the pH where the phenolphthalein remained, the more the phenolphthalein was negatively charged, causing the peak to appear later. Thus the migration time for the 200 s injection was longer than that of the 60 s injection. In this case the hydroxide ions in the sample zone moved backwards to the anode and interacted with the BGE positioned behind the sample plug (back BGE) in the capillary when the voltage was applied, causing the pH change.

Two other kinds of control experiments were carried out to further evaluate the nature of the pH junction in a multi-section electrolyte system. These are illustrated schematically as (C) and (D) in Figure 2.3.

Introducing the dye into the BGE makes it easy to monitor the BGE pH change. Phenolphthalein in a part of the BGE adjacent to the sample was also found to focus in both cases.

For condition (C), the electropherograms for the 60 s, 120 s, and 200 s injections are shown in Figure 2.7 (a), and the contour plot is shown in Figure 2.7 (b).

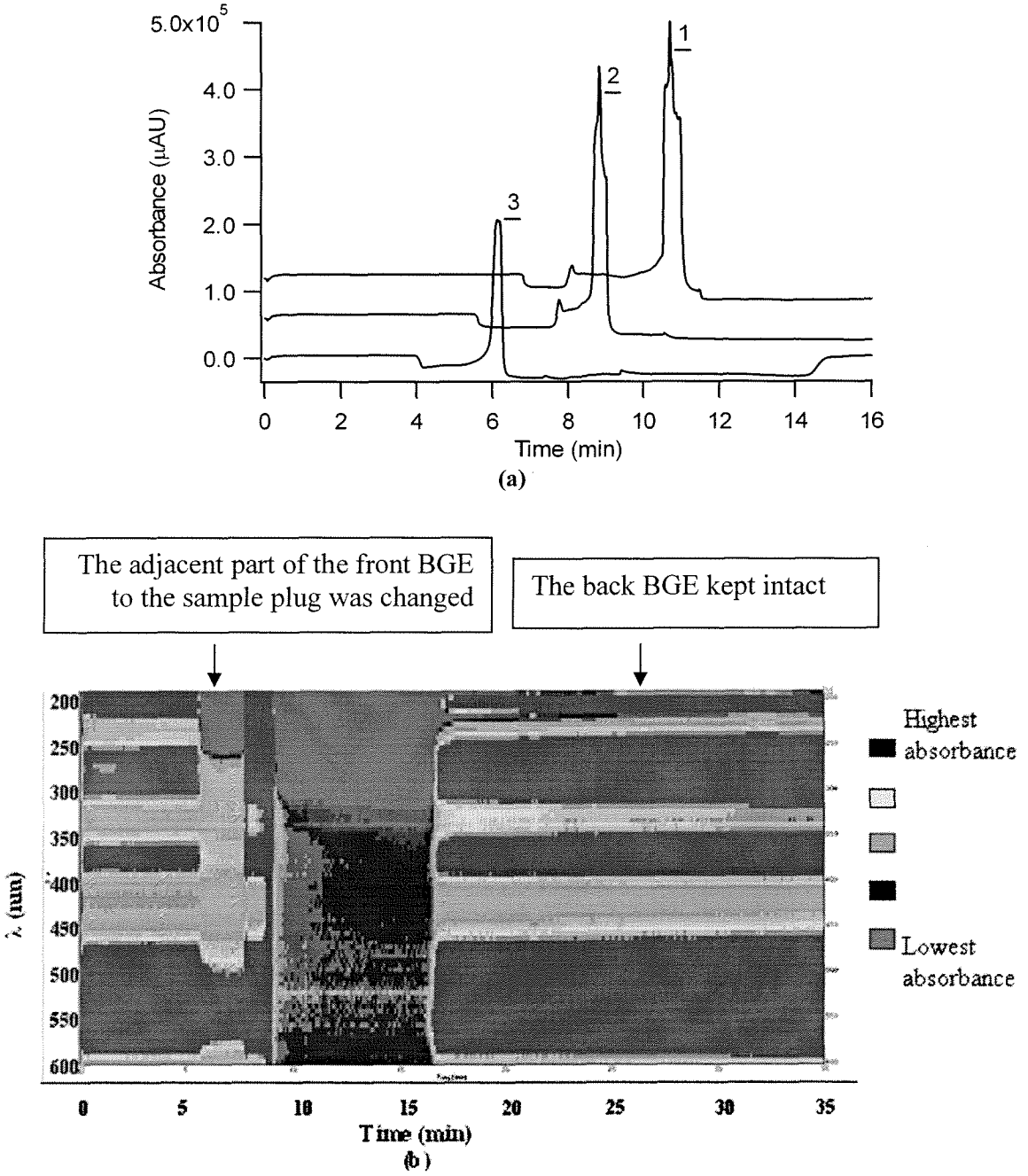

Figure 2.7 (a) Electropherograms for different injection times with a normal pH junction condition, condition (C) in Figure 2.3, where the dye was put into the BGE. 1-60 s (300 nL); 2- 120 s (600 nL); 3 - 200 s (1000 nL). Detection wavelength, 450 nm. (b) Contour plot of phenolphthalein in the normal pH junction condition where the BGE contained dye. Injection time was 120 s (600 nL). Conditions: BGE and sample matrix, 160 mM borate with 1 mM EDTA; BGE pH, 10.3; sample pH, 7.3; voltage, 15 kV.

For condition (D), the electropherograms for 60 s, 120 s, and 200 s injections are shown in Figure 2.8 (a), and the contour plot is shown in Figure 2.8 (b).

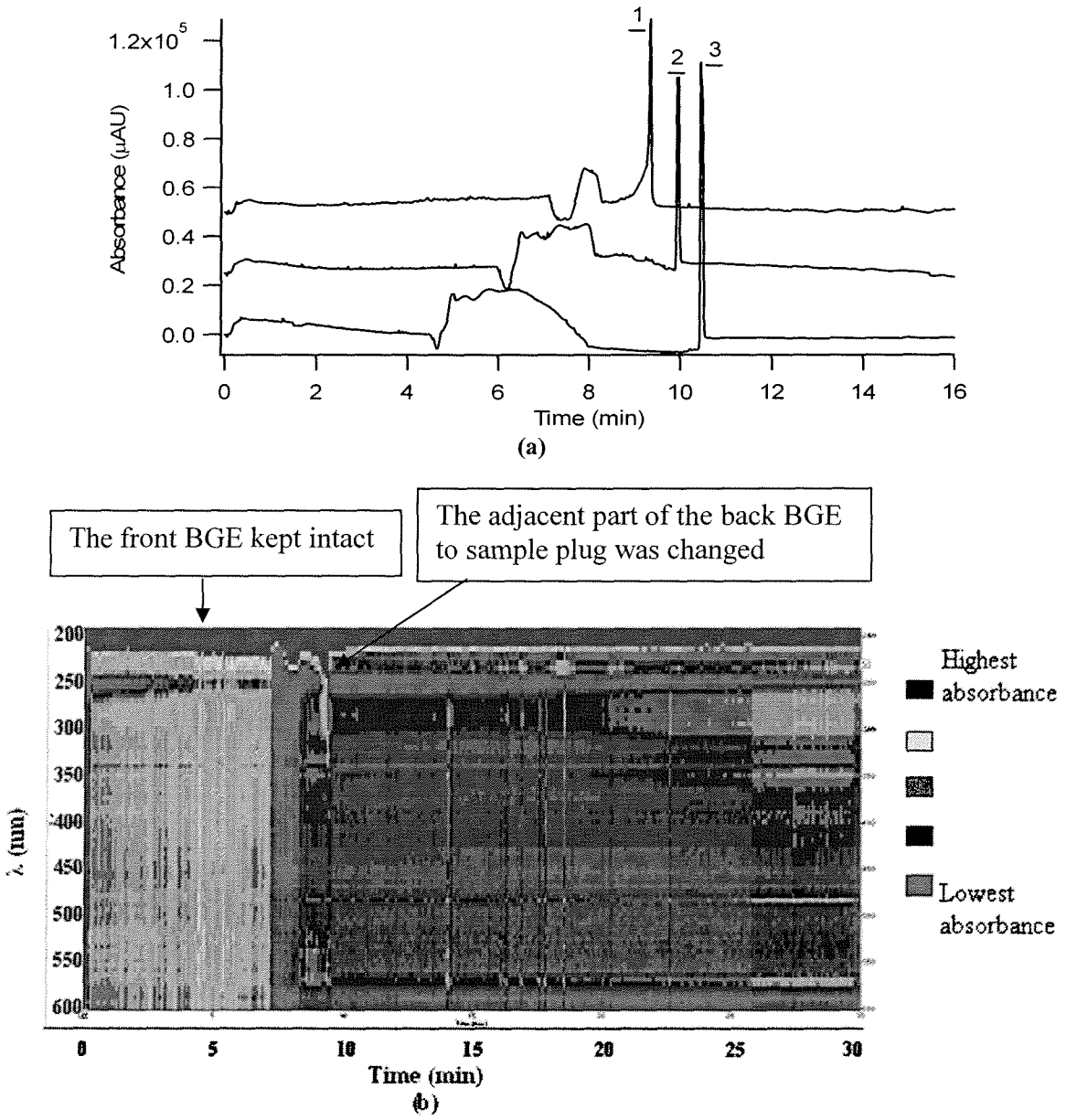

Figure 2.8 (a) Electropherograms for different injection times in the reverse pH junction condition, condition (D) in Figure 2.3, where the dye was put into the BGE. 1- 60 s (300 nL); 2- 120 s (600 nL); 3 - 200 s (1000 nL). Detection wavelength, 230 nm. (b) Contour plot of phenolphthalein in the reverse pH junction condition where the BGE contained dye. Injection time was 60 s (300 nL). Conditions: BGE, 160 mM borate with 1 mM EDTA; BGE pH, 7.3; sample pH, 10.3; voltage, 15 kV.

From the contour plot, we can tell whether the pH of the BGE was changed during the process according to the dye color. In the contour plot, the x-axis represents the migration time and the Y-axis represents the absorbance of dye at different wavelengths. The red color indicates high absorbance intensity, and the pink or blue color shows weak absorbance intensity. The contour plot shows the dye color in the capillary corresponding to migration time. The left part of the contour plot indicates the dye color of the front BGE and the right part of the contour plot indicates the dye color of the back BGE. The middle part represents the sample plug (void-no dye). The front junction is between the front BGE and the sample plug, and the back junction is between the back BGE and the sample plug. In case (C), where the sample pH was lower than that of the BGE, the dye color of the BGE at the back remained the same and the back junction remained intact, but the dye color of the adjacent part of the front BGE to sample plug changed and the original front junction disappeared. The pH calculated from the absorbance spectrum of the focused dye was different with those of the BGE and the sample plug. It could be inferred that the sample zone interacted with the adjacent part of the front BGE and changed the pH. This is mainly because the hydroxide ions in the front BGE move backwards to the anode once the voltage is applied and interact with the sample plug, causing the front junction to deteriorate. The dye in the adjacent part of the front BGE focused in the area where the sample plug and the BGE interacted. No significant inverse baseline shift was observed for the void sample (only BGE contained dye) in the electropherogram since the dye had a weak absorbance at the wavelength selected. In condition (D), the front junction remained intact, but the back junction disappeared. This is because the pH of the sample is higher than that of the BGE, and the hydroxide ions in

the sample plug move backwards to the anode and invade the back BGE when the voltage is applied, to cause the back junction to disappear. The dye in the part of the interaction between the sample plug and the back BGE also focused.

From the electropherograms of Figure 2.7 (a) and Figure 2.8 (a) for condition (C) and (D), it can be seen that the injection volumes also have similar effects on the migration times of phenolphthalein as (A) and (B) depending on the pH at the location of the phenolphthalein. In our previous research [10] it was thought that in a normal pH junction condition, when the electric field was applied, the neutral analyte molecules at the front of the injected sample acquired a negative charge as the hydroxide ions in the higher pH BGE invaded the sample zone, and migrated towards the anode. However, the analytes at the back of the sample zone migrated at the same speed as the EOF, which was faster than the negatively charged analytes, until the hydroxide ions reached the end of the sample zone. The pH of the solution in the entire capillary then equalized and the negatively charged analytes were carried to the detector by the EOF. From the above results, including the electropherograms and contour plots in Figure 2.4, 2.6, 2.7, and 2.8, it can be seen that the pH of different regions in the capillary can be different after the interaction. The resultant pH of the sample plug may not be the same as that of the BGE and is dependent on the injection volumes.

2.3.3 The effect of the BGE and sample pH on focusing

The influence of the BGE pH on focusing was examined. Figure 2.9 depicts a series of electropherograms in which the BGE pH ranged from 7.3 to 10.3 while the sample pH was fixed at 7.3.

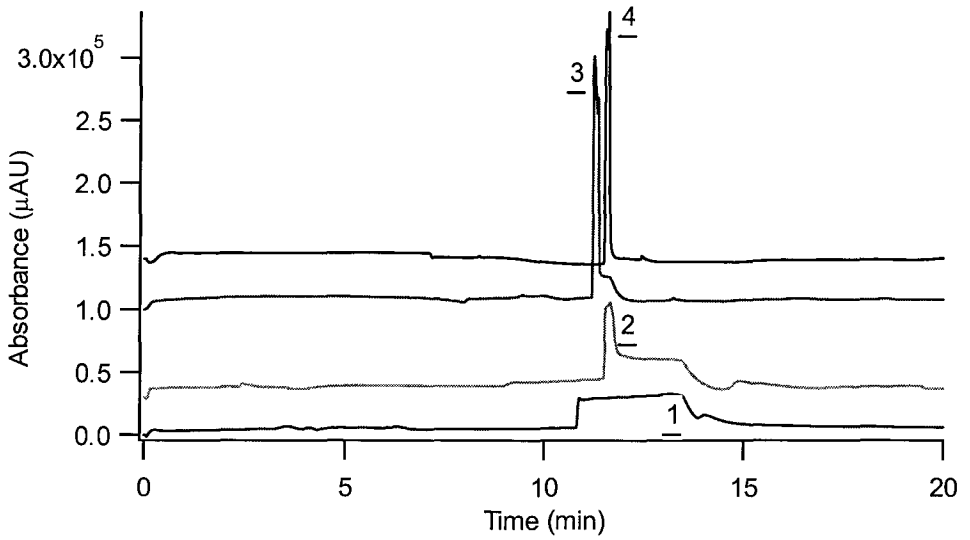

Figure 2.9 Electropherograms showing the effect of the BGE pH on phenolphthalein focusing. The injection time was 99 s (500 nL) and the sample matrix pH was fixed at 7.3. 1 – BGE pH 7.3; 2 – BGE pH 8.5; 3 – BGE pH 9.3; 4 – BGE pH 10.3. Conditions: BGE and sample matrix, 160 mM borate with 1 mM EDTA; phenolphthalein concentration, 1.5 x 10^{-5} M; detection wavelength, 230 nm; voltage, 15 kV.

Phenolphthalein migrated as a long and diffuse plug, as shown in trace 1, when the BGE pH was the same as that of the sample. When the BGE pH increased, the band narrowed. When the pH of the BGE was greater than the pK_a of phenolphthalein (9.5), the phenolphthalein focused into a sharp peak, as shown in trace 4. The peak height increased as the phenolphthalein band narrowed. It should be noted that the peak height increase is also related to a higher molar absorptivity of phenolphthalein at higher pH.

In our group's previous research [10] on epinephrine focusing using a dynamic pH junction, the pH of the BGE was fixed at 10.2, but the pH of the sample varied from 10.2 to 8.5 (epinephrine is neutral at pH 8.5). It was found that no focusing was observed when the sample and the BGE had the same pH. A gradual decrease of the sample pH relative to that of the BGE resulted in pronounced focusing. The best focusing was achieved when the pH of the sample was lowered to 8.5, which was below the pK_a of the analyte.

From the above results, it can be seen that the pH of the sample and BGE are crucial for focusing. This is ascribed to the different velocities of the same analyte in the sample zone and BGE caused by the changes in the deprotonation of the analyte at different pH. The optimum focusing results can be obtained by using pH under the pK_a and above the pK_a of the analyte, for the sample and the BGE, respectively, as the different pH could cause a significant change in the analyte velocity. In the previous work, [10, 18] it was thought that the velocity of the analyte was also changed by the different borate complexation in the sample zone and BGE, thus the borate buffer was important to the focusing as well. We tried several other buffer systems for different analytes (such as amino acids), and the same good focusing was achieved. Therefore, the difference in pH between the sample and the BGE is the most important factor for focusing with a dynamic pH junction.

2.3.4 Mechanism

A major characteristic of dye molecules is that their spectra change corresponding to protonation or deprotonation in solutions of different pH. In condition (A) as shown in Figure 2.3 (normal pH junction), the sample pH was lower than that of the BGE. When the voltage was applied, the hydroxide ions in the front BGE, which had a higher pH, moved backwards and invaded the sample zone and soon formed a pH gradient from the sample plug to the adjacent part of the front BGE. This pH gradient is similar to a pH gradient investigated by Rae *et al.* [26] The breadth of the gradient zone is a complicated relationship between the relative buffer capacities of the BGE and sample and the sample injection volumes. [26] The pH gradient in the normal pH junction condition was shown by Quintás *et al.* [27] in the study of on-line monitoring of pH junctions for myglobin focusing using Fourier transform infrared spectrometry. When the pH of the BGE was under 9.5, most of the phenolphthalein molecules were neutral. The dye moved with the EOF, so no focusing was achieved and a broad band was observed. However, when the pH of the BGE was above the pK_a of phenolphthalein, phenolphthalein in the high pH area in the gradient became negatively charged. The negative ions moved towards the anode until reaching the area of lower pH where protonation of the species occurred, resulting in significantly lower velocity and leading to focusing, as shown in Figure 2.10.

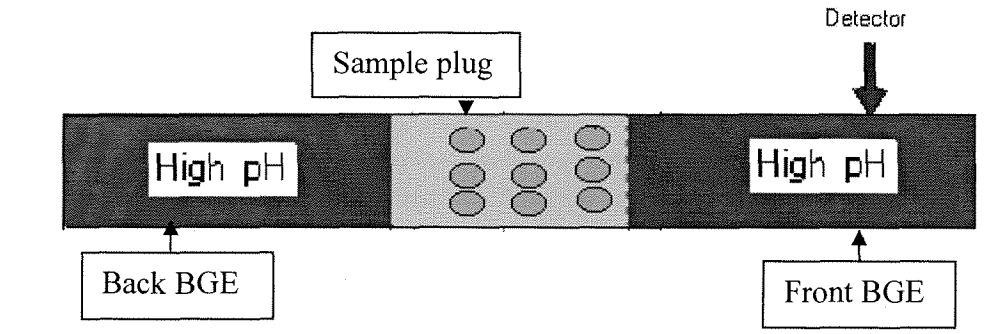

(a)

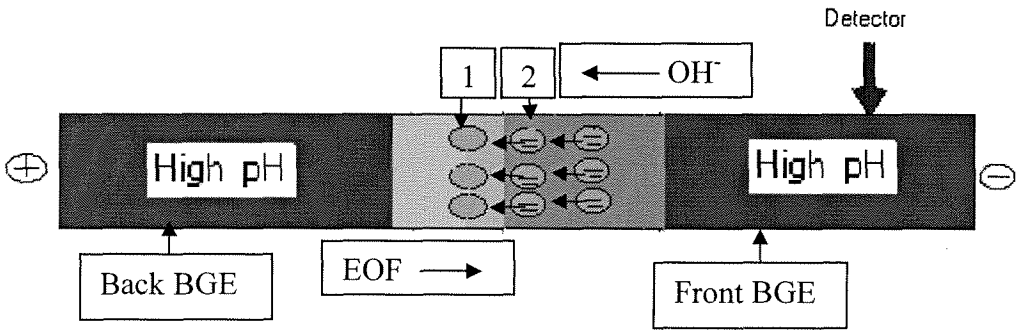

(b)

Figure 2.10 Proposed mechanism of focusing using a dynamic pH junction (normal pH junction). (a) A large sample plug with a lower pH electrolyte is injected into a capillary filled with a higher pH BGE. (b) pH gradient forms due to the invasion of hydroxide ions from the front BGE to the sample zone under the electric field, different color bands represent the pH gradient from the sample zone to the adjacent part of the front BGE. 1- Phenolphthalein is neutral. 2- Phenolphthalein is negatively charged.

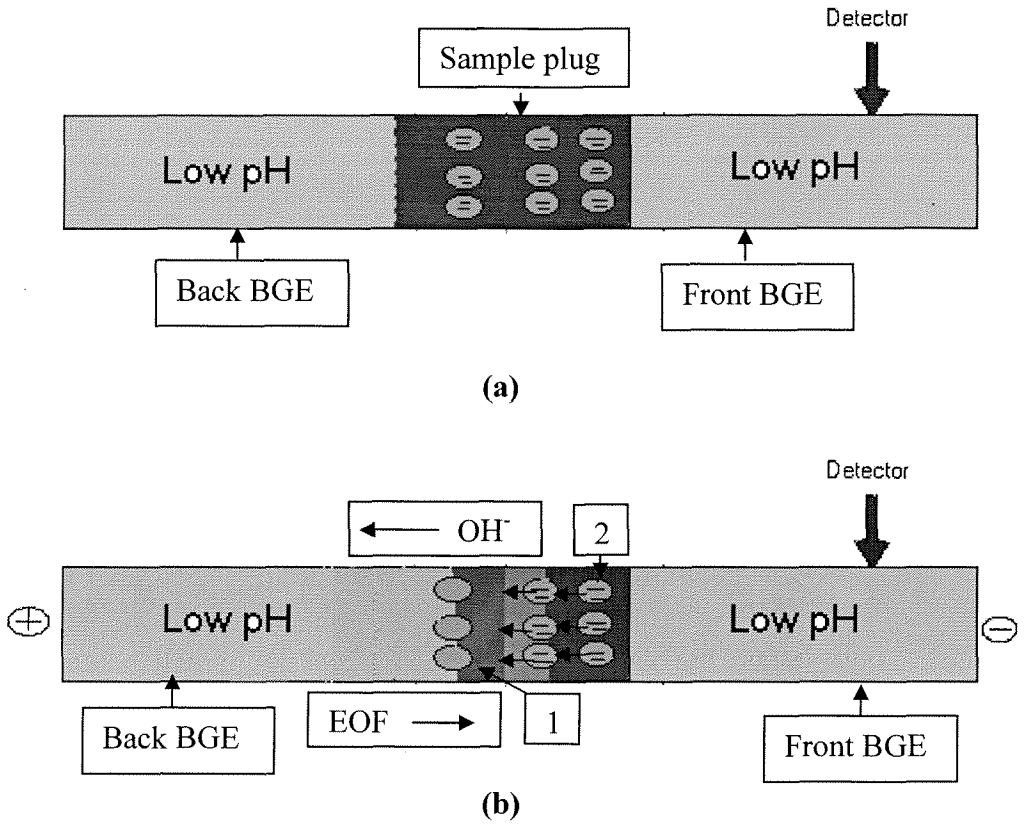

Figure 2.11 Proposed mechanism of focusing using a dynamic pH junction (reverse pH junction). (a) A large sample plug with a higher pH electrolyte is injected into a capillary filled with a lower pH BGE. (b) pH gradient forms due to the invasion of hydroxide ions from the sample zone to the back BGE under the electric field, different color bands represent the pH gradient from the sample zone to the adjacent part of the back BGE. 1- Phenolphthalein is neutral. 2- Phenolphthalein is negatively charged.

In condition (B) as shown in Figure 2.3 (reverse pH junction), the sample pH was higher than that of the BGE. When the voltage was applied, the hydroxide ions in the higher pH sample plug invaded the back BGE zone and formed a pH gradient from the sample plug to the adjacent part of the back BGE. The focusing process is similar to that of the normal pH junction and is depicted in Figure 2.11.

After the pH gradient was formed, the pH of the different bands in the gradient kept changing due to the continuous movement of hydroxide ions under the electric field.

The resultant pH of the low pH area in the gradient where the phenolphthalein focused depends on the length of the sample plug and the pH difference between the sample and the BGE. The longer the sample plug, the more it affects the pH of the gradient. For example, in condition (A) shown in Figure 2.3, the resulting electropherograms are shown in Figure 2.4. The pH indicated by the focused dye was different for 60 s, 120 s and 200 s injections. Because the pH of the sample was lower than that of the BGE, the resultant pH in the gradient was lower for the 200 s injection than for the 60 s and 120 s injections. The lower the pH where phenolphthalein remained, the less the phenolphthalein was negatively charged, and the earlier the peak came out in the electropherograms. Therefore, the peak came out earliest for the 200 s injection in this condition.

2.4 Conclusions

The mechanism of velocity-difference induced focusing was developed based on the experimental results by using phenolphthalein to monitor the pH of the sample and BGE during the focusing process. It was found that the pH difference between the sample and the BGE was the most important factor for focusing using a dynamic pH junction. Differences in pH resulting in different charge states for analytes in the sample and the BGE were determined to cause focusing through changes in analyte velocities in different pH segments in the pH gradient formed by the sample and adjacent BGE. The pK_a of an

analyte was found to be a key criterion for selecting the pH for the sample and the BGE to obtain optimum focusing. This mechanism only applies to analytes that have different charge states at different pH. Further investigation is needed with a wider variety of analytes.

2.5 References

1. Albin, M.; Grossman, P. D.; Moring, S. E. *Anal. Chem.* 1993, *65*, 489A-497A
2. Burgi, D. S.; Chien, R. L. *Anal. Chem.* 1991, *63*, 2042-2047
3. Kruaysawat, J.; Marriott, P. J.; Hughes, J.; Trenerry, C. *Electrophoresis* 2003, *24*, 2180-2187
4. Wolf, S. M.; Vouros, P. *Anal. Chem.* 1995, *67*, 891-900
5. Chen, Y. R.; Tseng, M. C.; Chang, Y. Z.; Her, G. R. *Anal. Chem.* 2003, *75*, 503-508
6. Manetto, G.; Tagliaro, F.; Crivellente, F. *Electrophoresis* 2000, *21*, 2891-2898
7. Zhang, C. X.; Thormann, W. *Anal. Chem.* 1996, *68*, 2523-2532
8. Burgi, D. S.; Chien, R. L. *Anal. Chem.* 1992, *64*, 1046-1050
9. Zhao, Y. P.; McLaughlin, K.; Lunate, C. E. *Anal. Chem.* 1998, *70*, 4578-4585
10. Britz-McKibbin, P.; Chen, D. D. Y. *Anal. Chem.* 2000, *72*, 1242-1252
11. Jenkins, M; Ratnaike, S; *Clin. Chem. Lab Med.* 2003, *41*, 747-754
12. Huang, T.; Wu, X. Z.; Pawliszyn, J. *Anal. Chem.* 2000, *72*, 4758-4761
13. Wei, W.; Xue, G.; Yeung, E. S. *Anal. Chem.* 2002, *74*, 934-940
14. Quirino, J. P.; Terabe, S. *Science* 1998, *282*, 465-468
15. Quirino, J. P.; Terabe, S. *Anal. Chem.* 1999, *71*, 1638-1644
16. Britz-McKibbin, P.; Kranack, A. R.; Paprica, A.; Chen, D. D. Y. *Analyst* 1998, *123*, 1461-1463
17. Britz-McKibbin, P.; Wong, J.; Chen, D. D. Y. *J. Chromatogr., A* 1999, *853*, 535-40
18. Britz-McKibbin, P.; Bebault, G. M.; Chen, D. D. Y. *Anal. Chem.* 2000, *72*, 1729-

1735

19. Kim, J.; Britz-McKibbin, P.; Hirokawa, T.; Terabe, S. *Anal. Chem.* 2003, *75*, 3986-3993

20. Breadmore, M. C.; Mosher, R. A.; Thormann, W. *Anal. Chem.* 2006, *78*, 538-546

21. Duso, A. B. *M. Sc. Thesis, Determination of on-capillary pH and Proton and Hydroxide Mobility in capillary electrophoresis,* UBC, 2002

22. Timperman, A.; Tracht, S.; Sweedler, J. *Anal. Chem.* 1996, *68*, 2693-2698

23. Macka, M.; Andersson, P.; Haddad, P. *Anal. Chem.* 1998, *70*, 743-749

24. Merck Index, 13th edition, Merck & Company, Whitehouse Station, NJ, 2001, Page 7325

25. Bowser, M. T.; Bebault, G. M.; Peng, X.; Chen, D. D. Y. *Electrophoresis* 1997, *18*, 2928-2934

26. Rae, W. E.; Wong, J. E.; Lucy, C. A. *J. Chromatogr., A* 1997, *781*, 3-10

27. Quintás, G.; Nuñez, E.; Vellekoop, M.; Lendl, B. *Anal. Bioanal. Chem.* 2007, *387*, 287-292

CHAPTER 3

Velocity-Difference Induced Focusing (V-DIF) of Serotonin in Capillary Electrophoresis with a Dynamic pH Junction

3.1 Introduction

Serotonin is a monoamine neurotransmitter involved in a variety of physiological processes including central nervous system neurotransmission and blood pressure regulation. [1] It is also associated with hypertension, [2] Alzheimer's [3] and Parkinson's disease. [4] The structure of serotonin is shown in Figure 3.1. [5] The pK_1 (α-$^+NH_3$) and pK_2 (α-OH) of serotonin are 9.98 and 11.26, respectively. [6] The pI is 10.62.

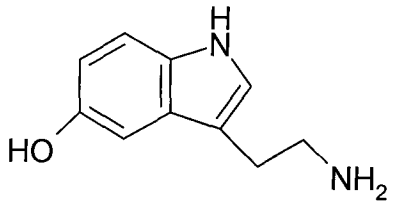

Figure 3.1. Serotonin structure.

Serotonin in plasma, platelets, and whole blood is often measured for diagnosis of disease and in psychiatric disorders research. [7-13] The technique employed for the analysis of serotonin is usually high-performance liquid chromatography (HPLC) with electrochemical [7, 14] or fluorimetric [10, 11, 15] detection. However, the cost is high for routine analysis with HPLC due to the high volume consumption of solvents and expensive columns. Although electrochemical detection is very sensitive, problems of maintenance, limited life time of the electrode and variability of sensitivity [16] require frequent repacking / repolishing of the electrodes. [17] Fluorimetric detection also has high sensitivity, but is not wide-spread. CE is a high-speed and high-efficiency analytical technique that has the advantage of minimal consumption of buffer and other materials. UV detection has proven to be the most universal and easiest to use. If CE with UV detection could be used to measure serotonin in plasma, it would bring greater simplicity and convenience to clinical diagnosis and related research. However, because the

concentration of serotonin in human plasma is at 10^{-6} M level, [13, 18] the commonly used CE methods with UV detection are not sufficiently sensitive. The sensitivity in these methods needs to be improved.

Several on-line focusing methods have been developed for CE to improve the concentration sensitivity. Sample stacking is one of the most common approaches to concentrate the analyte, through dissolving the sample in a diluted buffer that leads to amplification of the field strength in the sample zone. [19] This technique often requires desalting for biological and environmental samples. In large–volume sample stacking, more than a 100-fold increase in sensitivity can be achieved. [20] Another strategy, on-line transient isotachophoresis-capillary electrophoresis (ITP-CE), has been used to focus large-volume diluted samples [21] by adding high concentrations of leading and terminating co-ions to the sample and BGE, respectively. Quirino and Terabe [22] introduced sample sweeping to stack neutral analytes in micellar electrokinetic chromatography (MEKC). Palmer *et al.* [23] developed a technique for stacking with a high salt matrix by combining sample sweeping and micelle stacking.

Pesek *et al.* used CE with sample stacking in a coated capillary to analyze serotonin [24] and Musijowski *et al.* applied MEKC with sample stacking for the serotonin analysis [25]. The similar LODs were achieved with the two methods using UV detection, and both of them were at submicromolar levels. However, for serotonin analysis in plasma samples, desalting the samples is necessary in order to obtain sample stacking in the two methods.

Velocity-difference induced focusing (V-DIF) using a dynamic pH junction, discussed in chapter 2, has been applied to catecholamines and weakly acidic compounds. [26, 27] Higher concentration sensitivities were achieved. It is possible to apply this technique to improve the limit of detection for serotonin. Smadja [28] *et al.* used the dynamic pH junction focusing in CE for the determination of serotonin with LIF detection after derivatizating the serotonin. However, derivatization makes the sample preparation complicated and the derivatization reagent interferes with analysis. This investigation was conducted in an attempt to detect serotonin using V-DIF in CE-UV to see if the concentration sensitivity of this technique is sufficient to measure serotonin in human plasma. The pH difference between the BGE and the sample that influences the focusing of serotonin in a V-DIF CE system is also studied.

The LOD is 7.0×10^{-8} M with the focusing technique, which is much lower than the normal serotonin concentration in human plasma. This method has the potential to simplify the analysis of serotonin in human plasma because CE-UV is easy to operate and maintain. In actual practice, plasma samples could be extracted by solid phase extraction (SPE).[13] After the evaporation of the extraction solvent, the extracted residue can be reconstituted with a sample matrix which has different pH from that of BGE to perform V-DIF. A specific method using this technique for the analysis of serotonin in human plasma should be developed and validated in the future.

3.2 Experimental Section

3.2.1 Chemicals.

An aqueous BGE was prepared with 160 mM borate (Sodium tetraborate, 99.5-105.0%, Sigma Chemical Co., St. Louis, MO) and 1 mM ethylenediaminetetraacetic acid (EDTA, ACS reagent, BDH Chemicals, Toronto, Ont., Canada), or 50 mM H_3PO_4 (85% H_3PO_4, ACS reagent, BDH Chemicals, Toronto, ON, Canada), 50 mM NaH_2PO_4 (Certified, Fisher Scientific, Fair Lawn, NJ), and 50 mM Na_2HPO4 (Certified, Fisher Scientific, Fair Lawn, NJ). The pH of the borate BGE was adjusted with either 1.0 M NaOH (Certified, BDH Chemicals, Toronto, ON, Canada) or 1.0 M HCl (Certified, Fisher Scientific, Nepean, ON, Canada), and the pH of the phosphate BGE was adjusted by adding 50 mM H_3PO_4 to 50 mM NaH_2PO_4 or 50 mM Na_2HPO4. The sample was prepared with the phosphate BGE. Serotonin creatinine sulphate complex was purchased from Sigma.

3.2.2 Apparatus and Procedure

The apparatus and procedure are described in Chapter 2. The stock solution of serotonin was prepared by dissolving 1.00 mg serotonin in 1.0 mL deionized water, and the standard solutions were made by dilutions of the stock solution with appropriate sample matrix.

3.3 Results and Discussion

3.3.1 Serotonin Focusing.

The effect of pH differences between the BGE and the sample on serotonin focusing was first examined. A series of electropherograms in which the sample pH is 2.5 while the

BGE pH ranges from 5.5 to 8.8, corresponding to pH differences from 3.0 to 6.3, are shown in Figure 3.2.

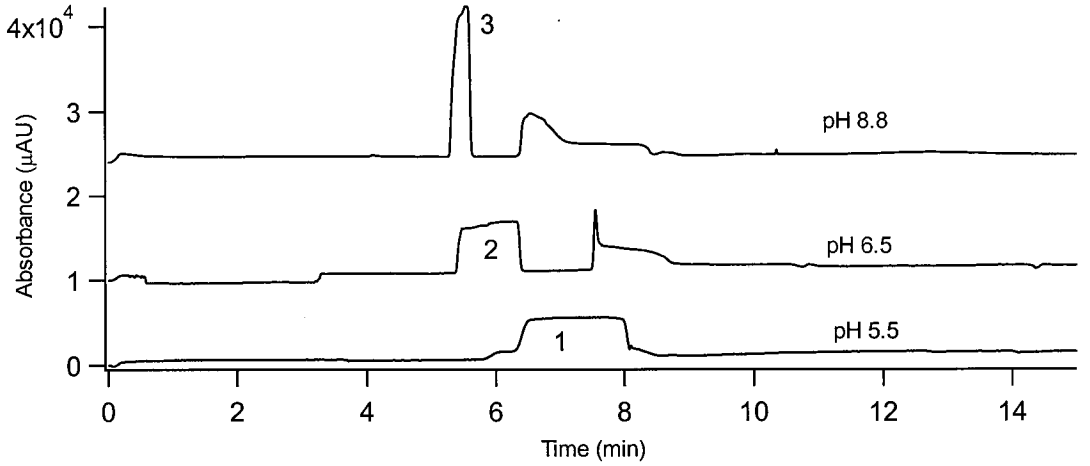

Figure 3.2 Electropherograms showing the use of a dynamic pH junction on serotonin focusing. The BGE and sample matrix were prepared with 50 mM NaH_2PO_4 or 50 mM Na_2HPO_4 and their pH was adjusted with 50 mM H_3PO_4, The pH of the sample was 2.5 and the pH of the BGE was 5.5, 6.5, and 8.8 for runs 1-3, respectively. The concentration of serotonin was 2.6 x 10^{-5} M; injection time, 99 seconds (500 nL); detection wavelength, 220 nm; voltage, 15 kV.

When the pH of the BGE was 5.5, the pH difference between the sample and the BGE was 3.0 pH units. This should be sufficient for V-DIF as demonstrated in previous work where focusing was achieved for epinephrine with only 1.9 pH units difference. [26] However, serotonin migrated as a broad plug. Then the BGE pH was increased to 6.5 and 8.8. The corresponding pH differences were 4.0 and 6.3 pH units, respectively. No sharp peaks were found. This result showed that focusing cannot be achieved only with large pH differences. However, as the pH of the BGE increased the serotonin band narrowed. The explanation is discussed in section 3.3.2. The slightly longer retention time in trace 1 is due to the lower EOF at lower BGE pH.

In light of the results in Figure 3.2, we decided to use a higher pH BGE to increase the focusing. Because the pH of the phosphate buffer cannot exceed 10.0, borate was used. The buffer solution was made with 160 mM borate and 1 mM EDTA. In order to examine if a mixed buffer system for sample and BGE also works for focusing with a dynamic pH junction, we used the phosphate buffer to prepare the sample. In our previous work, [26] we mainly used single buffer systems for focusing with a dynamic pH junction. Here we attempt to investigate whether the buffer system is also important for this focusing technique. The BGE pH was adjusted to 10.5. The sample was prepared with 50 mM H_3PO_4 and 50 mM NaH_2PO_4 at pH 2.5. Figure 3.3 shows the resulting electropherogram.

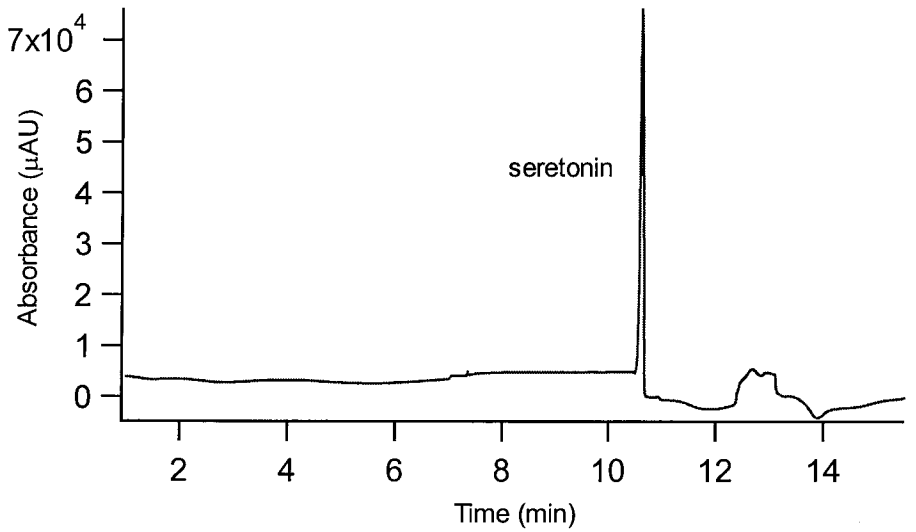

Figure 3.3 Electropherogram showing the use of a dynamic pH junction to focus serotonin. The buffer solution contained 160 mM borate and 1 mM EDTA with a pH of 10.5. The sample matrix was prepared with 50 mM H_3PO_4 and 50 mM NaH_2PO_4, at pH 2.5. The concentration of serotonin was 2.6 x 10^{-5} M; injection time, 120 seconds (600 nL); detection wavelength, 220 nm; voltage, 15 kV.

Serotonin focused into a sharp peak with these conditions. The separation efficiency is 1.4 x 10^5 theoretical plates. The degree of focusing can be evaluated by the detector-to-

injection bandwidth ratio (DIBR). [26] The injection bandwidth can be calculated by the injection time and the injection speed under the pressure of 0.5 psi. The injection speed measurement is as described in chapter 2. The detector bandwidth (the bandwidth of analyte migrating through the detector window) can be calculated by the peak width and the speed of the analyte crossing the detection window. [26] The DIBR is around 0.068. Therefore the initial injection zone is narrowed approximately 15-fold.

The mixed buffer system for sample and BGE also worked for focusing with a dynamic pH junction. The ionic strength of the BGE was around 1.5 times the sample matrix in this case. The field amplified focusing effect was limited with such large injection volumes. The important factor here was that the BGE pH was increased to 10.5, which was higher than the pK_1 of serotonin (9.98). The mechanism for this is discussed in detail in section 3.3.2.

When the pH of the BGE remained at 10.5, and the pH of the sample was increased to 7.0, Focusing was also achieved as shown in Figure 3.4. The separation efficiency is 4 x 10^4 theoretical plates. The DIBR is around 0.10. Thus the initial injection zone is narrowed approximately 10-fold.

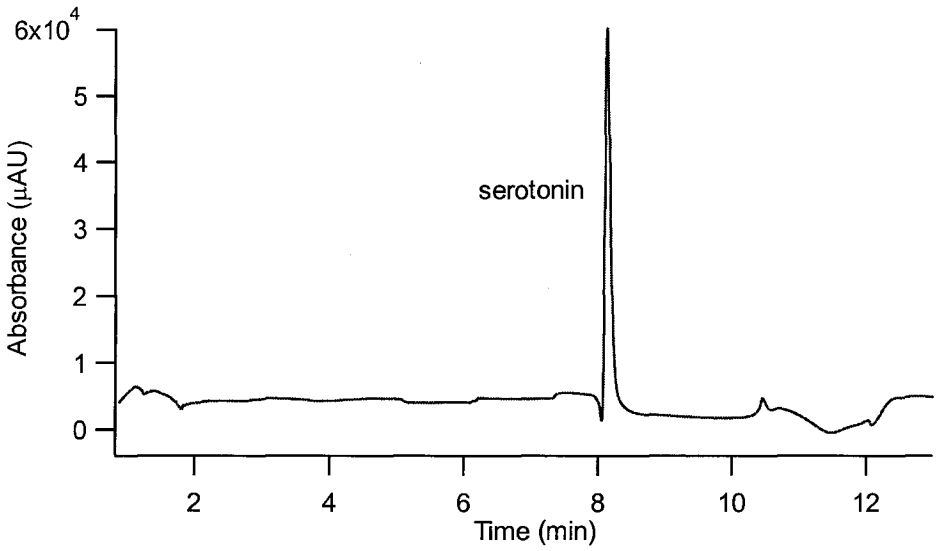

Figure 3.4 Electropherogram showing serotonin focusing with the sample pH at 7.0. The BGE contained 160 mM borate and 1 mM EDTA with a pH of 10.5, the sample matrix was prepared with 50 mM Na_2HPO4 and 50 mM H_3PO_4, at pH 7.0. Other conditions were the same as those in Figure 3.3.

This is because the pH of the sample solution still remains under the pK_1 while the pH of the BGE is higher than the pK_1 of serotonin. The above results confirm the finding in chapter 2 that it is crucial to maintain the pH of the BGE and the sample at different levels, one above the pK_a of the analyte and the other under the pK_a of the analyte, to obtain focusing.

The peak shape in Figure 3.3 is sharper than that in Figure 3.4. Given that the pH values of sample and BGE encompass the pK_a of the analyte, a larger pH difference results in a sharper peak. This may be because the pH of the lower pH area (where the serotonin is positively charged) remains low for a longer period, resulting in better focusing and sharper peaks.

3.3.2 Proposed Mechanism

Figure 3.5 depicts the mechanism of this focusing.

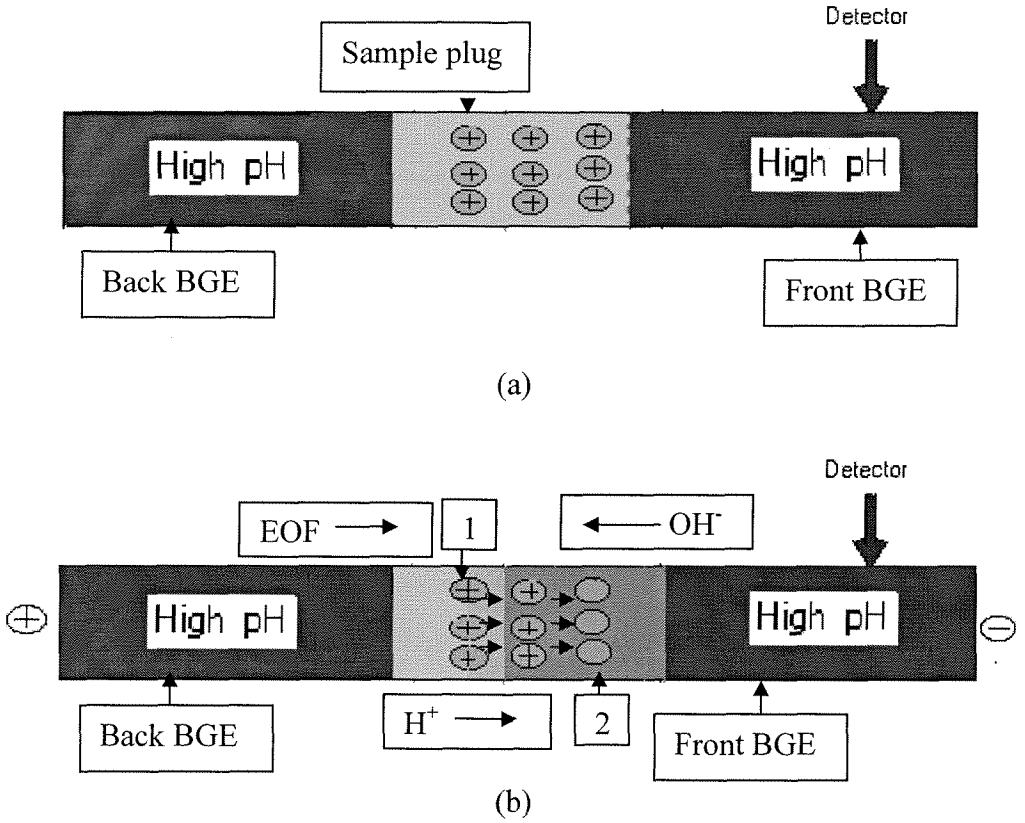

Figure 3.5 Proposed mechanism of focusing using a dynamic pH junction. (a) A large sample plug with a lower pH electrolyte is injected into a capillary filled with a higher pH BGE. (b) pH gradient formed due to the movement of protons and hydroxide ions between the front BGE and the sample zone under the electric field, different color bands represent the pH gradient from the sample zone to the adjacent part of the front BGE. 1- serotonin is positively charged. 2- serotonin is neutral.

When the pH of the BGE was higher than that of the sample, upon application of a potential, a pH gradient from the sample plug to the front BGE formed due to the movement of protons and hydroxide ions. Serotonin was distributed in the different parts of the gradient. When the pH of the BGE was much lower than 9.98 (the pK_1 of serotonin), most of the serotonin was positively charged within the gradient. There was practically no charge state change of serotonin in the gradient and very little focusing was

obtained, as seen in Fig. 3.2. When the pH of the BGE was increased, more and more positive ions in the higher pH area were deprotonated. The positive ions in the lower pH area moved towards the cathode until they reached an area of higher pH, where deprotonation of the ions occurred. This neutralized their positive charge, resulting in significantly lower velocity and leading to focusing. When the BGE pH was increased to a value higher than the pK_1 of serotonin, most of the positive ions were neutralized in the higher pH area, leading to sharp peak focusing.

3.3.3 Limit of detection (LOD) of serotonin using V-DIF

Although the peak was sharper and peak height was higher in Figure 3.3 than in Figure 3.4, the baseline was more stable in the latter case. The baseline fluctuation was caused by the different compositions between the sample matrix and the BGE. The conditions in Figure 3.4 were used to determine the LOD. A series of standard solutions were analyzed and the concentrations of the standards were 2.6×10^{-5} M, 1.3×10^{-5} M, 6.5×10^{-6} M and 3.2×10^{-6} M, respectively. The data were plotted by software Igor (Wavemetrics, Lake Oswego, OR, USA). The reproducibility of this focusing technique was tested by triplicate injections of 2.6×10^{-5} M serotonin solution. The RSD values are 2.0% and 4.5% for retention time and peak height, respectively.

The calibration curve is shown in Figure 3.6. The curve is linear and the correlation coefficient is 0.99.

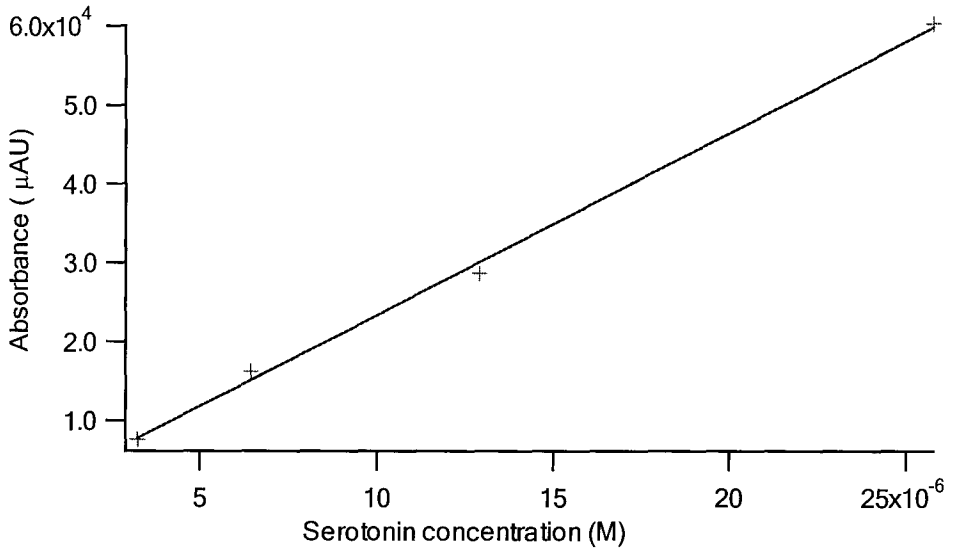

Figure 3.6 Peak height obtained for serotonin versus the concentration of serotonin. Conditions are the same as in Figure 3.4.

The LOD of serotonin is determined from

$$LOD = 3\sigma / k \quad (1)$$

Where σ is the standard deviation of the background UV absorption and k is the slope of the calibration curve. The LOD was calculated to be 7.0×10^{-8} M, which is lower than the normal serotonin concentration in human plasma. The LOD is around one order of magnitude lower than the two methods of CE with sample stacking using UV detection for serotonin analysis [24, 25]. However, this LOD is higher than those with LIF detection [28, 29, 30], which are at nmol/mL levels or lower.

3.4 Conclusions

Velocity-difference induced focusing (V-DIF) of serotonin was obtained by using a dynamic pH junction in CE. Mixed buffer systems also worked for focusing. Analyte focusing was caused by the difference in analyte velocities in the different segments of

electrolytes with different pH, and the pH gradient formed between the sample and the BGE. It is most important to maintain the BGE and the sample at different pH values, one above the pK_a of the analyte and the other under the pK_a of the analyte, to obtain good focusing. In comparing serotonin and phenolphthalein, it seems that the major requirement for normal V-DIF is that the analyte's electrophoretic mobility must decrease significantly at the front or back sample/BGE interface to achieve focusing; i.e., the analyte charge must go from positive to zero (case of serotonin) or from negative to zero (case of phenolphthelain).

The LOD for serotonin with this focusing technique using CE-UV is 7.0×10^{-8} M. This technique has the potential to make CE-UV a convenient alternative for plasma serotonin measurement. A practical method based on this V-DIF technique using CE-UV for plasma serotonin analysis should be further developed and validated.

3.5 References

1. Pazos, A.; Palacios, J. M. *Brain Res.* 1985, *346*, 205-249
2. Kamal, L. A.; Le Quan-Bui, K. H.; Meyer, P. *Hypertension* 1984, *6*, 568-573
3. Middlemiss, D. N.; Palmer, A. M.; Edel, N.; Bowen, D. M. *J. Neurochem.* 1986, *46*, 993-996
4. Scatton, B.; Javoy-Agid, F.; Rouquier, L.; Dubois, B.; Agid, Y. *Brain Res.* 1983, *275*, 321-328
5. Merck Index, 13th edition, Merck & Company, Whitehouse Station, NJ, 2001, Page 1518
6. Weber, O. A.; Simeon, V. I. *J. Inorg. Nucl. Chem.* 1971, *33*, 2097-2101
7. Pussard, E.; Guigueno, N.; Adam, O.; Giudicelli, J. F. *Clin. Chem.* 1996, *42*, 1086-1091
8. Maurer-Spurej, E.; Dyker, K.; Gahl, W. A.; Devine, D. V. *British Journal of Haematology* 2002, *116*, 604-611
9. Harenberg, J.; Huhle, G.; Giese, C.; Wang, L. C.; Hoffmann, U.; Song, X. H. *British Journal of Haematology* 2000, *109*, 182-186
10. Xiao, R.; Beck, O.; Hjemdahl, P. *Scand. J. Clin. Lab Invest.* 1998, *58*, 505-510
11. Aymard, N.; Honore, P.; Carbuccia, I. *Prog. Neuropsychopharmacol Biol. Psychiatry* 1994, *18*, 77-86
12. Kremer, H. P.; Goekoop, J. G.; Van Kempen, G. M. *J. Clin. Psychopharmacol.* 1990, *10*, 83-87
13. Peterson, Z. D.; Lee, M. L.; Graves, S. W. *J. Chromatogr., B* 2004, *810*, 101-110
14. Korpi, E. R. *Clin. Chem.* 1984, *30*, 487-488

15. Humble, M.; Bejerot, S.; Bergqvist, P. B. F.; Bengtsson, F. *Biol. Psychiatry* 2001, *49*, 360-368

16. Nagao, T.; Tanimura, T. *J. Chromatogr.* 1989, *496*, 39-53

17. Anton, A. H. *Life Sci.* 1984, *35*, 79-85

18. Kema, I. P.; Meijer, W. G.; Meiborg, G.; Ooms, B.; Willemse, P. H. B.; Vrise, E. G. E. *Clin. Chem.* 2001, *47*, 1811-1820

19. Chien, R.; Burgi, D. S. *Anal. Chem.* 1992, *64*, 1046-1050

20. Wolf, S. M.; Vouros, P. *Anal. Chem.* 1995, *67*, 891-900

21. Krivankova, L.; Bocek, P. *J. Chromatogr., B* 1997, *689*, 13-34

22. Quirino, J. P.; Terabe, S. *Anal. Chem.* 1999, *71*, 1638-1644

23. Palmer, J.; Landers, J. P. *Anal. Chem.* 2000, *72*, 1941-1943

24. Pesek, J. J.; Matyska, M. T. *J. Liq. Chromatogr. Relat. Technol.* 1998, *21*, 2923-2934

25. Musijowski, J.; Pobozy, E.; Trojanowicz, M. *J. Chromatogr., A* 2006, *1104*, 337-345

26. Britz-McKibbin, P.; Bebault, G. M.; Chen, D. D. Y. *Anal. Chem.* 2000, *72*, 1242-1252

27. Britz-McKibbin, P.; Chen, D. D. Y. *Anal. Chem.* 2000, *72*, 1729-1735

28. Smadja, C.; Potier, I. L.; Chaminade, P.; Jacquot, C.; Trouvin, J. H.; Taverna, M.; *Chromatographia* 2003, *58*, 79-85

29. Zhang, X.; Sweedler, J. V.; *Anal. Chem.* 2001, *73*, 5620-5624

30. Benturquia, N.; Couderc, F.; Sauvinet, V.; Orset, C.; Parrot, S.; Bayle, C.; Renaud, B.; Denoroy, L. *Electrophoresis* 2005, *26*, 1071-1079

CHAPTER 4

Velocity-Difference Induced Focusing (V-DIF) in Capillary Electrophoresis (CE) with a Dynamic pH Junction for Amino Acids, Peptides, and Proteins

4.1 Introduction

CE has become a very useful method for analyzing biological samples, [1, 2, 3] especially when only limited samples are available. The main advantages of CE are high separation efficiencies, minimum sample and buffer consumption, and low operation costs. A major weakness of CE is that it has lower concentration sensitivity than HPLC. Bubble cells [4, 5] and Z-cells [6, 7] have been used to improve the concentration sensitivity, but the sensitivity improvement with these techniques is much smaller than expected and they may reduce separation efficiency. [8] Improving the concentration sensitivity is critical to allow CE to be widely used in practical applications.

Higher concentration sensitivities and higher separation efficiencies were obtained using UV detection with the focusing technique that used a dynamic pH junction. [9, 10] This technique has previously been applied to catecholamines and weakly acidic compounds. It is possible to apply this V-DIF technique to amino acids, peptides, proteins, and other biological samples. Several papers have been published for focusing these biological samples by pH junctions in CE. [11, 12, 13, 14] This investigation aims to examine our findings that pKa is the most important criterion for the pH selection of the sample and BGE to achieve optimum focusing. The pI and pKa of an amino acid were both used as the criteria for the pH selection of the sample and the BGE in an attempt to identify the key factor for focusing. The criterion of pH selection for focusing was also examined by focusing a peptide (Phe-Leu-Glu-Glu-Leu) and a protein (bovine serum albumin).

4.2 Experimental Section

4.2.1 Chemicals.

The aqueous BGE consisted of 160 mM borate (Sodium tetraborate, 99.5-105.0%, Sigma Chemical Co., St. Louis, MO) and 1 mM ethylenediaminetetraacetic acid (EDTA, ACS reagent, BDH Chemicals, Toronto, Ont., Canada). Another BGE solution was prepared with 50 mM H_3PO_4 (85% H_3PO_4, ACS reagent, BDH Chemicals, Toronto, ON, Canada), 50 mM NaH_2PO_4 (Certified, Fisher Scientific, Fair Lawn, NJ), and 50 mM Na_2HPO4 (Certified, Fisher Scientific, Fair Lawn, NJ). The pH of the borate BGE was adjusted with either 1.0 M NaOH (Certified, BDH Chemicals, Toronto, ON, Canada) or 1.0 M HCl (Certified, Fisher Scientific, Nepean, ON, Canada), and the pH of the phosphate BGE was adjusted by adding 50 mM H_3PO_4 to 50 mM NaH_2PO_4 or 50 mM Na_2HPO_4. Tryptophan (ACS reagent), phenylalanine (ACS reagent), Phe-Leu-Glu-Glu-Leu (≥97%), and bovine serum albumin (BSA) (≥96%) were all purchased from Sigma. Water was purified using a Milli-Q Elix system (Millipore, Milford, MA, USA).

4.2.2 Apparatus and Procedure

Separations were performed on a P/ACE^{TM} MDQ automated CE system (Beckman-Coulter Inc., Mississauga, Ont., Canada). An uncoated capillary (Polymicro Technologies, Phoenix, AZ) with an inner diameter of 75 μm and a length of 60 cm was used.

The new capillary was first rinsed with 1.0 M NaOH (20 psi for 10 min) and then with BGE (20 psi for 10 min), and finally a voltage of 15 kV was applied for 10 min. For amino acids and peptides, each separation was preceded by a 1.5-min, 20 psi rinse with 1

M NaOH, followed by a 4-min rinse with BGE. For BSA, the separation was preceded by a 2-min, 20 psi rinse with 25 mM SDS, followed by a 2-min rinse with 1 M NaOH, and then a 2-min rinse with deionized water and a 2-min rinse with BGE. The samples were then injected by a pressure of 0.5 psi, and the separation was performed with normal polarity at 15 kV and room temperature or a temperature of 4 ^{0}C (for BSA).

Absorption detection was performed with a Beckman MDQ PDA detector with a wavelength range of 190-600 nm.

The stock solutions of amino acids were prepared by dissolving 1.00 mg of amino acids in 3.0 mL deionized water, and the stock solutions were further diluted 100 times with the appropriate sample matrix. The final concentrations of phenylalanine and tryptophan were 2.0 x 10^{-5} M and 1.6 x 10^{-5} M, respectively. The Phe-Leu-Glu-Glu-Leu stock solution was prepared by dissolving 1.00 mg Phe-Leu-Glu-Glu-Leu in 1.0 mL deionized water and the stock solution was further diluted 100 times with appropriate sample matrix, to a concentration of 1.5 x 10^{-5} M. The BSA stock solution was prepared by dissolving 10.00 mg BSA in 1.0 mL deionized water and the stock solution was further diluted 100 times with appropriate sample matrix to give a final concentration 1.5 x 10^{-6} M.

4.3 Results and Discussion

4.3.1 Amino acid focusing.

In the previous research discussed in chapters 2 and 3, we found the basis of the focusing technique was the charge state changes of the analytes. In practice, we used the pK_a of the analyte as a criterion for designing the conditions for focusing. Amino acids and their polymers are zwitterionic. Their charge states are determined by their pI and the pH of the solution. Both the pI and pK_a of an amino acid were used as the criteria for selecting the pH of the sample and the BGE for V-DIF. Based on the results; we attempt to understand the mechanism of this focusing technique in more detail.

4.3.1.1 Isoelectric point (pI) for focusing.

The pI is a very important characteristic of amino acids. The net electric charge of an amino acid can be judged by comparing the pI of the amino acid and the pH of the solution where the amino acid resides. When the pH of the solution equals the pI, the amino acid will be present in its zwitterionic form, fully ionized but without net charge. When the pH of the solution is higher than the pI, the amino acid will have a net negative charge. The amino acid will have a net positive charge when the pH of the solution is below its pI. In our previous research, it was found that the charge state change was very important for V-DIF. Therefore the pI, which contains important information about the charge of the amino acids, was examined first. The pI of tryptophan is 5.8 and of phenylalanine 5.7. [15] The BGE and the sample solutions were prepared with 50 mM H_3PO_4, 50 mM NaH_2PO_4, and 50 mM Na_2HPO_4. The pH was adjusted to 7.5 for BGE

(above pI of 5.8 and 5.7) and 3.5 for the samples (below pI of 5.8 and 5.7). The electropherograms for phenylalanine and tryptophan are shown in Figure 4.1.

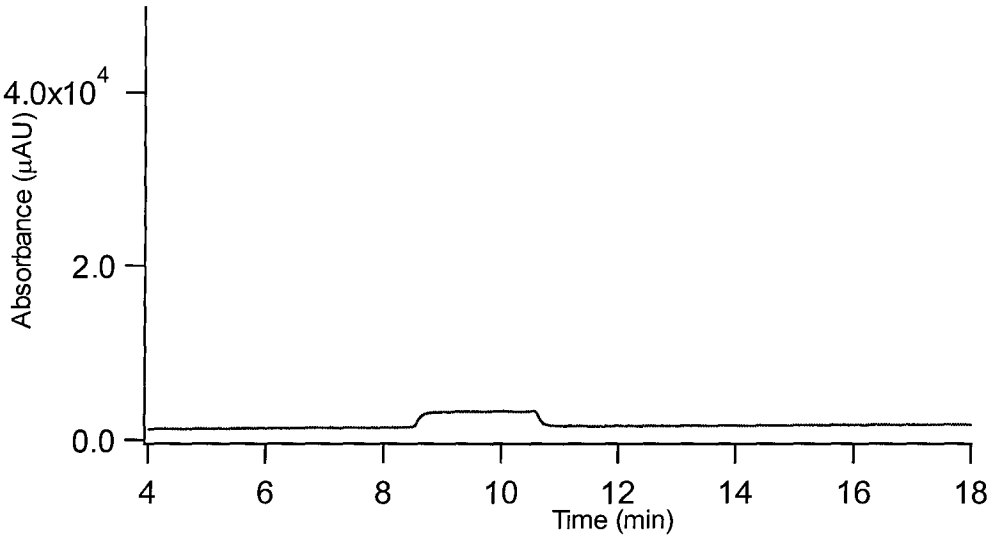

(a)

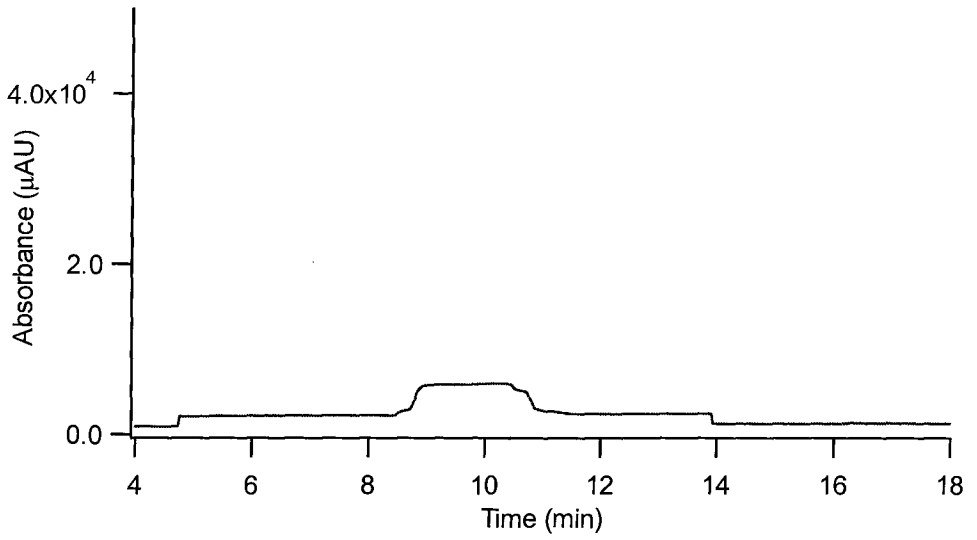

(b)

Figure 4.1 Electropherograms of phenylalanine (a) and tryptophan (b) where the pH of the sample was 3.5 and the pH of the BGE was 7.5. The BGE and sample matrix were prepared with 50 mM NaH_2PO_4 or 50 mM Na_2HPO4 and their pH were adjusted with 50 mM H_3PO_4. The concentrations of phenylalanine and tryptophan were 2 x 10^{-5} M and 1.6 x 10^{-5} M, respectively; injection time, 99 seconds (500 nL); detection wavelengths, 214 nm for phenylalanine and 225 nm for tryptophan; voltage, 15 kV.

The phenylalanine and tryptophan did not focus into sharp peaks with these conditions. The explanation is discussed in section 4.3.2.

4.3.1.2 pK_a for focusing.

The pK_a is another important characteristic of amino acids. It is a convenient notation for the equilibrium constant for deprotonation. There are two pK_a values (α-COOH and α-$^+NH_3$) for tryptophan and phenylalanine. The pK_2 (α-$^+NH_3$) is 9.3 [15] for both tryptophan and phenylalanine. Borate was used as the BGE. The pH was adjusted to 11.0 for the BGE (above pK_2 of 9.3) and 7.5 for the samples (below pK_2 of 9.3). The electropherograms for phenylalanine and tryptophan are shown in Figure 4.2.

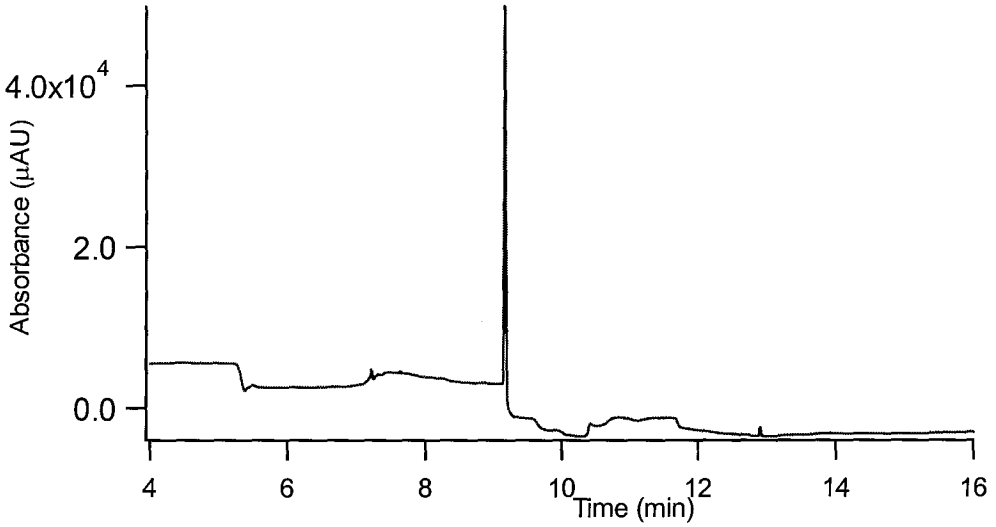

(a)

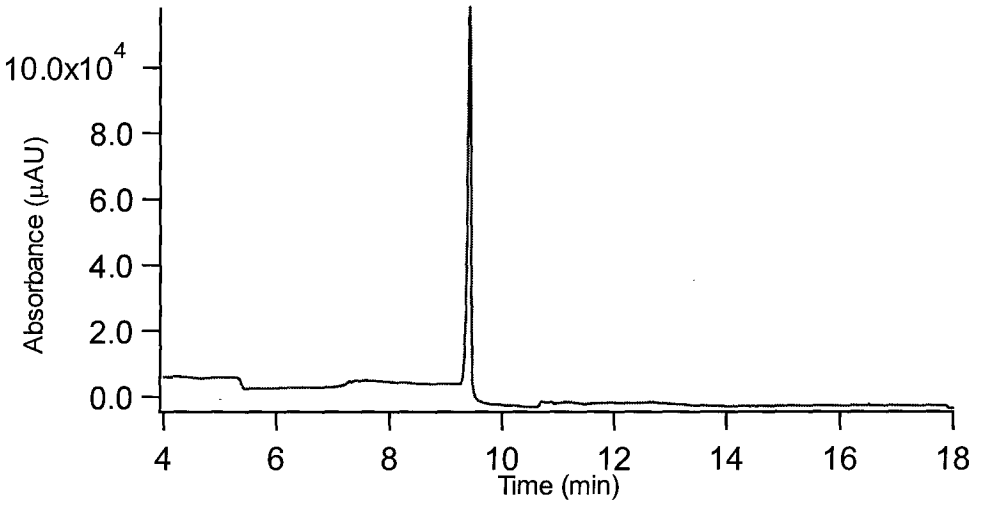

(b)

Figure 4.2 Electropherograms of phenylalanine (a) and tryptophan (b) where the pH of the sample was 7.5 and the pH of the BGE was 11.0. The BGE and sample matrix were prepared with 160 mM borate and 1 mM EDTA. Other conditions were the same as those in Figure 4.1.

Phenylalanine and tryptophan both focused into sharp peaks. The separation efficiencies for phenylalanine and tryptophan are 5.5 x 10^5 and 1.1 x 10^5 theoretical plates, respectively. The detector-to-injection bandwidth ratio (DIBR) for phenylalanine is about 0.046, thus the initial injection zone is narrowed around 21-fold. The DIBR for

tryptophan is about 0.10, and the initial injection zone is narrowed approximately 10-fold. The pK_a is found to be important for choosing the pH of the BGE and the sample to focus the amino acids with a dynamic pH junction.

4.3.2 Focusing Mechanism.

The ratio of different species of amino acids in the various pH solutions can be estimated by using the Henderson-Hasselbalch equation

$$pH = pK_a + \log([A^-] / [HA]) \qquad (4.1)$$

For phenylalanine, the different charged species at various pH values are:

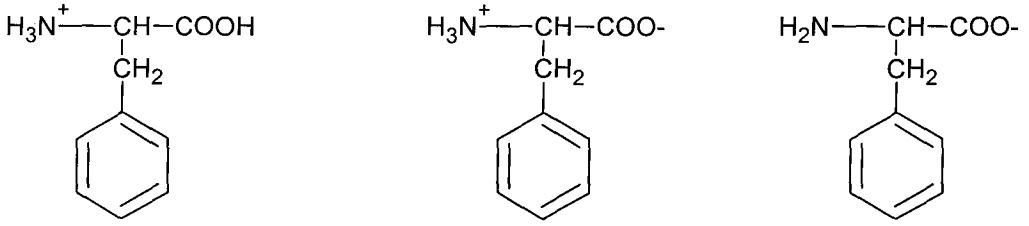

A B C

Figure 4.3 Differently charged species of phenylalanine at various pH values. A: net charge +1. B: net charge 0. C: net charge –1.

The pK_1 (α-COOH) and pK_2 (α-$^+NH_3$) are 2.2 and 9.3 respectively for phenylalanine. [15] At pH 3.5, the major species are A and B. From the Henderson-Hasselbalch equation, A is about 4.8% and B is about 95.2% of the phenylalanine. At pH 7.5, B and C are approximately 98.5% and 1.5% of the phenylalanine, respectively. At pH 11.0, B is about 2.0% and C is about 98.0% of total phenylalanine.

With the pH of the BGE higher than that of the sample, when the voltage was applied, the junction between the sample zone and the front BGE dissipated and a pH gradient formed due to the movement of protons and hydroxide ions under the electric field.

When the pH of the BGE was 7.5, approximately 98% of the phenylalanine molecules existed in the neutral form B. The neutral species did not move separately, but moved with the sample plug. For this reason, there was no focusing in such a situation. When the pH of the BGE was increased to 11.0, approximately 98% of phenylalanine molecules were in form C (the negatively charged form). The negative ions moved towards the anode until they reached a lower pH region, where they were protonated. This neutralized their negative charges, leading to a significantly lower velocity, thus forming the sharp peak.

A similar mechanism led to the focusing of tryptophan. The mechanism discussed in chapter 2 applies.

4.3.3 Peptide (Phe-Leu-Glu-Glu-Leu) Focusing.

Phe-Leu-Glu-Glu-Leu contains ionizable groups on its side chains, which causes the peptide to have different charge states in solutions of different pH. The pK_a of amino acid R-groups (side chain) in peptides can be different from those in free amino acids; they are dependent on neighboring amino acids as well as on the tertiary structure in larger peptides. [16, 17] Hilser *et al.* [16] confirmed that the modified values used by Richard [17] were a better match than the values of the individual amino acids. The modified pK_a for

the R-group of Glu in the peptide is 4.5. The buffer and the sample solutions were then prepared with 50 mM H_3PO_4, 50 mM NaH_2PO_4, and 50 mM Na_2HPO4. The pH was 6.7 for the BGE and 3.0 for the sample. In order to evaluate the focusing effect, the sample was also prepared at the same pH as the BGE. The electropherograms for Phe-Leu-Glu-Glu-Leu are shown in Figure 4.4.

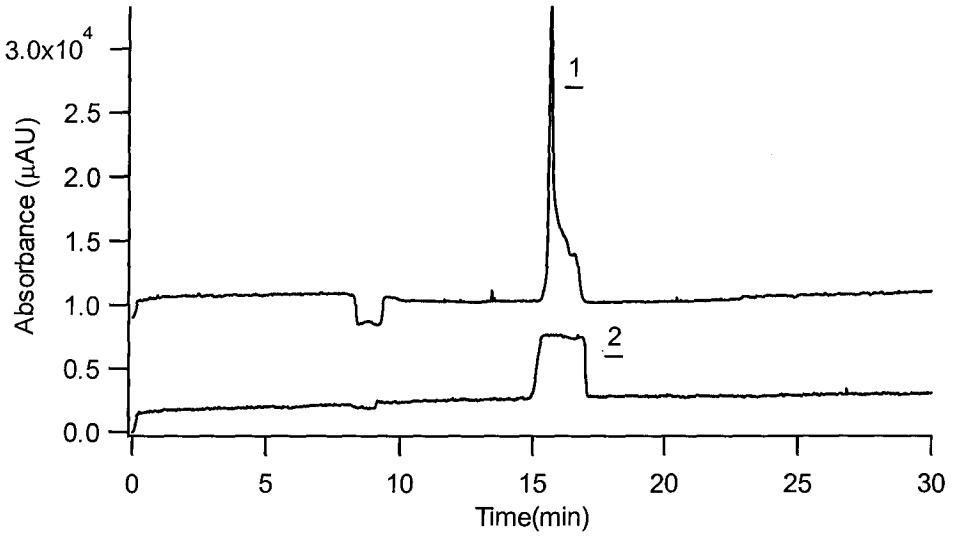

Figure 4.4 Electropherograms showing the use of a dynamic pH junction on Phe-Leu-Glu-Glu-Leu focusing. The BGE and the sample matrix were prepared with 50 mM NaH_2PO_4 or 50 mM Na_2HPO4 and their pH were adjusted with 50 mM H_3PO_4. 1. BGE pH=6.7, sample pH=3.0. 2. BGE pH=6.7, sample pH=6.7. The concentration of Phe-Leu-Glu-Glu-Leu was 1.5 x 10^{-5} M; injection time, 60 seconds (300 nL); detection wavelength, 214 nm; voltage, 15 kV.

Phe-Leu-Glu-Glu-Leu also focused into a sharp peak with a dynamic pH junction, but the peak shape was not as narrow as those of the amino acids. This may be due to the interaction between the peptide and the capillary inner wall. However, when the BGE and sample were prepared with the same pH, the peptide migrated as a broad band and the signal was much lower. Here the protons in the sample zone moved towards cathode and invaded the front BGE when the voltage was applied, and a pH gradient formed from

the sample plug to the adjacent part of the front BGE. At pH 3.0, the peptide is positively charged. The positive ions moved towards the cathode until they reached an area of lower pH, where deprotonation occurred and neutralized their positive charges, resulting in lower velocity and leading to focusing. At pH 6.7, which is higher than the pK_r of the peptide, most of the peptide molecules are negatively charged (two ionizable R-groups, q = -2, where q is the electric charge). The negative ions in the higher pH area moved towards anode until they reached the area of lower pH where protonation of the species took place, resulting in lower velocity and leading to focusing.

4.3.4 Bovine Serum Albumin (BSA) Focusing.

After the amino acids and peptides were focused successfully with a dynamic pH junction using the pKa of the analytes as criteria for pH selection, the application of this V-DIF technique for BSA was examined. BSA is a protein with a molecular weight of ~66k Da. [18] The properties of a protein are much more complicated than those of an amino acid, but some of its properties are based on its primary structure. As with amino acids, proteins have different charge states in different pH solutions, and this may be useful in CE-V-DIF. However, it is very difficult to know the specific charge state of a protein at a certain pH because proteins have many pK_a which are influenced by many factors. First, we selected pH 10.5 for the BGE and pH 5.5 for the sample to examine the V-DIF for BSA because the pK_2 of most amino acids are within this range.

The BSA did not focus with these conditions; it migrated as a broad band. It is possible that BSA stuck to the capillary wall due to the electrostatic interactions between BSA and

the fused silica surface because BSA contains many charged moieties, therefore restricting its motion. The electropherogram for BSA is shown in Figure 4.5.

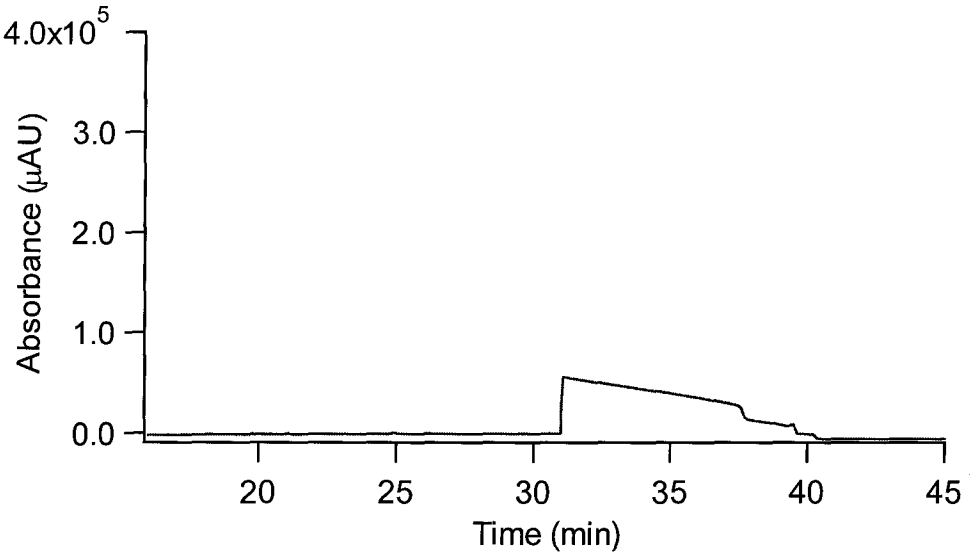

Figure 4.5 Electropherogram showing the use of a dynamic pH junction on bovine serum albumin focusing. The BGE contained 160 mM borate and 1 mM EDTA, and the sample matrix was prepared with 50 mM NaH_2PO_4 and 50 mM Na_2HPO4. The pH of the sample was 5.5 and the pH of the BGE was 10.5. The concentration of BSA was 1.5 x 10^{-6} M; injection time, 60 seconds (300 nL); detection wavelength, 280 nm; voltage, 15 kV.

A low pH focusing strategy was then selected to minimize the wall effects within the capillary. At pH values below 4, most of the silanols are not deprotonated and most proteins will not adhere to the capillary wall electrostatically. A solution of 0.1 M HCl was used as the sample matrix in order to decrease the pH to 1.0. A series of different pH BGE were tested. The best result was achieved when the BGE pH was adjusted to 3.7. The electropherogram is shown in Figure 4.6.

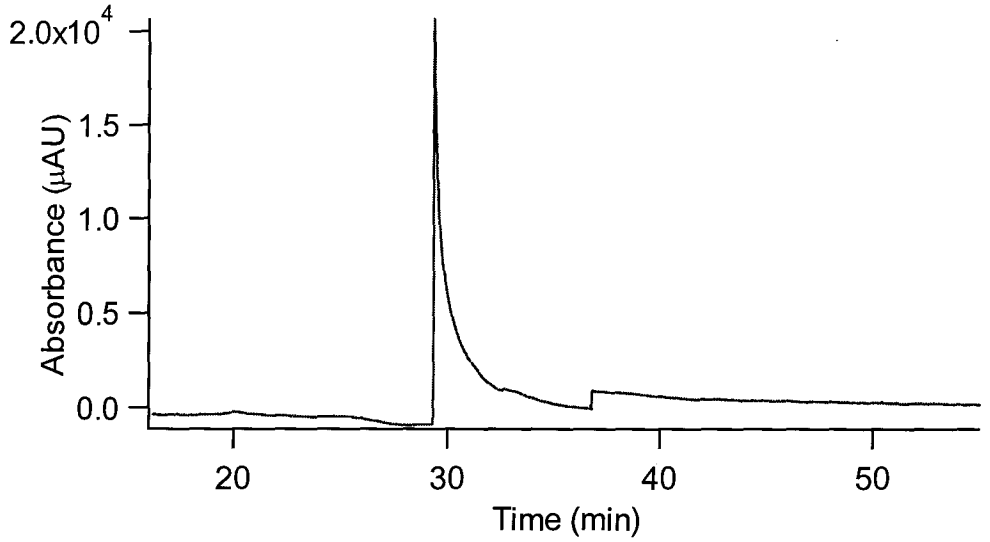

Figure 4.6 Electropherogram showing the use of a dynamic pH junction on BSA focusing with a BGE pH of 3.7. The BGE was prepared with 50 mM H_3PO_4 and 50 mM NaH_2PO_4 and the sample matrix was prepared with 0.1 M HCl. The pH of the sample was 1.0 and the pH of the BGE was 3.7. Other conditions were the same as those in Figure 4.5.

BSA focused at low pH with the dynamic pH junction. The asymmetry of the peak shape may be due to the hydrophobic adsorption of the protein on the capillary wall.

When the BGE pH was increased to 5.0, BSA stuck to the capillary wall and migrated as a broad band, and the peak shapes were also distorted and exhibited extensive tailing. The electropherogram is shown in Figure 4.7.

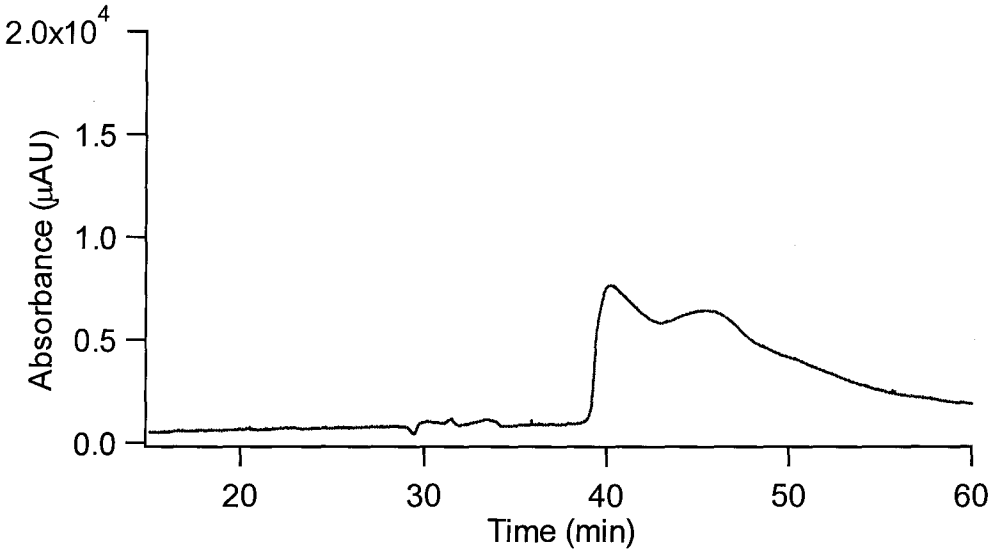

Figure 4.7 Electropherogram showing the use of a dynamic pH junction on bovine serum albumin focusing with a BGE pH of 5.0. The buffer solution was prepared with 50 mM NaH_2PO_4 and 50 mM Na_2HPO_4 and the sample matrix was prepared with 0.1 M HCl. The pH of the sample and the BGE was adjusted to 1.0 and 5.0, respectively. Other conditions were the same as those in Figure 4.5.

4.4 Conclusions

Velocity-difference induced focusing (V-DIF) of amino acids, peptides, and proteins using a dynamic pH junction was achieved in CE. Analyte focusing resulted from different mobilities associated with the different charge states of the analyte at different pH values. The pK_a values rather than the pI values, were found to be most important for selecting the pH for sample and BGE in order to focus amino acids. The focusing results for proteins were not as good as those of amino acids because they have many charged moieties that will stick to capillary wall. This study was mainly conducted with bare silica capillaries; further experiments applying V-DIF to proteins with a coated capillary, which can eliminate wall effects, should be performed to optimize the focusing conditions.

4.5 References

1. Burnner, L. J., Dipiro, J. T. *Electrophoresis* 1998, *19*, 2848-2855
2. Shihabi Z. K. *J. Chromatogr., A* 1998, *807*, 27-36
3. Guzman, N. A. *J. Chromatogr., B* 1997, *697*, 37-66
4. Hempel, G.; Lehmkuhl, D.; Krumpelmann, S.; Blaschke, G.; Boos, J. *J. Chromatogr., A* 1996, *745*, 173-179
5. Olgemoller, J.; Hempel, G.; Boos, J.; Blaschke, G. *J. Chromatogr., B* 1999, *726*, 261-268.
6. Chervet, J. P.; Van Soest, R. E. J.; Ursem, M. *J. Chromatogr.* 1991, *543, 439-449*
7. Mrestani, Y.; Neubert, R. *Electrophoresis* 1998, *19*, 3022-3025
8. Albin, M.; Grossman, P. D.; Moring, S. E. *Anal. Chem.* 1993, *65*, 489A-497A
9. Britz-McKibbin, P.; Bebault, G. M.; Chen, D. D. Y. *Anal. Chem.* 2000, *72*, 1242-1252
10. Britz-McKibbin, P.; Chen, D. D. Y. *Anal. Chem.* 2000, *72*, 1729-1735
11. Ptolemy, A. S.; Britz-McKibbin, P. *Analyst* 2005, *130*, 1263-1270
12. Wang, S. J.; Tseng, W. L.; Lin, Y. W.; Chang, H. T. *J. Chromatogr., A* 2002, *979*, 261-270
13. Monton, M. R. N.; Imami, K.; Nakanishi, M.; Kim, J.; Terabe, S. *J. Chromatogr., A* 2005, *1079*, 266-273
14. Imami, K.;Monton, M. R. N.; Ishihama, Y.; Terabe, S. *J. Chromatogr., A* 2007, *1148*, 250-255

15. Harris, D. C. *Quantitative Chemical Analysis*, W. H. Freeman and Co. New York, 6th ed., 2003

16. Hilser, V. J.; Worosila, G. D.; Rudnick, S. E. *J. Chromatogr., A* 1993, *630*, 329-336

17. Richard, E. C.; Strohl, M. M.; Nielsen, R. G. *Anal. Biochem.* 1991, *197*,197-207

18. Trigatti, B. L.; Gerber, G. E. *Biochem. J.* 1995, *308*, 155-159

CHAPTER 5

Comparison of photodiode array (PDA) and mass spectrometry (MS) detection for aromatic amino acids in capillary electrophoresis (CE) with velocity-difference induced focusing (V-DIF) using a dynamic pH junction

5.1 Introduction

Because longitudinal diffusion is minimized in CE due to the flat profile of the EOF, the separation efficiency of CE is often very high. The principal detection method in CE is UV absorption, but UV absorption does not contain sufficient information for peak identification. Furthermore, migration time variations in CE lead to greater difficulty in the identification of analytes. Photodiode array (PDA) detectors record light absorption at different wavelengths and can provide spectra of the analytes. This is useful in identifying unknowns. Mass spectrometry (MS) is a better detector for unknowns. It gives an unambiguous molecular weight of an analyte and provides structural information. When coupled with CE or HPLC, MS can separate co-eluting analytes with different mass to charge ratios. Electrospray ionization (ESI) is the first choice [1, 2, 3, 4, 5] for coupling CE to MS. The solution from the capillary in CE can be transferred to the ESI-MS via an interface. Large molecules are usually multiply-charged in ESI-MS, which allows them to be detected within the limited mass range of most mass spectrometers. [6] Because ESI is a soft ionization method, it is also suitable for the detection of fragile and thermally labile analytes. For CE-ESI-MS coupling, a sheath-flow interface is commonly used in commercial instruments, because it can be easily and reproducibly constructed.

One major disadvantage of CE is the relatively high concentration detection limit. Although MS offers high sensitivity, the eluent from the capillary is diluted at the mixing point in CE-ESI-MS with a sheath-flow interface. This lowers the signal. A variety of on-line focusing methods have been developed to improve the concentration sensitivity in

CE. Sample stacking is one of the most commonly used techniques to focus the analytes. The sample is dissolved in a dilute buffer which amplifies the field strength in the sample zone. [7, 8] Shihabi developed a stacking method by adding large amounts of acetonitrile and salt [9, 10] to the samples. Adding salts in these methods introduces another source of chemical background and suppresses the signal in ESI-MS. On-line transient isotachophoresis is another technique used to focus dilute samples, [11, 12] in which high concentrations of leading and terminating co-ions are added to the sample and the BGE, respectively. Isotachophoresis is also difficult to couple with ESI-MS due to the high levels of leading and terminating ions present in the system. However, applications with focusing such as isoelectric focusing (IEF) in CE-MS have also been published. [13] The focusing technique using a dynamic pH junction [14, 15, 16] discussed in the last several chapters is found to be simple and easy to apply to CE-ESI-MS. It makes CE a suitable technique for coupling to MS for the analysis of dilute biological samples.

In this study, we apply V-DIF with PDA or MS detection for amino acids, and optimize the detection parameters and separation conditions for the two methods with V-DIF. Three aromatic amino acids were selected because of their relatively high UV absorbance. The highly alkaline and volatile organic base diethylamine (DEA) was selected as the running buffer for focusing according to the pK_a values of the amino acids. The buffer system was the same for both CE-PDA and CE-MS. The results, such as limits of detection (LOD), are compared.

5.2 Experimental.

5.2.1 Chemicals.

The reagents used to prepare the buffer, sample, and sheath liquid were analytical grade. Diethylamine and 2-propanol were from Fisher Scientific (Fair Lawn, NJ). Ammonium acetate was from BDH Chemicals (Toronto, Ont., Canada). Tryptophan, phenylalanine, and tyrosine were purchased from Sigma. Water was purified using a Milli-Q Elix system (Millipore, Milford, MA, USA).

5.2.2 Apparatus and Procedure

5.2.2.1 CE-PDA system

Separations were performed on a P/ACE^{TM} MDQ automated CE system (Beckman-Coulter Inc., Mississauga, Ont., Canada). An uncoated capillary (Polymicro Technologies, Phoenix, AZ) with an inner diameter of 75 μm and a length of 80 cm was used. The new capillary was first rinsed with 1.0 M NaOH (20 psi for 10 min) and then rinsed with BGE (20 psi for 10 min). A voltage of 30 kV was applied for 10 min. Each separation was preceded by a 1.5-min, 20 psi rinse with 1.0 M NaOH, followed by a 4-min rinse with the BGE. The samples were then injected by a pressure of 0.5 psi, and the separation was performed with normal polarity at 30 kV and a temperature of 20 ^{0}C. Absorption detection was performed with a Beckman MDQ PDA detector over a wavelength range of 190-600 nm. The stock solutions of amino acids were prepared by dissolving 1.00 mg of each amino acid in 4.0 mL of deionized water, and the stock solutions were then further diluted 100 times with the appropriate sample matrix.

5.2.2.2 CE-MS system

The automated CE system was the same as described in section 5.2.2.1, and the MS was an LCQ (Finnigan MAT, San Jose, CA, USA) ion-trap mass spectrometer equipped with a tricoaxial pneumatically assisted electrospray (ESI) ion source. Negative ion mode was used. The working conditions for ESI were: electrospray capillary potential, -3.5 kV; temperature of the heated capillary, 200 °C; sheath liquid flow rate ranging between 2-10 μL/min was optimized to produce optimum electrosprays; The sheath liquid was 2-propanol/water (80/20, v/v) with 0.25% DEA. Full-scan data acquisition was performed from m/z 100 to 300 in centroid mode. The selected ion monitoring (SIM) mode recorded all selected m/z ratios with a dwell time of 50 ms over the full time range.

5.3 Results and discussion

5.3.1 CE-PDA

5.3.1.1 BGE and sample matrix effects on focusing

Since introduction of non-volatile materials into an MS ion source over time may block the orifice and requires frequent cleaning, and non-volatile materials also suppress the MS signal, the running buffer for CE-MS is often made from volatile components. Separation in a CE capillary filled with volatile buffers is usually inferior to separation in borate, phosphate, and other buffers containing non-volatile components. In order to examine if the focusing technique using a dynamic pH junction also works with a volatile buffer system, and to compare CE-PDA and CE-MS with the focusing technique, the same buffer system with volatile materials was used for both CE-PDA and CE-MS. In our research on focusing with a pH junction described in the previous chapters, the pK_a

of the analyte was found to be the key criterion for the BGE and the sample pH selection. All the three amino acids have more than one pK_a. Here we utilize the pK_2 (α-$^+NH_3$). The pK_2 for the three aromatic amino acids ranges from 9.1 to 9.4, so the highly alkaline and volatile organic base diethylamine (DEA) was selected as the electrolyte in running BGE. To evaluate the effects of the buffer concentrations on focusing, 10 mM – 50 mM DEA was used as the BGE and the sample matrix was prepared with 10 mM – 50 mM ammonium acetate. The pH of the BGE was 11.2-11.6 and of the sample matrix 6.5-6.7. Because discontinuous buffer systems were used for the BGE and the sample matrix, the UV absorbance difference between the BGE and the sample plug increased with the buffer concentrations. Higher concentrations of buffers are not suitable for CE-PDA, especially for separations, since the baseline fluctuates very severely. Moreover, high currents will be produced with high concentrations of buffers, resulting in high resistive heating which will cause serious band broadening in CE.

The concentration of tryptophan was 1.2×10^{-5} M. A large volume of sample (380 nL) was injected, with an injection time of 99.9 seconds at pressure of 0.5 psi. The focusing results with different buffer concentrations are shown in Figure 5.1.

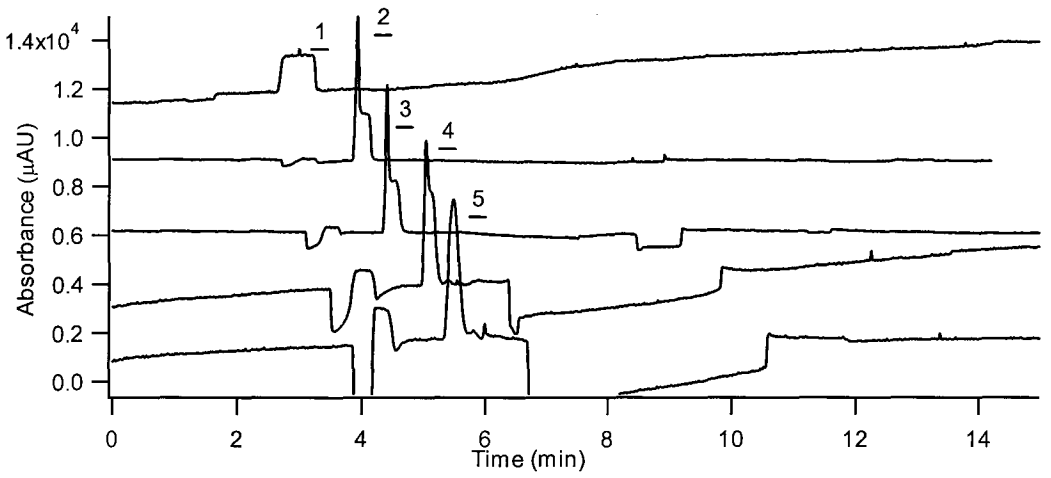

Figure 5.1 Electropherograms showing the use of a dynamic pH junction for tryptophan focusing. The BGE and the sample matrix were prepared with DEA or ammonium acetate; The concentration of tryptophan was 1.2 x 10^{-5} M; The time for all injections was 99.9 seconds (380 nL); detection wavelength, 225 nm; voltage, 30 kV. Note the axes for the electropherograms are shifted horizontally and vertically for clarity of presentation.

1. BGE: 20mM DEA, pH=11.3; Sample: 20mM DEA, pH=11.3;
2. BGE: 5mM DEA, pH=10.94; Sample: 5mM CH_3COONH_4, pH=6.7;
3. BGE: 10mM DEA, pH=11.2; Sample: 10mM CH_3COONH_4, pH=6.7;
4. BGE: 20mM DEA, pH=11.3; Sample: 20mM CH_3COONH_4, pH=6.7;
5. BGE: 50mM DEA, pH=11.6; Sample: 50mM CH_3COONH_4, pH=6.8;

When the pH of the sample equalled that of the BGE, tryptophan did not focus and migrated as a broad band. However, as the pH of the sample decreased to 6.7, tryptophan focused with all the different BGE concentrations. The concentrations of the buffer influenced peak shapes and baselines. From Figure 5.1, it can be seen that the peak shape improved as the concentrations of BGE increased. The peak heights are similar in all the cases. The conductivity of the sample matrix in all the cases was higher than that of the BGE, except in case 1, where they were equal. Therefore, there was no field-amplified focusing effect here. The improvement of peak shape with increasing concentrations of BGE may be caused by improved focusing resulting from a sharper pH gradient (thus smaller width of the gradient region) caused by the higher concentrations of BGE.

However, the baseline fluctuated more when the concentration of the buffer system increased.

5.3.1.2 Buffer system and sample matrix effects on separation.

Although the peak shape improved when the buffer concentrations increased, the baseline became less stable due to the absorbance difference between the BGE and the sample matrix. The BGE of 10 mM was used for separation considering both the peak shape and the baseline.

A contour plot for the separation of tryptophan, phenylalanine, and tyrosine with pH junction focusing is shown in Figure 5.2. The UV absorption spectra of the amino acids obtained from the PDA detector in CE are shown in Figure 5.3. The concentrations of tryptophan, phenylalanine, and tyrosine were 1.2×10^{-5} M, 1.5×10^{-5} M, and 1.4×10^{-5} M, respectively. The contour plot for a separation without pH junction focusing is shown in Figure 5.4, and a comparison of the two separations with and without pH junction focusing is shown in Figure 5.5.

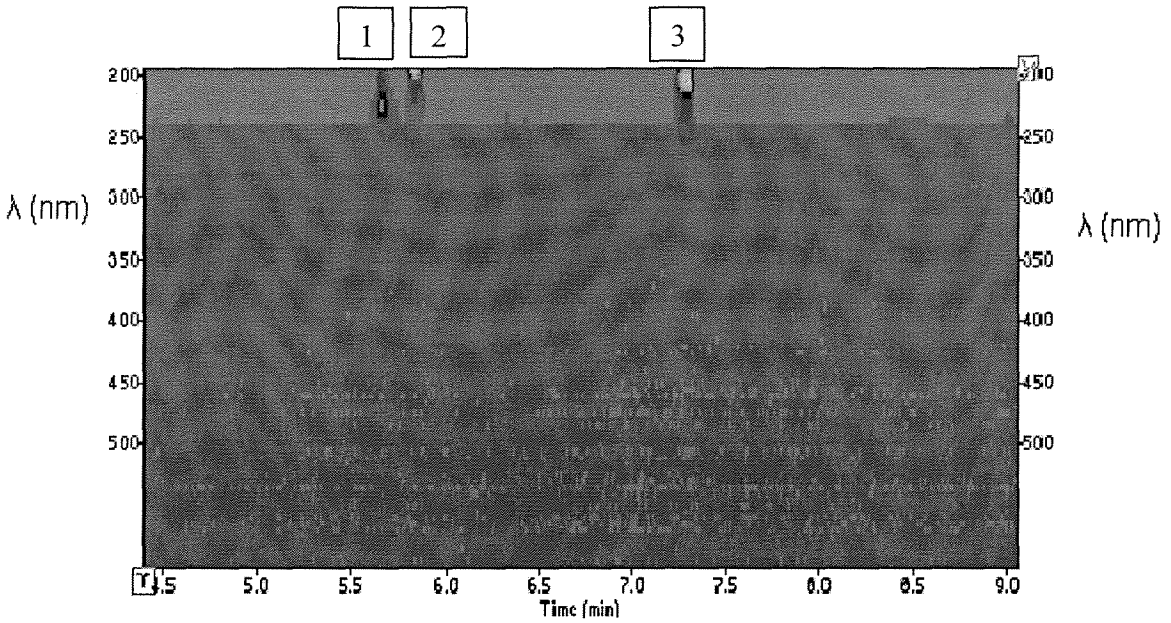

Figure 5.2 Contour plots for the separation of tryptophan, phenylalanine, and tyrosine with pH junction focusing. The BGE was prepared with 10 mM DEA and the sample matrix was prepared with 10 mM ammonium acetate. The pH for the BGE and the sample was 11.2 and 6.7, respectively. The concentrations for tryptophan, phenylalanine, and tyrosine were 1.2 x 10^{-5} M, 1.5 x 10^{-5} M, and 1.4 x 10^{-5} M, respectively; injection time, 99.9 s (380 nL); voltage, 30 kV. 1-Tryptophan; 2-Phenylalanine; 3-Tyrosine.

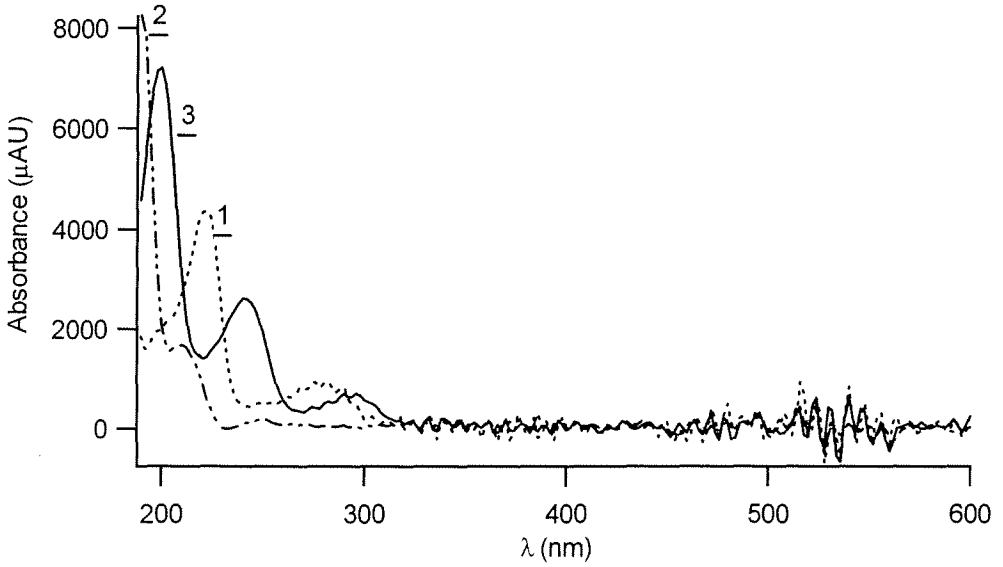

Figure 5.3 UV absorption spectra of the three amino acids obtained from PDA. 1-Tryptophan; 2-Phenylalanine; 3-Tyrosine. The conditions are the same as in Figure 5.2.

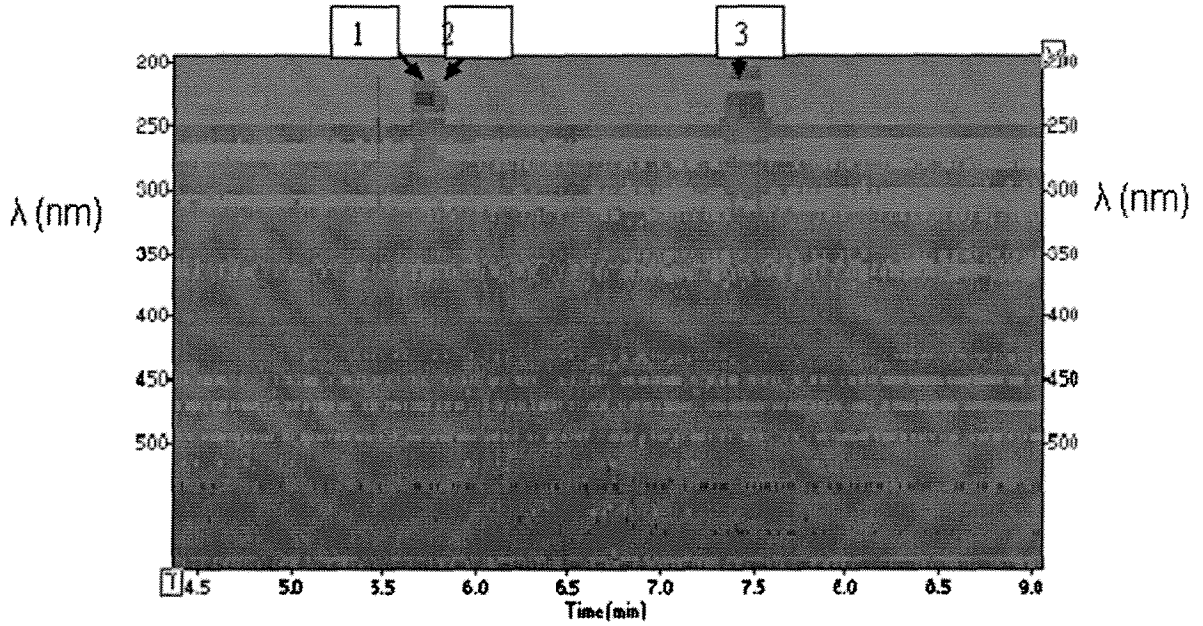

Figure 5.4 Contour plots for the separation of tryptophan, phenylalanine, and tyrosine without pH junction focusing. The BGE and the sample matrix were both prepared with 10 mM DEA, and the pH for both of them was 11.2. Other conditions were the same as those in Figure 5.2. 1-Tryptophan; 2-Phenylalanine; 3-Tyrosine.

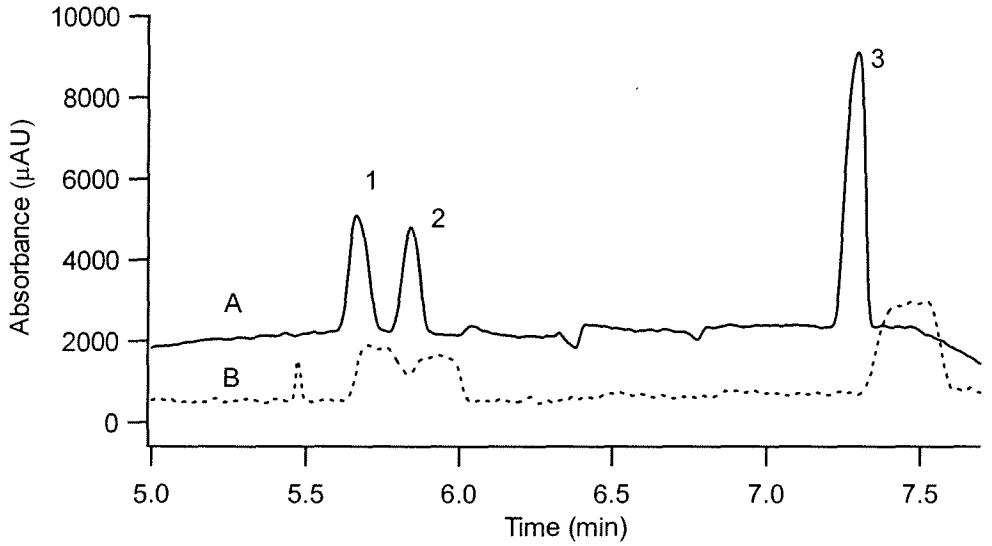

Figure 5.5 Comparison of two separations with and without pH junction focusing. A: using pH junction focusing with the conditions of Figure 5.2; B: without pH junction focusing with the conditions of Figure 5.4. Detection wavelength was 200 nm; injection time, 99.9 s (380 nL). 1-Tryptophan; 2-Phenylalanine; 3-Tyrosine. Note the axes for the electropherograms are shifted vertically for clarity of presentation.

With a pH junction, baseline separation was achieved for the three species despite such a large sample volume injected (380 nL). Three sharp peaks were observed as shown in Figure 5.5. It should be noted that the x-axis (time) for the electropherograms in Figure 5.5 is expanded in order to compare clearly the results of the two separations with and without pH junction focusing. The separation efficiencies for tryptophan, phenylalanine and tyrosine are 2.9 x 10^4, 4.3 x 10^4, and 6.3 x 10^4, respectively. The DIBR values are around 0.12, 0.11, and 0.095 for tryptophan, phenylalanine and tyrosine, respectively. Therefore the corresponding initial injection zones are narrowed approximately 8-fold, 9-fold, and 11-fold. It can also be seen from the contour plot of Figure 5.2 that three spots with strong absorbance are obvious. Corresponding to each spot, a UV spectrum can be obtained from the PDA. The spectra for the three spots in the contour plot are shown in Figure 5.3. From these UV spectra, the three species were identified. Number 1 was tryptophan; 2 was phenylalanine and 3 was tyrosine. However, without a dynamic pH junction, the tryptophan and phenylalanine coeluted and appeared as one spot as shown in Figure 5.4, and the two peaks overlapped to form a broad band in Figure 5.5. Moreover, the absorbance was also low for the three species due to band broadening. The focusing by a dynamic pH junction significantly improved the separation efficiency and thus the concentration sensitivity for the 380 nL sample volume injected.

5.3.2 CE-MS

5.3.2.1 BGE and sample matrix effects on focusing.

The charges carried by an analyte depend on its structure and the carrier solvent. In ESI-MS, the buffer and buffer strength both have a significant effect on MS response. [17]

Therefore, it is important to choose these conditions correctly. According to the pK_2 values of the three amino acids (ranges from 9.1 to 9.4) and the previous work, the strongly alkaline and volatile base DEA was selected as the electrolyte used in the BGE. In CE-ESI-MS with a sheath-flow interface, higher concentrations of BGE can be used. This is due to the low conductivity of the sheath liquid which serves as the outlet vial to complete the CE voltage circuit. The current is not high with high buffer concentrations. Thus it will not generate high Joule heating. Diethylamine concentrations between 50 mM and 300 mM, corresponding to pH values in the range of 11.6-12.1, were investigated. Samples were prepared with 5 mM ammonium acetate (pH 6.7). Higher concentrations of ammonium acetate were not used because high concentration salts may lead to decreased analyte response in ESI. [18] The conductivity of the sample matrix prepared with 5 mM ammonium acetate is lower than that of the BGE, which will produce field-amplified focusing. In order to evaluate this focusing effect in the absence of V-DIF, a DEA of 5 mM was used as sample matrices as well. A DEA of 100 mM was used as sample matrix in order to compare the focusing results with and without a dynamic pH junction.

The results with different concentration BGE using selected ion monitoring (SIM) mode in MS (m/z = 203) are shown in Figure 5.6. The tryptophan concentration was 1.2 x 10^{-5} M.

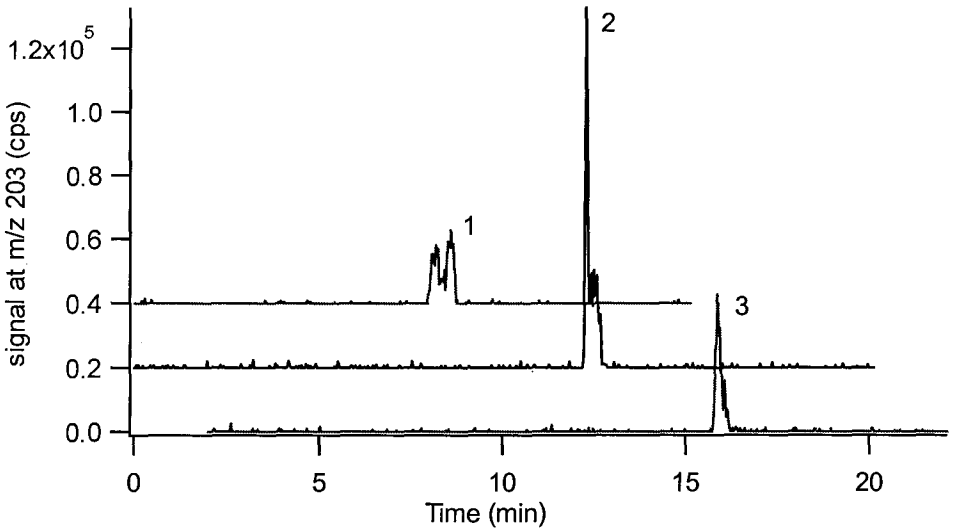

Figure 5.6 CE-MS SIM electropherograms of tryptophan. Conditions: sample matrix, 5 mM ammonium acetate (pH = 6.7); BGE: 1-50 mM DEA (pH = 11.6); 2-100 mM DEA (pH = 11.8); 3-300 mM DEA (pH = 12.1); injection, 99.9 s (380 nL); CE potential, 30 kV; sheath liquid, 5 µL/min of 0.25% DEA in 2-propanol/water, 80/20 (v/v). Note the axes for the electropherogram 3 is shifted horizontally by 2 min; 1 and 2 are shifted vertically for clarity of presentation.

When the BGE concentration was 50 mM, peak splitting was pronounced. As the BGE concentration increased, the peak shape improved. This may be due to the improved focusing caused by higher BGE concentrations as discussed in section 5.3.1.1. However, when the BGE concentration increased to 300 mM, the peak height lowered. This was due to the suppression resulting from the high concentration of BGE. The DEA of 100 mM gave the best result; the peak 2 in Figure 5.6 was much higher than the other two traces.

Because the conductivity of 5 mM ammonium acetate is lower than the BGE, it will produce field amplification focusing in addition to the V-DIF. A DEA of 5 mM, which has similar conductivity as 5 mM ammonium acetate and a pH slightly different from

BGE, was used to evaluate the field amplification focusing effect in this case. A DEA of 100 mM was used to prepare the sample to compare the results with and without pH junction focusing. Results for different sample matrices are shown in Figure 5.7.

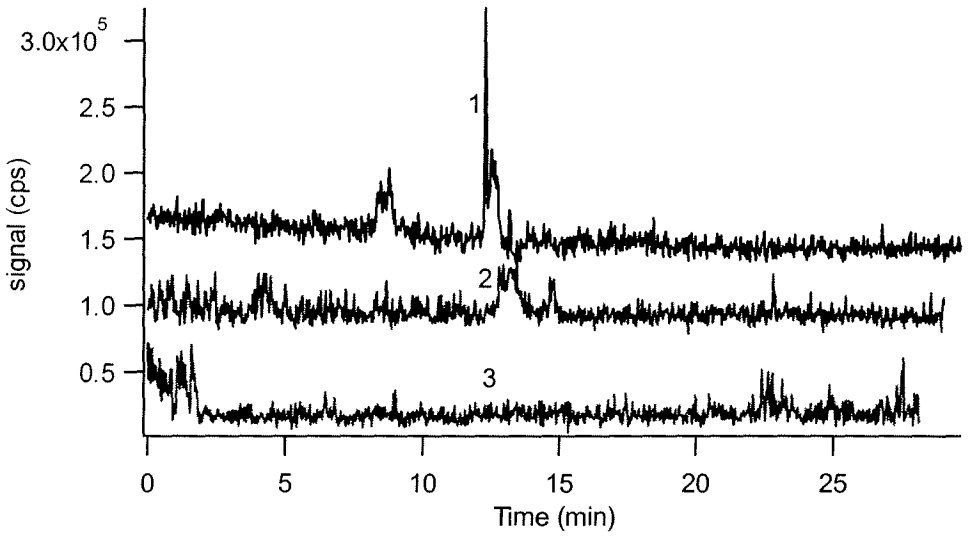

(a)

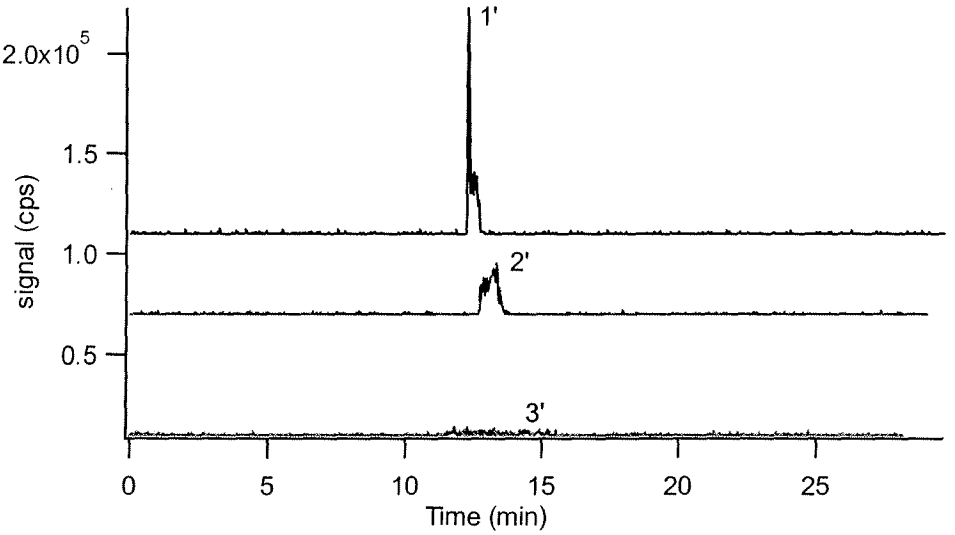

(b)

Figure 5.7 (a) CE-MS Total ion current (TIC) electropherograms of tryptophan, MS scan range 100-300 m/z. Conditions: BGE, 100 mM DEA (pH = 11.8); sample matrix: 1- 5 mM ammonium acetate (pH = 6.7); 2- 5 mM DEA (pH = 11.0); 3- 100 mM DEA (pH = 11.8); (b) CE-MS SIM electropherograms of tryptophan. BGE, 100 mM DEA (pH = 11.8); sample matrix: 1'- 5 mM ammonium acetate (pH = 6.7); 2'- 5 mM DEA (pH = 11.0); 3'- 100 mM DEA (pH = 11.8); injection, 99.9 s (380 nL); CE potential, 30 kV; sheath liquid, 5 μL/min of 0.25% DEA in 2-propanol/water, 80/20 (v/v).

Note the axes for the electropherograms are shifted vertically for clarity of presentation.

When 5 mM ammonium acetate (pH = 6.7) was used to prepare the sample, tryptophan focused into a sharp peak. A signal to noise ratio (S/N) of 58 was achieved with SIM detection. In the TIC electropherograms, the peak was easily observed. The result of preparing a sample with 5 mM DEA (pH = 11.0), while keeping all other conditions the same, is shown as peaks 2 and 2' in Figure 5.7. The pH of the sample is just slightly different from that of the BGE, so little or no V-DIF is occurring. The conductivity of the sample is lower. This produces the field amplification effect which also leads to focusing. However, the peak broadened and the peak height was much lower than that of peak 1. The field amplification focusing effect was limited in this case. When the sample was prepared with BGE, the pH difference no longer existed and no signal was observed with such large injection volumes. The dynamic pH junction played a key role in focusing.

5.3.2.2 Buffer system and sample matrix effects on separation

Because 100 mM DEA BGE and 5 mM ammonium acetate sample matrix gave the best focusing, we used these conditions to separate the three amino acids. In order to investigate the focusing effect caused by the dynamic pH junction on separation, the 100 mM DEA was also used to prepare the sample for the separation. The results are shown in Figure 5.8 and Figure 5.9. The concentrations of tryptophan, phenylalanine, and tyrosine were 1.2×10^{-5} M, 1.5×10^{-5} M, and 1.4×10^{-5} M, respectively.

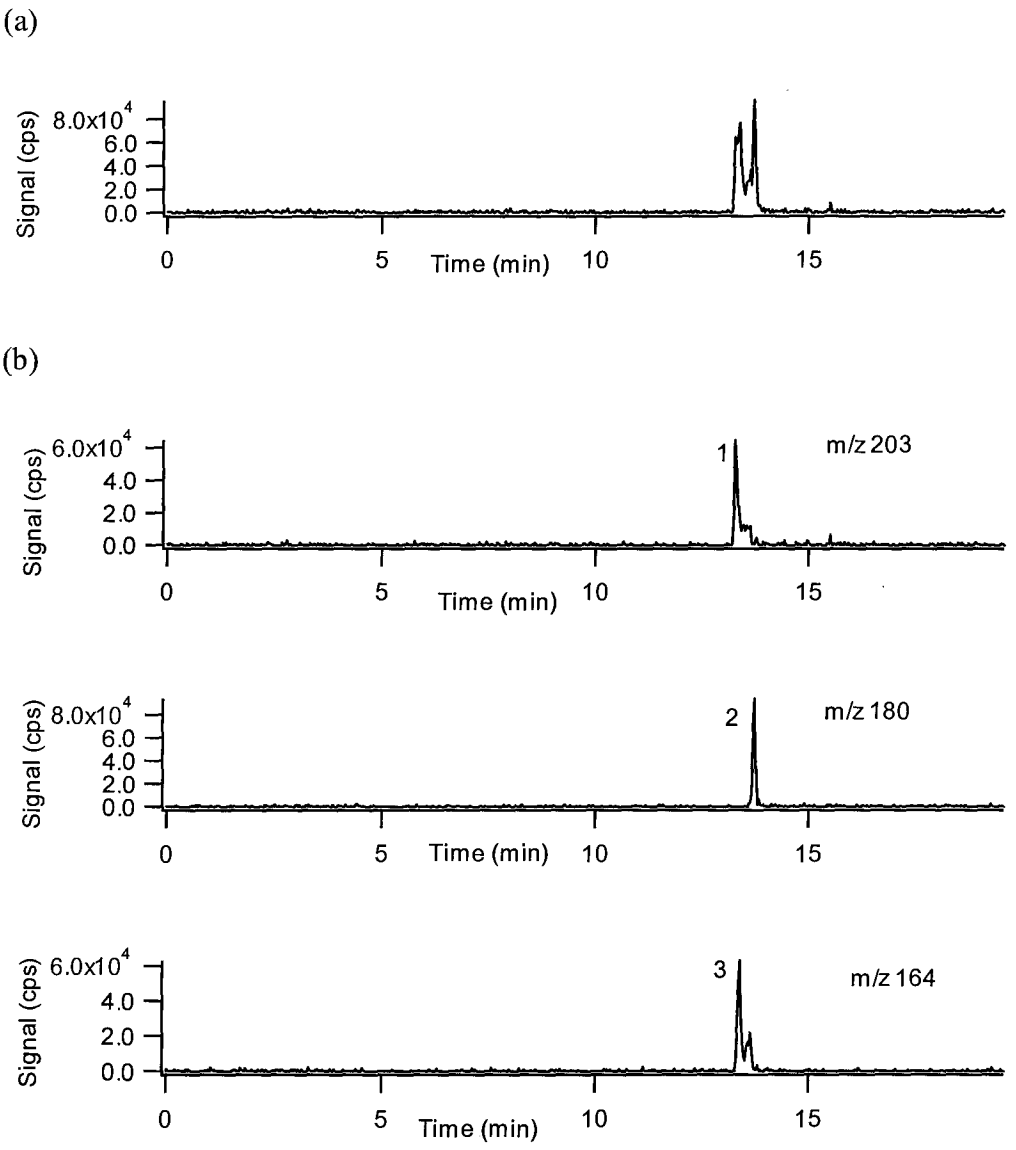

Figure 5.8 Separation of three amino acids with a dynamic pH junction. (a) CE-MS SIM electropherograms for the three amino acids. (b) CE-MS SIM electropherograms for the individual amino acids. Peaks: 1-tryptophan; 2-tyrosine; 3-phenylalanine. Conditions: BGE, 100 mM DEA (pH = 11.8); sample matrix, 5 mM ammonium acetate (pH = 6.7); concentrations, 1.2 x 10^{-5} M for tryptophan, 1.4 x 10^{-5} M for tyrosine, and 1.5 x 10^{-5} M for phenylalanine; injection, 99.9 s (380 nL); CE potential, 30 kV; sheath liquid, 5 µL/min of 0.25% DEA in 2-propanol/water, 80/20 (v/v).

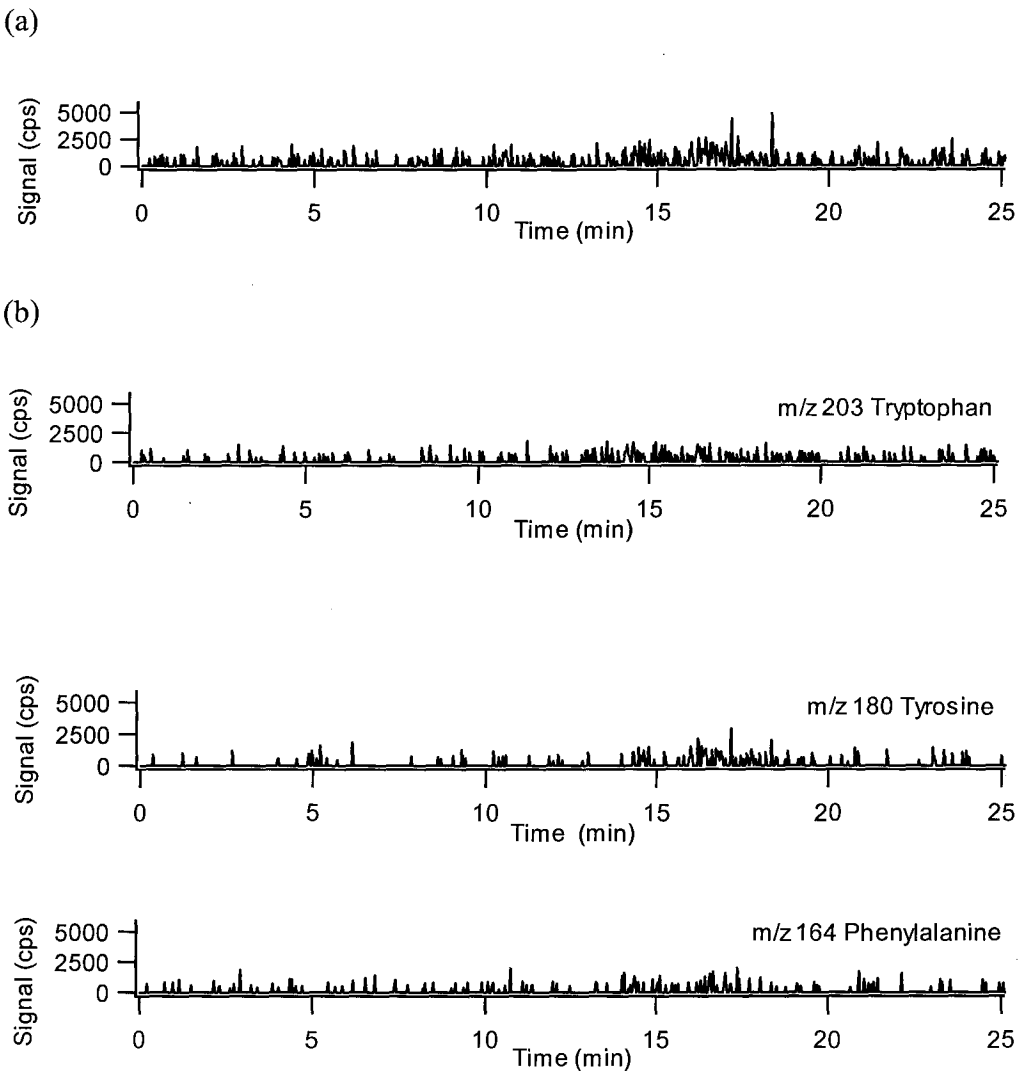

Figure 5.9 Separation of three amino acids without a dynamic pH junction. (a) CE-MS SIM electropherograms for the three amino acids separation. (b) CE-MS SIM electropherograms for the individual amino acids. Conditions: BGE, 100 mM DEA (pH = 11.8); sample matrix, 100 mM DEA (pH = 11.8); other conditions are the same as in Figure 5.8.

The SIM electropherograms for a separation of the mixture of three amino acids with a dynamic pH junction are shown in Figure 5.8. All of the three selected masses were detected in the SIM mode as shown in Figure 5.8 (b). The signal was high for all of them and the peaks were also narrow. Signal to noise ratios (S/N) of 55, 88, and 86 for tryptophan, tyrosine, and phenylalanine were achieved. The separation efficiencies for

tryptophan, tyrosine, and phenylalanine are 1.2 x 10^5, 2.2 x 10^5, and 1.3 x 10^5 theoretical plates, respectively. However, The CE resolution was less than that in CE-UV, possibly due to the band broadening caused by post-separation mixing during transfer from the outlet of the capillary to the mass spectrometer. However, MS can separate the co-eluted amino acids based on their different mass to charge ratios (m/z) if SIM mode is used. Without a dynamic pH junction for such large injection volumes, no signal can be obtained for any of the analytes.

5.3.2.3 Optimization of CE-MS detection parameters

The CE-MS interface is shown in Figure 5.10. [17]

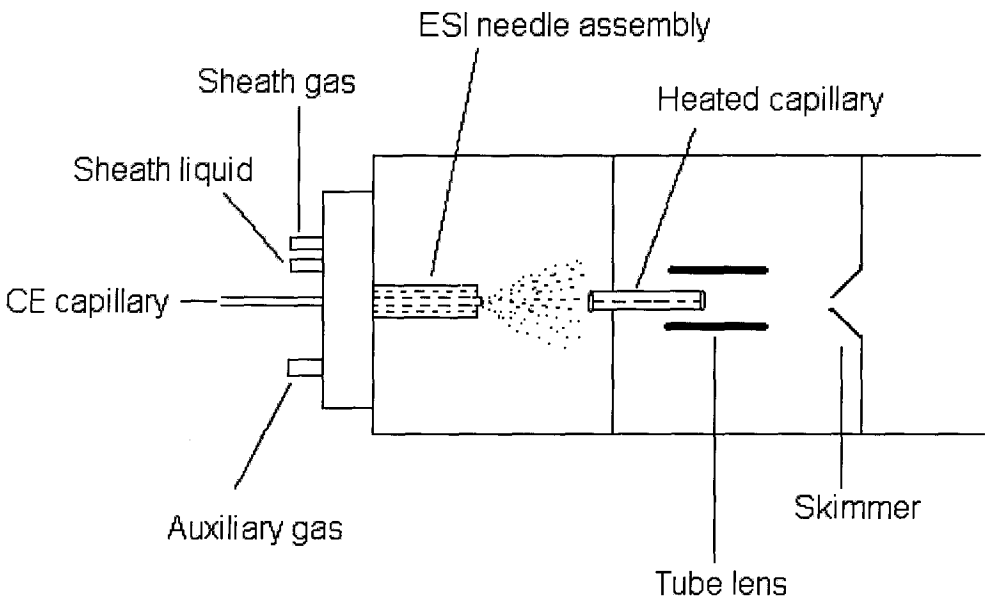

Figure 5.10 CE-MS interface.

The ESI-MS capillary tip position, sheath liquid composition, and flow rate were adjusted to optimize sensitivity and stability.

The capillary tip position may seriously affect the performance of the system. [19, 20] It needs to be adjusted for optimal performance, while maintaining electrical continuity [13] for CE separation. If the tip is too far out of the sheath liquid, it may generate an unstable spray. Furthermore, the tip may dry out, leading to the loss of the electrical connection and immediate termination of the CE separation. If the tip is too far back in the sheath liquid, it may form drops of the sheath liquid and result in sputtering and intermittent electrical continuity. The CE capillary tip was adjusted by the micrometer attached to the interface, in order to get a stable spray and optimum signal.

The sheath liquid is critical to the performance of the CE-MS system. [21] It helps to establish a stable ESI in CE-MS, makes electrical contact between the solution inside the capillary and the probe tip, and changes the post capillary solution chemistry to improve ESI characteristics and ionization efficiency [22] as well. 2-Propanol is selected as it produces a more stable signal than methanol or ethanol in the negative ionization mode. [19] Sheath liquids containing 2-propanol/water (80%/20% v/v) with 0 - 1% DEA were tested. The optimum sheath liquid composition was found to be 2-propanol/water (80/20, v/v) with 0.25% DEA. Finally, sheath liquid flow rates ranging between 2 - 10 μL/min were examined. Since the most satisfactory results were obtained between 5 and 10 μL/min, 5 μL/min was selected.

5.3.3 Detection limits for CE-PDA and CE-MS with V-DIF

Detection limits for tryptophan, phenylalanine, and tyrosine in CE-PDA and CE-MS with V-DIF are given in Table 5.1. The detection limits were determined as described in chapter 3.

Compound	**Limit of detection (10^{-7} M)**	
	CE-PDA	**CE-MS (SIM)**
Tryptophan	0.5	7.4
Phenylalanine	11.0	3.9
Tyrosine	0.7	5.1

Table 5.1 Detection limits for tryptophan, phenylalanine, and tyrosine in CE-PDA and CE-MS. Wavelengths of 225 nm, 203 nm and 200 nm were used for the determination of LODs for tryptophan, tyrosine and phenylalanine, respectively.

LOD values between 0.5 x 10^{-7} M and 11 x 10^{-7} M in CE-PDA and between 3.9 x 10^{-7} M and 7.4 x 10^{-7} M in CE-MS were obtained. Detection limits for trypothan and tyrosine using CE-PDA are considerably lower than those using CE-MS. However, the detection limit for phenylalanine is a little higher in CE-PDA. This may be attributed to the different molar absorptivities which depend on the detection wavelengths for the individual compounds in CE-UV systems.

5.4 Conclusions

The results presented in this work indicate that the V-DIF using a dynamic pH junction was achieved for both CE-PDA and CE-MS with volatile buffers. Both PDA and ESI-MS are suitable for CE detection, especially for peak identification. However, CE-ESI-MS

results are affected by more factors such as sheath liquid composition and flow rate, and the optimization parameters may be different for different compounds. The optimized BGE concentrations and sample matrix for focusing are also different between CE-PDA and CE-MS. For different analytes, different conditions can be selected for focusing to improve the separation efficiency and thus improve concentration sensitivity.

5.5 References

1. Figeys, D.; Van Oostveen, I.; Ducret, A.; Aebersold, R. *Anal. Chem.* 1996, *68*, 1822-1828.
2. Wu, J. T.; Qian, M. K.; Li, M. X.; Zheng, K.; Huang, P.; Lubman, D. M. *J. Chromatogr., A* 1998, *794*, 377-389.
3. Hernández-Borges, J.; Neusüß, C.; Cifuentes, A.; Pelzing, M. *Electrophoresis* 2004, *25*, 2257-2281
4. Simpson, D. C.; Smith, R. D. *Electrophoresis* 2005, *26*, 1291-1305
5. Klampfl, C. W. *Electrophoresis* 2006, *27*, 3-34
6. Loo, J. A.; Edmonds, C. G.; Smith, R. D. *Anal. Chem.* 1991, *63*, 2488-2499
7. Liu, S. J.; Chen, X. J.; Hu, Z. *Electrophoresis* 2002, *23*, 3392-3397
8. Burgi, D. S.; Chien, R. L. *Anal. Chem.* 1991, *63*, 2042-2047.
9. Shihabi, Z. K. *J. Chromatogr., A* 1993, *652*, 471-475
10. Shihabi, Z. K. *J. Chromatogr., A* 1996, *744*, 231-240
11. Krivankova, L.; Bocek, P. *J. Chromatogr., B* 1997, *689*, 13-34
12. Gebauer, P.; Thormann, W.; Bocek, P. *Electrophoresis* 1995, *16*, 2039-2050
13. Monton, M. R. N.; Terabe, S. *Anal. Sci.* 2005, *21*, 5-13
14. Imami, K.;Monton, M. R. N.; Ishihama, Y.; Terabe, S. *J. Chromatogr., A* 2007, *1148*, 250-255
15. Britz-McKibbin, P.; Wong, J.; Chen, D. D. Y. *J. Chromatogr., A* 1999, *853*, 535-540
16. Britz-McKibbin, P.; Chen, D. D. Y. *Anal. Chem.* 2000, *72*, 1242-1252
17. Schnute, W. C. *Finnigan CE/MS getting started*, ThermoQuest, 1999

18. Ikonomou, M. G.; Blades, A. T.; Kebarle, P. *Anal. Chem.* 1990, *62*, 957-967

19. Tsai, C. Y.; Her, G. R. J. *Chromatogr., A* 1996, *743*, 315-321

20. Jauregui, O.; Moyano, E.; Galceran, M. T. *J. Chromatogr., A* 2000, *896*, 125-133

21. Moseley, M. A.; Shabanowitz, J.; Hunt, J. F.; Tomer, K. B. *J. Am. Soc. Mass Spectrom.* 1992, *3*, 289-300

22. Banks, J. F. *Electrophoresis* 1997, *18*, 2255-2266

CHAPTER 6

Non-aromatic Amino Acid Focusing in Capillary Electrophoresis (CE)-Electrospray Ionization Mass Spectrometry (ESI-MS) with a Dynamic pH Junction

6.1 Introduction

The detection and identification of amino acids [1] are very important in many research and industrial fields including biochemical analysis, [2] medical diagnostics, [3, 4, 5] and food analysis. [6] The analysis of amino acids is used to determine the primary structure of proteins in biochemistry, and the assay of amino acids in urine or other body fluids is very helpful for the diagnosis of diseases. The analysis of amino acids also plays an important role in the food industry in which they are analyzed to monitor fermentation and assess the quality of food products. [6] Since most of the amino acids are non-aromatic and have little UV absorbance, it is very difficult to detect them directly with UV absorption. They have commonly been derivatizated with UV chromophores or fluorophores before their detection. [7, 8] The derivatization process can be time consuming and labour intensive. Mass spectrometry is a good method for detecting these non-aromatic amino acids without the need for derivatization.

As mentioned in the previous chapters, CE has one major drawback: its relatively low concentration sensitivity. Although MS offers higher sensitivity, in CE-ESI-MS with a sheath-flow interface, the capillary eluent is diluted and the signal is significantly decreased. A variety of focusing techniques have been explored to improve the concentration sensitivity in CE. [9-13] Each method has certain shortcomings when coupled to MS. The V-DIF technique using a dynamic pH junction, which has been discussed in previous chapters, is very suitable for application in CE-ESI-MS because it is simple and easy to operate.

Due to their zwitterionic nature, amino acids can be analyzed as positive ions using low pH carrier electrolytes [14, 15] or as negative ions using carrier electrolytes with a high pH. [14] In this study of non-aromatic amino acids, we used both modes and applied the V-DIF technique with a dynamic pH junction with different conditions in CE-MS to improve the concentration sensitivity. The non-aromatic amino acids Asp, Glu, and Leu were selected. The highly alkaline and volatile organic base diethylamine (DEA) was selected as the electrolyte for the BGE in the negative ion mode and formic acid was selected as the electrolyte for the BGE in the positive ion mode.

6.2 Experimental

6.2.1 Chemicals

The reagents used to prepare the buffer, sample and sheath liquid were analytical grade. Diethylamine, formic acid, methanol and 2-propanol were from Fisher Scientific (Fair Lawn, NJ). Ammonium acetate was from BDH Chemicals (Toronto, Ont., Canada). Aspartic acid, glutamic acid, and leucine were all purchased from Sigma (St. Louis, MO, USA). Water was purified using a Milli-Q Elix system (Millipore, Milford, MA, USA).

6.2.2 Apparatus and Procedure

CE was performed using a P/ACE^{TM} MDQ (Beckman-Coulter Inc., Mississauga, Ont., Canada). Uncoated capillaries (Polymicro Technologies, Phoenix, AZ) with inner diameters of 75 μm and lengths of 80 cm were used. In the positive ion mode, the BGE was 1 M formic acid. New capillaries were first rinsed with 1.0 M formic acid for 20 min (20 psi), and before each run, the capillary was prerinsed for 5 min with the BGE. For

negative ion mode operation, new capillaries were first rinsed with 1.0 M NaOH (10 min, 20 psi) and then the BGE (10 min, 20 psi), and finally 30 kV was applied for 10 min. Each separation was preceded by a 1.5-min, 20 psi rinse with 1 M NaOH, followed by a 4-min rinse with the BGE. The samples were then injected by a pressure of 0.5 psi, and the separation was performed with normal polarity at 30 kV and ambient temperature. The amino acid stock solutions were prepared by dissolving each amino acid (1.00 mg for Asp and Leu, 2.00 mg for Glu) in 4.0 mL of deionized water and the stock solutions were then further diluted 10 times with appropriate sample matrix.

The mass spectrometer was an LCQ (Finnigan MAT, San Jose, CA, USA) ion-trap mass spectrometer equipped with a tricoaxial pneumatically assisted electrospray ion source. The working conditions for ESI were: temperature of the heated capillary, 200 ^{0}C, electrospray capillary potential, 3.5 kV for the positive ion mode and -3.5 kV for the negative ion mode. The sheath liquid was methanol/water (50/50, v/v) with 5 mM ammonium acetate for the positive ion mode and 2-propanol/water (80/20, v/v) with 0.25% DEA for the negative ion mode. The auxiliary gas is not needed due to the low sheath liquid flow rate. The selected ion monitoring (SIM) mode recorded all selected m/z ratios with a dwell time of 50 ms over the full time range.

6.3 Results and discussion

6.3.1 Positive ion mode

6.3.1.1 Asp focusing

In our previous work with focusing using a pH junction, the pK_a for the analyte was found to be key for the buffer and sample pH selection, whether at low or high pH. Asp and Glu have three pK_a values [pK_1 (α-COOH), pK_2 (α-$^+NH_3$), and pK_r (side chain)] and Leu has two pK_a values [pK_1 (α-COOH) and pK_2 (α-$^+NH_3$)]. The pK_1 (α-COOH) are 2.0, 2.2 and 2.3 for Asp, Glu and Leu, [16] respectively. The buffer composition should have sufficient volatility to ensure compatibility with the MS detection. Formic acid is a good choice for the electrolyte in the BGE. The concentration of the formic acid was 1M to give the low pH (1.8). To create the pH junction, the sample was prepared with 5 mM ammonium acetate (pH 6.7). Formic acid, 5 mM, was also used as sample matrix in order to evaluate the field-amplified focusing effect in the absence of V-DIF, and 1M formic acid was used as sample matrix to compare the results with and without pH junction focusing. The Asp concentration was 1.9×10^{-4} M.

The results with different sample matrices are shown in Figure 6.1.

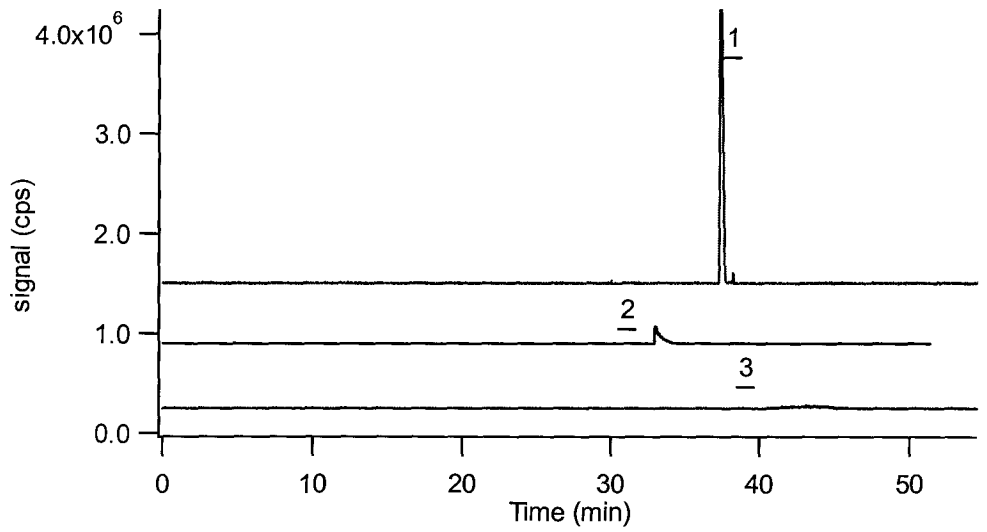

Figure 6.1 CE-MS SIM electropherograms of aspartic acid. The Asp concentration was 1.9 x 10^{-4} M. Conditions: BGE, 1 M formic acid (pH = 1.8); sample matrix: 1- 5 mM ammonium acetate (pH = 6.7); 2- 5 mM formic acid (pH = 2.8); 3-1 M formic acid (pH = 1.8); injection, 99 s (380 nL); CE potential, 30 kV; sheath liquid, 5 µL/min of 5 mM ammonia acetate in methanol/water, 50/50 (v/v). Note the axes for the electropherograms are shifted vertically for clarity of presentation.

When 5 mM ammonium acetate (pH = 6.7) was used to prepare the sample, aspartic acid (Asp) focused to a sharp peak and the signal was high (peak 1 in Figure 6.1). A signal to noise ratio (S/N) of 1180 and separation efficiency of 1.1 x 10^5 theoretical plates were obtained. The detector-to-injection bandwidth ratio (DIBR) was around 0.10, thus the initial injection zone was narrowed approximately 10-fold.

The conductivity of 5 mM ammonium acetate is lower than that of BGE. This will produce field amplification focusing. We use 5 mM formic acid as sample matrix to evaluate the effect of this field amplification focusing. The conductivity of 5 mM formic acid is similar to 5 mM ammonium acetate, and the pH of 5 mM formic acid only differs slightly from the BGE. The result with 5mM formic acid as sample matrix should be

sufficient to evaluate the effect of field amplified focusing. The result of preparing samples with 5 mM formic acid (pH = 2.8), while keeping all other conditions the same, is shown as peak 2 in Figure 6.1. However, the peak was broader and the peak height was significantly lower than that of peak 1. The field amplification effect in this case was weak. When the sample was prepared with the same solution as the BGE, there was no pH difference and no signal was observed at this large injection volume. The pH junction focusing caused by the difference in pH between the sample and the BGE is crucial for the Asp focusing.

6.3.1.2 Effect of focusing by a dynamic pH junction on separation

In order to examine the focusing effect caused by the dynamic pH junction on other non-aromatic amino acids and separation, three non-aromatic amino acids Glu, Asp and Leu were used. Formic acid (1M) was still used as the BGE. The 5 mM ammonium acetate and 1 M formic acid were used to prepare the samples in order to compare the focusing effects caused by the dynamic pH junction. The results are shown in Figure 6.2 and Figure 6.3. The concentrations of Asp, Glu, and Leu were 1.9×10^{-4} M, 3.3×10^{-4} M, and 1.9×10^{-4} M, respectively.

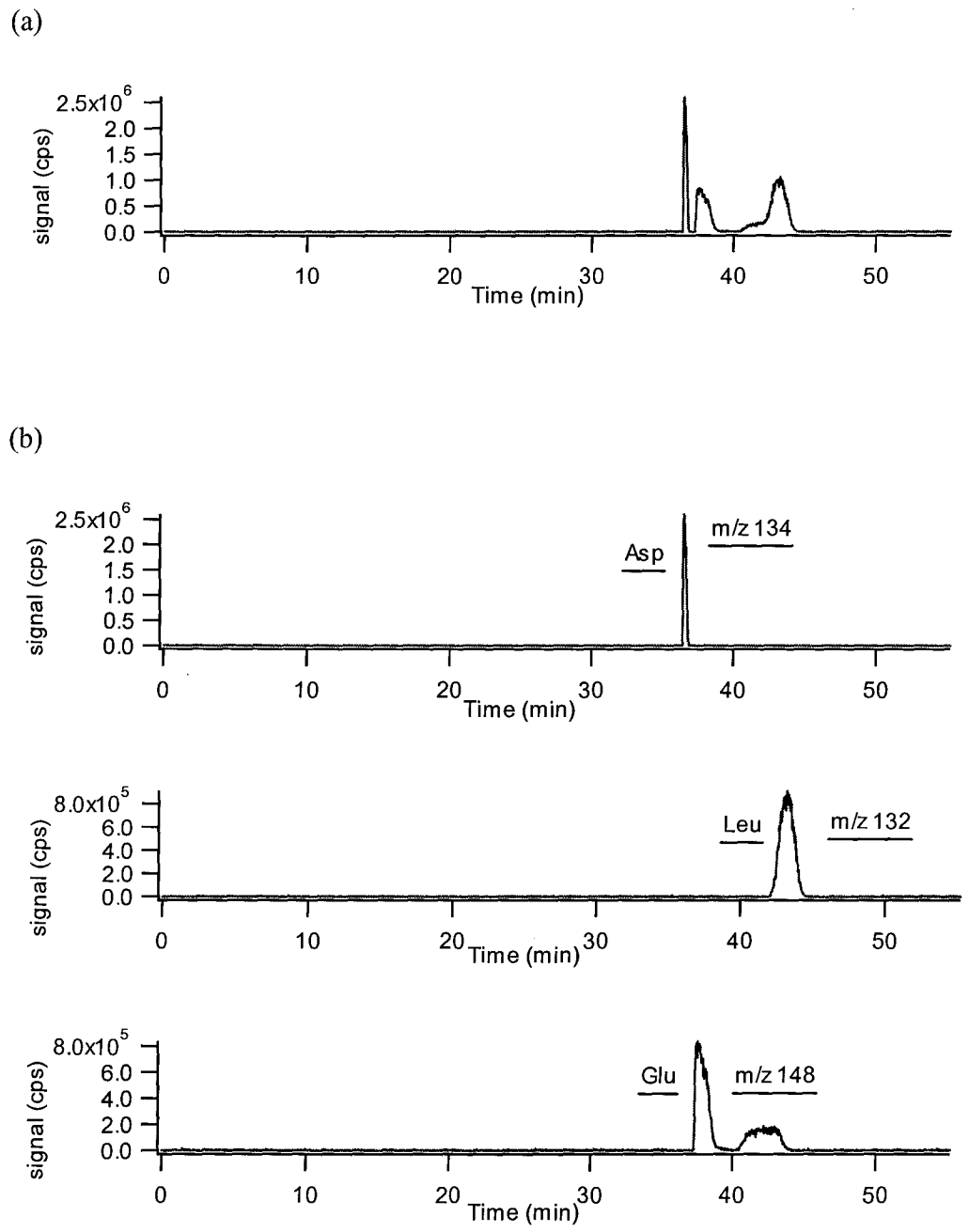

Figure 6.2 Separation of three amino acids with a dynamic pH junction. (a) CE-MS SIM electropherogram for the three amino acids. (b) CE-MS SIM electropherograms for the individual amino acid. The concentrations of Asp, Glu, and Leu were 1.9 x 10^{-4} M, 3.3 x 10^{-4} M, and 1.9 x 10^{-4} M, respectively. Conditions: BGE, 1M formic acid (pH = 1.8); sample matrix: 5 mM ammonium acetate (pH = 6.7); injection, 99 s (380 nL); CE potential, 30 kV; sheath liquid, 5 µL/min of 5 mM ammonium acetate in methanol/water, 50/50 (v/v).

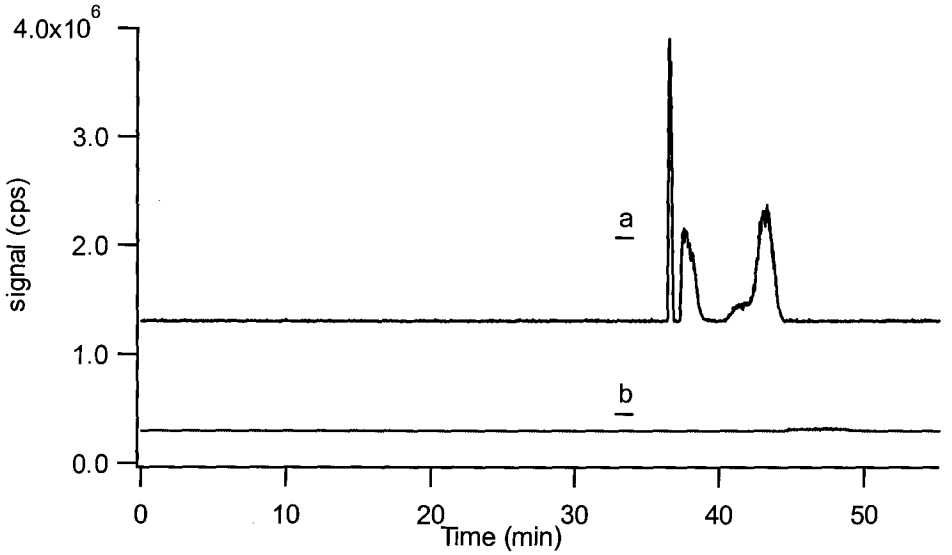

Figure 6.3 Comparison of the separation of three amino acids with and without a dynamic pH junction. The concentrations of Asp, Glu and Leu were the same as those in Figure 6.2. Conditions: a. with a dynamic pH junction: BGE, 1 M formic acid (pH = 1.8); sample matrix, 5 mM ammonium acetate (pH = 6.7); b. without a dynamic pH junction: BGE, 1 M formic acid (pH = 1.8); sample matrix, 1 M formic acid (pH = 1.8); injection, 99 s (380 nL); CE potential, 30 kV; sheath liquid, 5 µL/min of 5 mM ammonia acetate in methanol/water, 50/50 (v/v). Note that the axes for the electropherograms are shifted vertically for clarity of presentation.

The SIM electropherogram for a mixture of three amino acids with a dynamic pH junction is shown in Figure 6.2. All of the three selected masses were detected in the SIM mode. The signals were very high for all of them. Signal to noise ratios (S/N) for Asp, Leu and Glu were 1220, 580, and 370, and separation efficiencies for Asp, Leu and Glu were 1.2×10^5, 6.0×10^3, and 8.5×10^3 theoretical plates, respectively. Glu appeared as a split peak, which may be attributed to an electromigrative interaction of the sample with BGE. [16] This phenomenon often occurs when a sample is preconcentrated to increase the separation efficiency and is related to the sample concentration. [17] The possible reason that Asp appeared as a single peak while Glu appeared as split peaks may be due to the higher sample concentration of Glu. Further experiments should be performed to

verify the cause of Glu peak splitting. The comparison of the separation of the three amino acids with and without a dynamic pH junction is shown in Figure 6.3. Trace (a) shows the signal-to-noise with a dynamic pH junction. Very good separation was achieved. However, without a dynamic pH junction, in which the sample was prepared with 1 M formic acid, shown as trace (b), just one broad band can be seen, no separation was achieved, and the signal was also very low. The pH junction focusing is critical for the detection and separation. It improves the separation efficiency significantly and therefore improves concentration sensitivity.

6.3.2 Negative ion mode

6.3.2.1 Asp focusing

The pK_2 for the Asp, Glu, and Leu are 10.0, 9.9 and 9.7, [16] respectively. The highly alkaline and volatile organic base diethylamine (DEA) was selected as the electrolyte in the BGE in which the analytes were negatively charged. In the negative ion mode, alkylamines are better electrolyte than ammonium hydroxide because of their lower volatility, increasing the stability of the electrolyte concentration. [18] Diethylamine (100 mM, pH = 11.8) was used in the BGE and samples were prepared in 5 mM ammonium acetate (pH = 6.7). The concentration of Asp was the same as that used in the positive ion mode experiments, 1.9×10^{-4} M. The injection time was 99.9 seconds at 0.5 psi. In order to evaluate the field amplification effect and compare the focusing results with or without a dynamic pH junction, 5 mM DEA and 100 mM DEA were also used to prepare the sample. The results with different sample matrix compositions are shown in Figure 6.4.

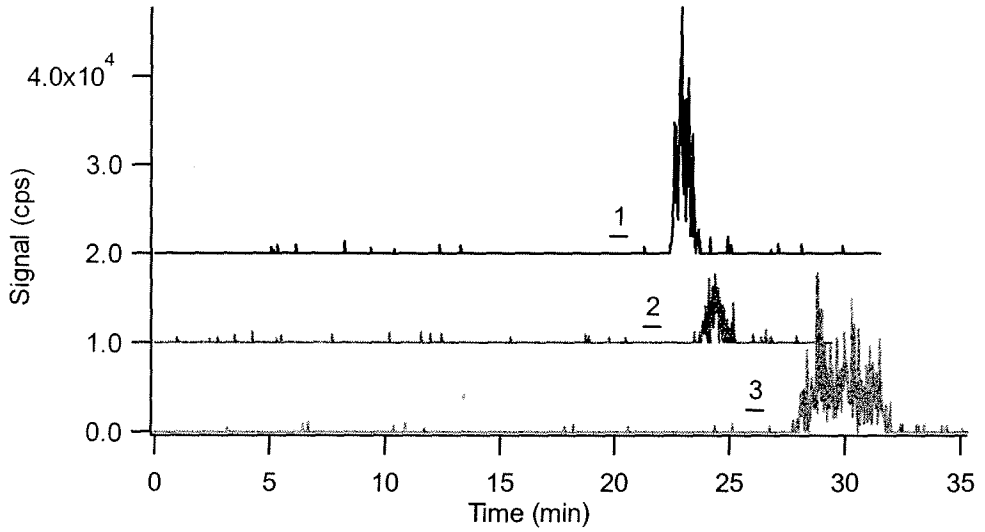

Figure 6.4 CE-MS SIM electropherograms of Asp. The concentration of Asp was 1.9 x 10^{-4} M. Conditions: BGE, 100 mM DEA (pH = 11.8); sample matrix: 1- 5 mM ammonium acetate (pH = 6.7); 2- 5 mM DEA (pH = 11.0); 3- 100 mM DEA (pH = 11.8); injection, 99 s (380 nL); CE potential, 25 kV; sheath liquid, 5 µL/min of 0.25% DEA in 2-propanol/water, 80/20 (v/v). Note the axes for the electropherograms are shifted vertically for clarity of presentation.

When 5 mM ammonium acetate (pH = 6.7) was used to prepare the sample, Asp was somewhat focused, but not as narrow as those of other amino acids such as phenylalanine and tryptophan. This may be due to the different charge state changes during the focusing process which are directly related to the velocity changes. For phenylalanine and tryptophan, their charges changed from -1 to neutral during the focusing, resulting in abrupt changes in the velocities and thus sharp focusing. The Asp, charge changed from -2 to -1 during the focusing process (this is described in section 6.3.3). Asp with charge -1 at the lower pH area also moved towards the anode during the focusing. Therefore the velocity did not change abruptly and no sharp focusing was achieved.

The result of preparing the sample with 5 mM DEA (pH 11.0), while keeping all other conditions the same, is shown as peak 2 in Figure 6.4. The peak broadened and the height was lower than that of peak 1. The field amplification effect was also limited here. When the sample was prepared with the same solution as the BGE (peak 3), the peak broadened. The pH dynamic junction focusing narrowed the band approximately 2.5-fold, and the improvement in concentration sensitivity for Asp in these conditions was not significant.

6.3.2.2 Effect of focusing by a dynamic pH junction on separation

The three non-aromatic amino acids Glu, Asp and Leu were also used to examine the effect of focusing caused by a dynamic pH junction on separation at high pH. Diethylamine (100 mM) was used as the electrolyte in the BGE and samples were prepared with 5mM ammonium acetate (with a dynamic pH junction), and 100 mM DEA (without a dynamic pH junction). The results are shown in Figure 6.5. The concentrations of Asp, Glu, and Leu used in these experiments were 1.9×10^{-4} M, 3.3×10^{-4} M, and 1.9×10^{-4} M, respectively.

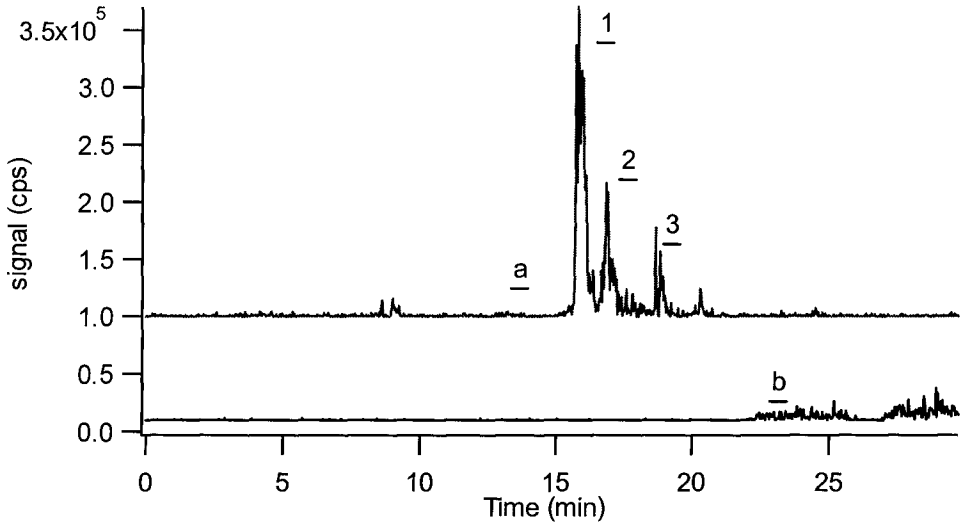

Figure 6.5 Comparison of the separation of three amino acids with or without a dynamic pH junction. Conditions: a. with a dynamic pH junction: BGE, 100 mM DEA (pH = 11.8); sample matrix, 5 mM ammonium acetate (pH = 6.7); b. without a dynamic pH junction: BGE, 100 mM DEA (pH = 11.8); sample matrix, 100 mM DEA (pH = 11.8); The concentrations for Asp, Glu, and Leu used in these experiments were 1.9 x 10^{-4} M, 3.3 x 10^{-4} M, and 1.9 x 10^{-4} M, respectively; injection, 99 s (380 nL); CE potential, 25 kV; sheath liquid, 5 µL/min of 0.25% DEA in 2-propanol/water, 80/20 (v/v). 1-Leu; 2-Glu; 3-Asp. Note the axes for the electropherograms are shifted vertically for clarity of presentation.

All three amino acids were observed and nearly baseline separation was achieved. The signal of Leu was stronger than Glu and Asp, which may be due to the better focusing for Leu. The focusing mechanism for Leu is the same as that of phenylalanine and the focusing of Leu is better than those for Asp and Glu as discussed in section 6.3.2.1. When the separation was performed without a dynamic pH junction, i.e. the sample was prepared with 100 mM DEA, two much broader peaks were observed and the signals were lower. Here the pH junction focusing also improved the separation efficiency, but the improvement was limited for Asp and Glu.

6.3.3 Proposed mechanisms for focusing using a dynamic pH junction.

Figure 6.6 and 6.7 depict the mechanism of the focusing for the cases of positive ion mode and negative ion mode detection.. For Asp, pK_1 (α-COOH) is 2.0, pK_2 (α-$^+NH_3$) 10.0, and pK_r (side chain) 3.9. [16] The major species of Asp at different pH could be estimated as described in chapter 4.

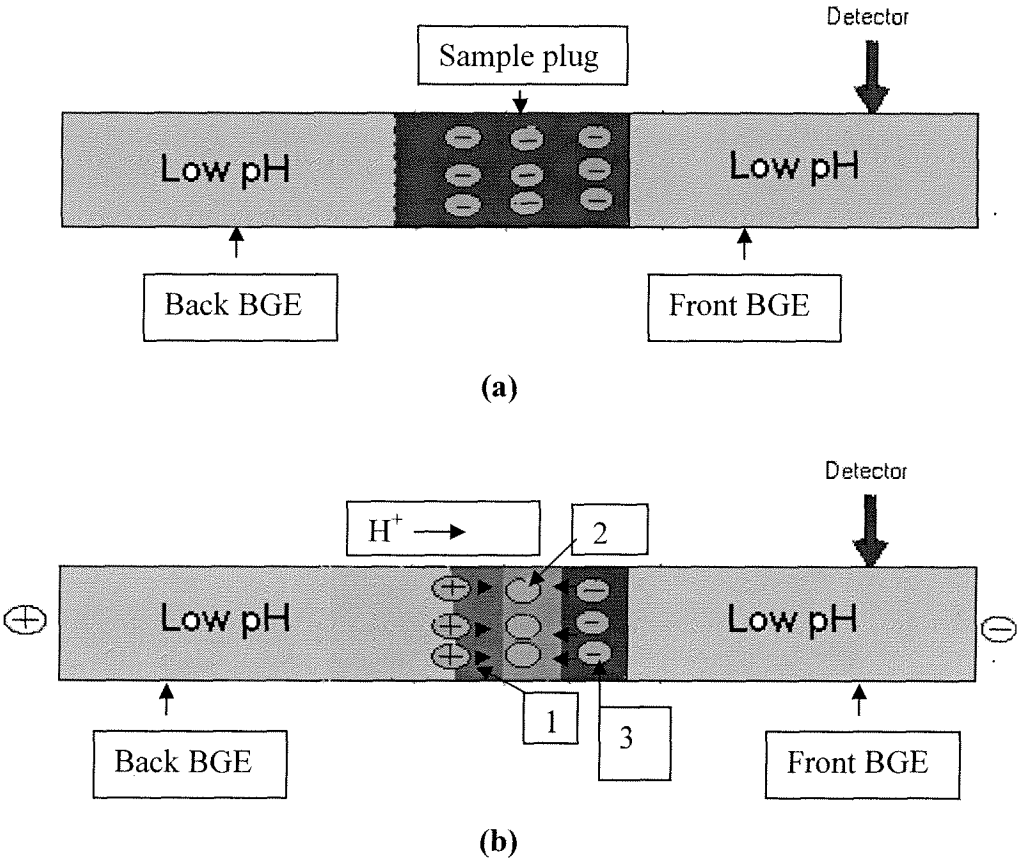

Figure 6.6 Proposed mechanism of focusing using a dynamic pH junction in CE-MS with the positive ionization mode. (a) A large sample plug with a higher pH electrolyte was injected into a capillary filled with a lower pH BGE. (b) pH gradient formed due to the invasion of protons from the back BGE to the sample zone under the electric field. Different color bands represent the pH gradient from the sample zone to the adjacent part of the back BGE. 1- Asp positively charged; 2- Asp neutral; 3-Asp negatively charged.

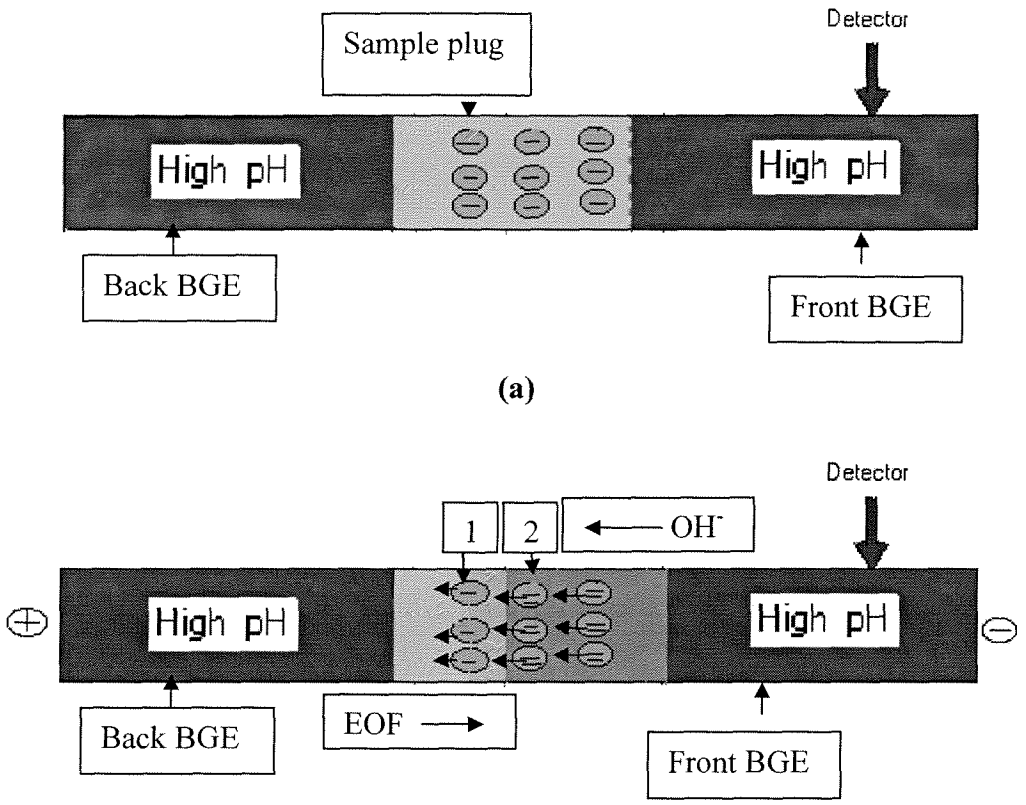

Figure 6.7 Proposed mechanism of focusing using a dynamic pH junction in CE-MS with the negative ionization mode. (a) A large sample plug with a lower pH electrolyte was injected into a capillary filled with a higher pH BGE. (b) pH gradient formed due to the invasion of hydroxide ions from the front BGE to the sample zone under the electric field, different color bands represent the pH gradient from the sample zone to the adjacent part of the front BGE. 1- Asp net charge -1. 2- Asp net charge -2.

For the positive ion mode, shown in Figure 6.6, when the pH of the sample was higher than BGE, once the voltage was applied, the junction between the sample zone and the back BGE disappeared and a pH gradient formed because of the movement of protons. Asp distributed in the different parts of the gradient. The Asp molecules in the lower pH area were protonated to become positively charged. These positive ions moved towards the cathode until they reached an area of higher pH, where deprotonation of the species

occurred and neutralized their positive charges, resulting in lower velocity and leading to peak focusing. The Asp in the higher pH area was negatively charged and moved towards the anode until it reached the area of lower pH where protonation of the species occurred, which neutralized its negative charge, resulting in peak focusing. After the focusing, Asp was further protonated to become positively charged due to the pH decreasing of the gradient caused by continuous movement of protons. The focusing mechanism for Glu is the same. For Leu, the mechanism is similar. The only difference is the species in the higher pH area is neutral and does not move towards the anode.

For the negative ion mode, shown in Figure 6.7, when the pH of BGE was higher than that of the sample, upon application of a potential, the junction between the sample zone and the front BGE disappeared and a pH gradient formed because of the movement of hydroxide ions. The Asp in the higher pH area gained more negative charges to become the species with net charge of -2. These more negatively charged ions moved towards the anode faster until reaching an area of lower pH, where protonation of the species occurred, which lowered their negative charges, resulting in lower velocity. This led to some peak focusing, but not as much as the situation described above. Asp at the lower pH area was also negatively charged (-1) and moved towards the anode as well during the focusing process. Therefore there were no abrupt changes in the analyte velocities and focusing was not as complete as in the case where the analytes were neutralized at the lower pH area. The mechanism of Glu focusing is the same as that of Asp, and of Leu is the same as that of phenylalanine described in chapter 4.

6.4 Conclusions

This study has shown that V-DIF using a dynamic pH junction is achieved for non-aromatic amino acids in CE-MS. Both pK_1 and pK_2 of the analytes can be used as criteria for the selection of the BGE and the sample pH for focusing. Either positive or negative ion mode detection can be chosen in CE-MS with V-DIF. However, focusing in the negative ion mode was limited for analytes such as Asp and Glu. Positive ion mode was better for focusing these types of analytes. The V-DIF with different ion modes can be chosen based on the analysis of the charge state changes of analytes. Optimum focusing is obtained when the charge state changes causing abrupt changes in the analyte velocities.

6.5 References

1. Poinsot, V.; Lacroix, M.; Maury, D.; Chataigne, G.; Feurer, B.; Couderc, F. *Electrophoresis* 2006, *27*, 176-194
2. Teerlink, T. *J. Chromatogr., B* 1994, *659*, 185-207
3. Prata, C.; Bonnafous, P.; Fraysse, N.; Treilhou, M.; Poinsot, V.; Couderc, F. *Electrophoresis* 2001, *22*, 4129-4138
4. Vecchione, G.; Margaglione, G.; Grandone, E.; Colaizzo, D.; Cappucci, G.; Fermo, I.; D'Angelo, A.; Di Minno, G. *Electrophoresis* 1999, *20*, 569-574.
5. Kelts, D. G.; Ney, D.; Bay, C.; Saudubray, J. M.; Nyhan, W. L. *Pediatr. Res.* 1985, *19*, 86-91
6. Marchelli, R.; Dossena, A.; Palla, G. *Trends Food Sci. Technol.* 1996, *7*, 113-119
7. Spackman, D. H.; Stein, W. H.; Moore, S. *Anal. Chem.* 1958, *30*, 1190-1206
8. Schuster, R. *J. Chromatogr.* 1988, *431*, 271-284
9. Naylor, S.; Benson, L. M.; Tomlinson, A. J. *J. Chromatogr., A* 1996, *735*, 415-438
10. Shihabi, Z. K. *J. Chromatogr., A* 1996, *744*, 231-240
11. Burgi, D. S. *Anal. Chem.* 1991, *63*, 2042-2047.
12. Krivankova, L.; Bocek, P. *J. Chromatogr., B* 1997, *689*, 13-34
13. Gebauer, P.; Thormann, W.; Bocek, P. *Electrophoresis* 1995, *16*, 2039-2050
14. Klampfl, C. W.; Ahrer, W. *Electrophoresis* 2001, *22*, 1579-1584
15. Soga, T.; Heiger, D. N. *Anal. Chem.* 2000, *72*, 1236-1241
16. Harris, D. C. *Quantitative Chemical Analysis*, W. H. Freeman and Co. New York, 6th ed., 2003

17. Ermakov, S. V.; Zhukov, M. Y.; Capelli, L.; Rightetti, P. G. *Anal. Chem.* 1994, *66*, 4034-4042

18. Tsai, C. Y.; Her, G. R. *J. Chromatogr. A* 1996, 743, 315-321

CHAPTER 7[1]

Effect of More Than One Capillary in a Continuous Electrophoretic Purification System

[1] A version of this chapter will be submitted for publication.

7.1 Introduction

Continuous electrophoretic purification (CEP) provides an alternative in analytical purification compared to fraction collection by liquid chromatography and conventional capillary electrophoretic methods. [1-5] A CEP system was developed in our group to purify individual analytes from multicomponent mixtures. [6, 7] We have demonstrated that in addition to being able to purify the fastest migrating component, it is feasible for the CEP system to purify any component in a complex mixture using a two-step procedure. With refined backpressure control and an appropriate choice of background electrolyte, individual analytes of appreciable amount can be isolated from a complex mixture and collected in the outlet vial by carrying out the electrophoretic purification through a capillary column.

The principle underlying flow counterbalanced capillary electrophoresis (FCCE) was first described by Dovichi *et al.* in a study on the interaction of CE with a sheath flow cuvette fluorescence detector. [8] Culbertson and Jorgenson used the FCCE technique for the analytical separation of closely migrating species. [9, 10] They used this technique to increase the residence time and extend the effective length of the separation column, thereby allowing closely migrating analytes to separate from each other. In order to reduce the broadening caused by the pressure induced parabolic flow profile, very small inner diameter (5 to 10 μm) capillaries had to be used. Chankvetadze *et al.* demonstrated the potential of FCCE for preparative operation in normal-scale capillaries by recovering pure fractions of a chiral compound and the α-isomer of a dipeptide, aspartame, from a binary mixture. [11] In continuous FCCE, a hydrodynamic counter pressure is applied

opposite to the direction of migration of the analytes. By choosing the appropriate counter pressure, faster migrating analytes are allowed to migrate continuously through the column under the electric field while the rest of the analytes remain in the inlet vial. However, only the fastest migrating species can be purified, severely limiting the usefulness of this technique.

Our group demonstrated, by carefully analyzing the direction and magnitude of mobilities induced by all forces, that one can purify any component in a sample in two cycles without any modification to the capillary wall or the BGE. [7] We use the term continuous electrophoretic purification (CEP) to emphasize the potential applications of such systems. The effects of the BGE components and capillary inner diameter on purification rate and yield were also studied. [7] Techniques including pressure ramping and buffer replenishment have been used to improve the yield. It is logical to expect that the throughput of such a system should be significantly improved if more than one capillary is used. This investigation demonstrates the feasibility of increasing the amount of purified analyte by using multiple capillaries.

7.2 Experimental

7.2.1 Chemicals.

2-(N-Cyclohexylamino)-ethanesulfonic acid (CHES), caffeine, tyrosine, and tryptophan were all purchased from Sigma (Sigma-Aldrich, Oakville ON, Canada). NaOH was from Fisher (Fisher Scientific, Nepean ON, Canada). The background electrolytes were 50 mM CHES. The pH of the buffer was adjusted to 9.0 using 1M NaOH. The sample

concentration used for preparative separation was approximate 0.73 mg / mL for caffeine, 0.70 mg / mL for tyrosine, and 0.67 mg / mL for tryptophan. For quantitative analysis of the analytes recovered at the outlet following the CEP process, the content of the outlet vial was briefly mixed and then analyzed on a P/ACE^{TM} MDQ automated CE system (Beckman-Coulter, Mississauga, ON, Canada). The peak area of the recovered analyte was compared to that of the original sample to determine the yield and final concentration of the purified component.

7.2.2 Apparatus.

Experiments were performed on home-built CEP systems similar to those described previously. [6, 7] The pressure required for injection or purification was generated by pumping nitrogen gas into the sealed inlet or outlet vials. The approximate pressure needed was set using a two-stage regulator, then adjusted to the desired value by a needle valve and monitored using a digital pressure gauge with 0.01 psi resolution (an order of magnitude greater than that available on most commercial CE systems). As depicted in Figure 7.1(a), when the voltage and pressure are set to the desired values, only one compound can migrate to the other side of the capillary and into the collection vial. The schematic diagrams of two-capillary and three-capillary systems are shown in Figure 7.1(b) and 7.1(c).

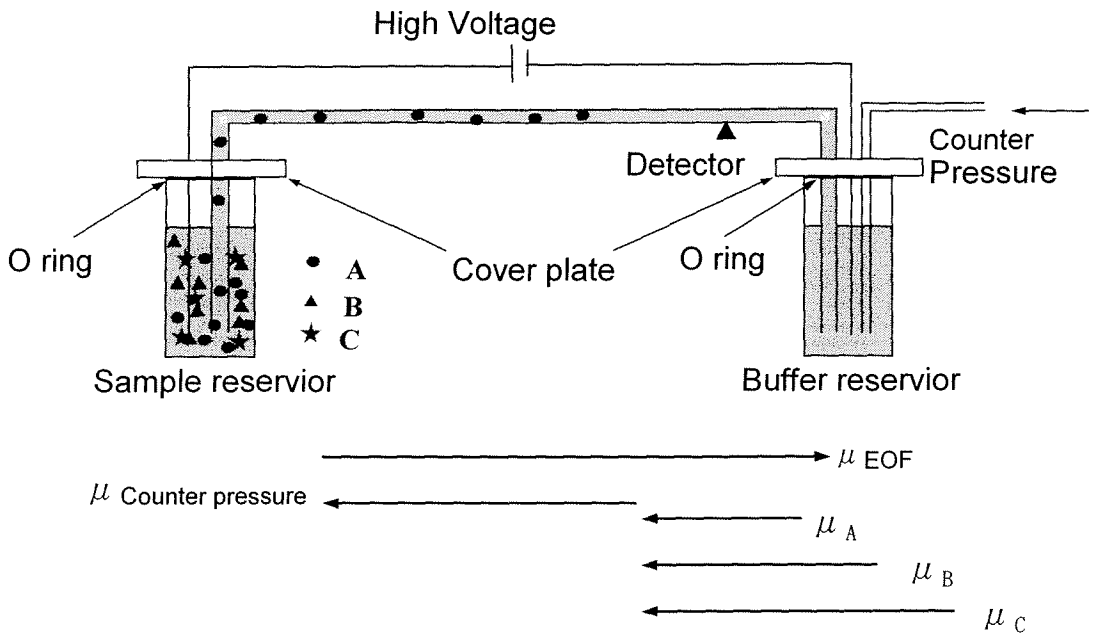

(a)

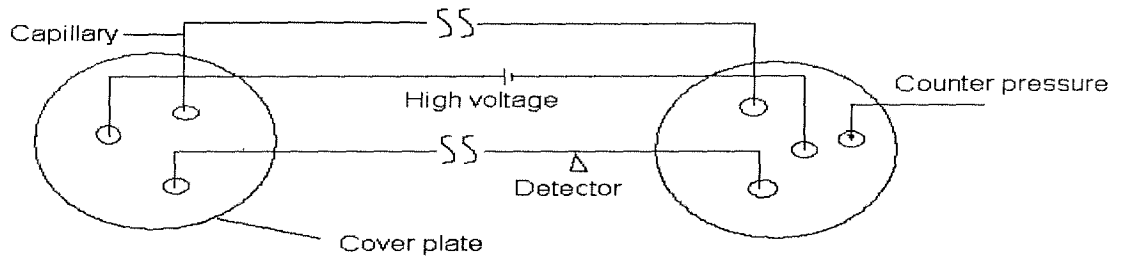

(b)

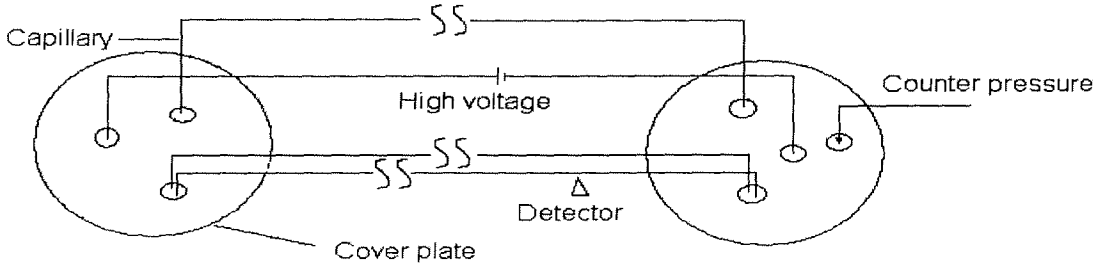

(c)

Figure 7.1 Schematic diagram of CEP and the two and three-capillary systems. (a) A mixture of three analytes (A, B, C) with negative electrophoretic mobilities. Components with greater negative electrophoretic mobilities have a net velocity toward the inlet and the component with the smallest electrophoretic mobility have a net velocity toward the outlet. (b) Schematic diagram of a two-capillary system. (c) Schematic diagram of a three-capillary system.

Fused silica capillaries (Polymicro Technologies, Phoenix, AZ) 40 cm in length (32.5 cm to the detector) with an internal diameter of 75 μm were used. New capillaries were first rinsed with 1M NaOH, followed by rinsing with the buffer, and finally a voltage of 10 kV was applied for 40 min prior to use. All separations were preceded by a 5 min, high-pressure rinse with 1M NaOH, followed by a 5 min, high-pressure rinse with the BGE. Separations were performed at 10 kV and ambient temperature using normal polarity.

A UV-Vis absorbance detector used in our system was purchased from Ocean Optics Inc. (Dunedin, FL, USA). The miniature fiber optic spectrometer consists of a dual channel, linear silicon CCD detector with a crossed Czerny-Turner configuration (Model SD2000). Light from the source (DT1000, deuterium-tungsten combination) travels to the detection window in the capillary via a 300 μm, solarization-resistant fiber optic cable (the same as the source fiber) and enters the spectrometer through a 25 μm slit. The signal from the detector is acquired using a data acquisition card interfaced to a desktop PC through a USB port (ADC 1000-USB).

7.3 Results and discussion

7.3.1 Determination of counter pressure.

Caffeine, tyrosine, and tryptophan were chosen because they have strong UV absorbance, which is convenient for the UV detector we used in the experiments. A representative CE separation of the three analytes studied is shown in Figure 7.2(a), and a typical detector

trace for a frontal capillary electrophoresis of a mixture of the three analytes is shown in Figure 7.2(b).

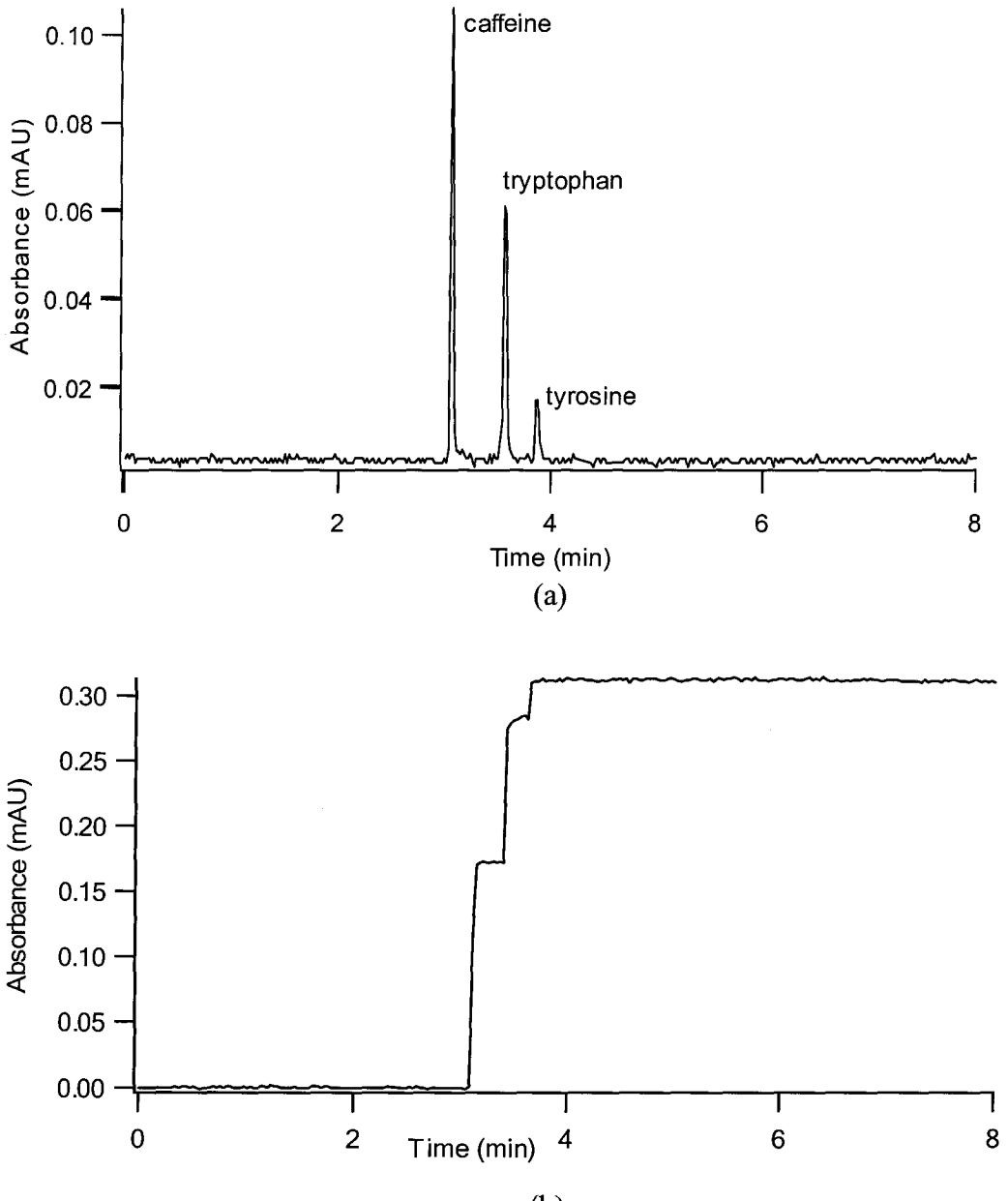

Figure 7.2 Separation of the three analytes. Capillary: 75 μm i.d.; 40 cm in length; BGE: 50 mM CHES, pH 9.0; Voltage: 10 kV, normal polarity. The concentrations of caffeine, tryptophan and tyrosine were 0.73 mg / mL, 0.70 mg / mL, and 0.67 mg / mL, respectively. (a) An electropherogram of a normal CE separation. (b) An electrophorerogram of a frontal CE with the same analytes.

Without the counter pressure, the three analytes arrive at the director one by one after a few minutes. Three distinct plateaus can be observed: the first marks the migration time of caffeine, the second, tryptophan, and the third, tyrosine. The counter pressure is determined using the method described previously, [6, 7] so that it is high enough to stop all analytes except the analyte of interest.

A plot of the forward (toward the outlet) linear velocities of each analyte as a function of counter pressure is constructed as shown in Figure 7.3. The curves were generated by injecting samples containing all 3 analytes and measuring their forward velocities when various counter pressures were applied at the outlet of the capillary.

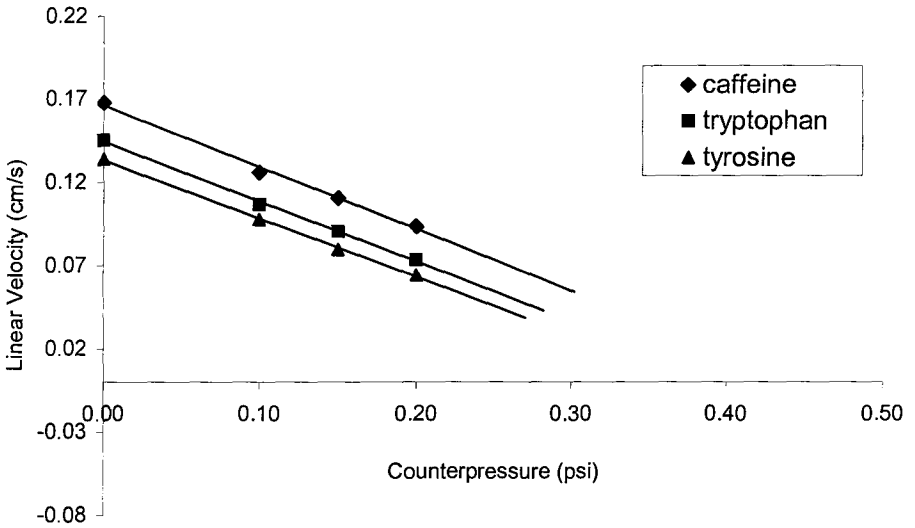

Figure 7.3 Forward velocities of analytes versus counter pressure.

The counter pressure necessary to stop each analyte is obtained by extrapolating the curved lines to the x-axis as described previously. [6, 7] The x-axis intercepts for caffeine, tryptophan, and tyrosine were: 0.45 psi, 0.40 psi, and 0.38 psi, respectively. A counter

pressure of 0.40 psi was selected because tryptophan had no net forward velocity while allowing caffeine to migrate at maximum forward velocity towards the outlet.

7.3.2 Preparative operations.

In the presence of a 0.40 psi counter pressure, caffeine migrated slowly and arrived at the detector after ca. 25 minutes. A stable plateau was observed as caffeine continued to migrate past the detector and reached the outlet vial. The purification of caffeine continued for ca. 60 minutes before the plateau began to increase because the second fastest analyte, tryptophan, migrated to the detector. The signal vs. time is shown in Figure 7.4(a).

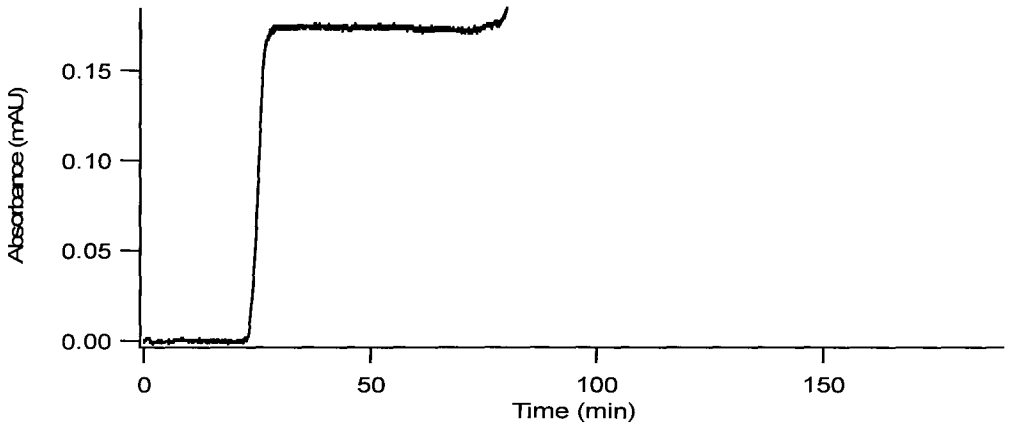

(a)

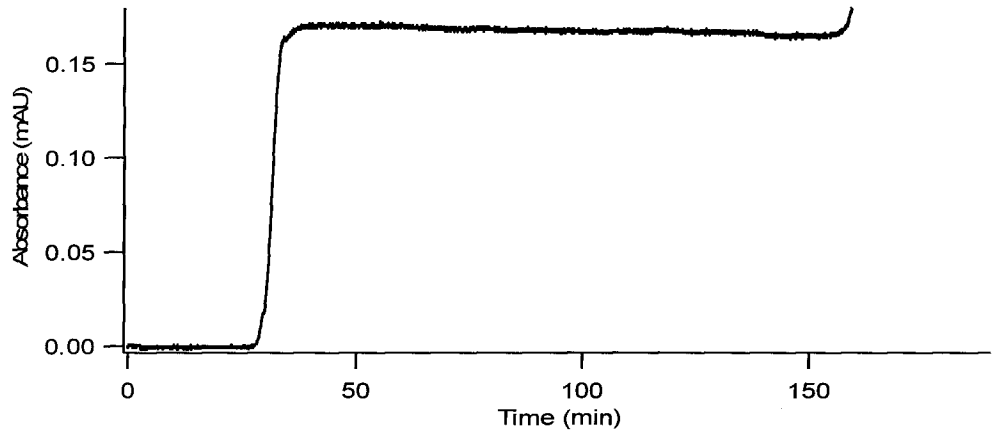

(b)

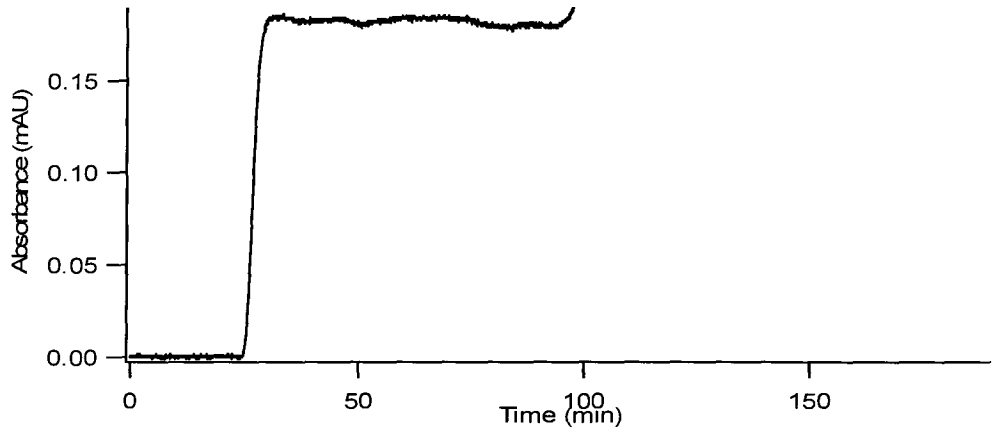

(c)

Figure 7.4 Signal vs. time plots for preparative operations. (a) one-capillary system. (b) two-capillary system. (c) three-capillary system.

The purification process has to be stopped when tryptophan reaches the detector because it will soon arrive at the outlet vial and contaminate the purified analyte. The change in the tryptophan mobility can be explained by the effects of buffer depletion at the capillary inlet. During the CEP process, electrolysis of water results in a decrease in pH in the anodic vial (inlet) and an increase in pH in the cathodic vial (outlet). [6, 7] Because of the zwitterionic nature of the amino acids, a decrease in pH leads to greater protonation of the amino acid, giving the analyte less net negative charge. This charge change results in an increased electrophoretic mobility towards the outlet, which finally overcomes the opposing counter pressure. This change in pH will affect different analyte-buffer systems differently, but in this case it represents a fundamental limit to the amount of pure caffeine that can be obtained through continuous collection without any remediation as described in previous papers. [6, 7] The component collected at the outlet vial was subsequently analyzed by P/ACE^{TM} MDQ automated CE.

The peak area of caffeine collected at the capillary outlet was compared to that of the original sample. A correction factor was used to account for the increase in volume in the outlet vial due to the bulk solution flow from the inlet as a result of EOF. [6,7] This was accomplished by weighing the outlet vials both before and after the continuous CEP runs and calculating the additional volume using the known density of the buffer solution, as described previously. [12]

With this one-capillary CEP system, the average yield for caffeine was 1.0%, corresponding to a mass of 3.7 μg. The highest yield obtained was 1.5%, corresponding

to a mass of 5.4 μg. It should be noted that the concentrations of the analytes used in this study are much higher than those in previous studies because an absorbance detector is used. When the sample volume is changed from 500 μL to 1500 μL, the current remained the same but the time for a single CEP run was nearly twice as long as the run time of the smaller volumes. This is because the extent of buffer depletion is in part dependent on the volumes in the reservoirs. [13] The electrolysis product diffuses into a larger reservoir volume, which results in a slower pH change. Therefore, the second fastest analyte stayed in the sample vial for a longer period of time, and the purification process lasted longer.

The average yield achieved using the larger vials decreased to 0.7%, but the mass yield was increased to 7.8 μg. The decrease in yield seems to be caused by the slow diffusion of the analyte through the depletion zone in a larger volume at the inlet.

7.3.3 Two-capillary system.

Another way to increase the recovery amount is to use multiple capillary systems. A two-capillary system was first used. The schematic of the home-built instrument is shown in Figure 7.1(b).

The separation voltage was kept the same as that for the single capillary system, but the current increased by a factor of 2 as expected. The signal of only one capillary was monitored. The two capillaries are the same length and are expected to have the same performance. Because there is a 7.5 cm distance between the detector and the outlet, a small variation, if any, in the migration rates, should not cause any contamination if the

purification is stopped as soon as the second analyte reaches the detector. The CEP runs last about 150 minutes when a 500 μl sample is used, as shown in Figure 7.4(b).

The yield improved more than expected when a two-capillary system was used, varying from 4.0% to 9.0% of the caffeine in the original samples, corresponding to 14.8 –33.3 μg. The higher yield may be caused by flow-induced convection between the two capillaries in the sample vial. A CEP process can be considered as an extended electrokinetic injection. The convection at the capillary inlets helps to introduce more analyte into the vicinity of the sampling spot, thus improving the yield. Protons produced by the electrolysis also diffused and were diluted more effectively due to this convection. The smaller pH change makes the run times of the CEP process much longer. All these factors work together to make the two-capillary systems more efficient.

The sample volumes were then increased to 1500 μL. The stable CEP lasted about 180 minutes, and the average yield was 2.7%. Considering the volumes increased three times compared to the 500 μl vials, the total average mass collected was about 30 μg.

7.3.4 Three-capillary system.

Due to the limited space on the lids of 500 μL vials, the design of the three-capillary system is almost the same as the two-capillary system except that one of the two capillaries was replaced by a plug which holds two capillaries together, as illustrated in Figure 7.1(c).

The separation voltage used was the same as other systems, but the current increased to three times that of the single capillary system. We still monitored the signal of one capillary only. The detector trace for the three-capillary system is shown in Figure 7.4(c). It was unfortunate that the stable CEP times for the three-capillary system were much shorter than those of the one or two-capillary systems as shown in Figure 7.4(c). The purification yield also decreased to an average of 3%. This may be caused by the much faster buffer depletion at the capillary inlet where two of the three capillaries are sampling the analyte from the same spot in the inlet vial. In addition, the electrolysis of water at the electrodes was faster than the one or two-capillary systems because of the larger current. The faster electrolysis leads to a faster decrease in pH in the inlet vial which results in greater protonation of the analytes, giving a less net negative charge for the analytes. The faster neutralization of analytes leads to an increased electrophoretic mobility for the second fastest analyte, tryptophan, making it arrive at the detector earlier. The purification process has to be stopped in a shorter time leading to lower overall yield. The results from the three systems are listed in Table 7.1.

Sample Volume	No. of Capillaries	% yield	mass
500 μL	1	1.0%	3.7 μg
	2	6.5%	24.1 μg
	3	3%	11.1μg
1500 μL	1	0.7%	7.8 μg
	2	2.7%	30 μg
	3	0.5%	5.6 μg

Table 7.1 Results of the average yield and masses for the three systems with different sample volumes

7.4 Conclusions

Doubling the number of capillaries provides better purification efficiency because of the increased number of paths for the analyte at different locations of the inlet vial to enter the capillary channels and migrate to the other side. Using 3 capillaries only improved the yield when the sample volume was small (500 uL). Based on the principles of CEP [7], if the length of the capillaries can be reduced significantly at the same time, the time required for the CEP process can also be significantly reduced. It is reasonable to predict that multi channel microfluid devices and even membranes can be used to replace the capillaries currently used in the CEP systems to dramatically improve the efficiency of purification.

7.5 References

1) Rose, D. J.; Jorgenson, J. W. *Journal of Chromatography A* 1988, *438*, 23-34

2) Huang, X.; Zare, R. N. *Analytical Chemistry.* 1990, *62*, 443-446.

3) Muller, O.; Foret, F.; Karger, B. *Analytical Chemistry* 1995, *67*, 2974-2980

4) Minarik, M.; Foret, F.; Karger, B. L. *Electrophoresis* 2000, *21*, 247-54.

5) Minarik, M.; Kleparnik, K.; Gilar, M.; Foret, F.; Miller, A. W.; Sosic, Z.; Karger, B. L. *Electrophoresis* 2002, *23*, 35-42.

6) McLaren, D. G.; Chen, D. D. Y. *Electrophoresis* 2003, 24, 2887-2895

7) McLaren, D. G.; Chen, D. D. Y. *Analytical Chem*istry 2004, 76, 2298-2305

8) Cheng, F. Y.; Wu, S.; Chen, D. D. Y.; Dovichi, N. J. *Analytical Chemistry* 1990, *62*, 496-503

9) Culbertson, C. T.; Jorgenson, J. W. *Analytical Chemistry* 1994, *66*, 955-962

10) Culbertson, C. T.; Jorgenson, J. W. *Journal of Microcolumn Separations* 1999, *11*, 175-183

11) Chankvetadze, B.; Burjanadze, N.; Bergenthal, D.; Blaschke, G. *Electrophoresis* 1999, *20*, 2680-2685.

12) McLaren, D. G. *Ph.D. thesis, New Studies and Developments in Capillary Electrophoresis for the Analysis and Purification of Biological Molecules*, UBC, 2003

13) Kelly, M. A.; Altria, K. D.; Clark, B. J.; *Journal of Chromatography A* 1997, *768*, 73-80

CHAPTER 8

Concluding Remarks

The material presented in this thesis provides a mechanistic study of the V-DIF technique and its applications in CE. Chapter 2 described the investigation of the mechanism of the focusing technique by monitoring the pH change in the capillary during the focusing process using the dye phenolphthalein. It was found that the pH difference between the sample and the BGE played a key role in this technique. Differences in pH resulting in different charge states for analytes in the sample and the BGE were determined to cause focusing through changes in analyte velocities in different pH segments in the pH gradient formed by the sample and BGE. The pK_a of an analyte was found to be a key criterion for selecting the pH for the sample and the BGE to obtain optimum focusing. Chapter 3 described an application of this focusing technique to the well-known neurotransmitter, serotonin. It was found that mixed buffer systems (borate and phosphate) also worked for V-DIF. The mechanism proposed in chapter 2 was confirmed. The LOD determined for serotonin with this method using CE-UV was found to be $7x10^{-8}$ M, which is lower than the normal serotonin concentration in human plasma. The focusing technique has the potential to simplify serotonin analysis in human plasma and a practical method should be further developed.

Chapter 4 discussed the application of the technique to amino acids, peptides and proteins. Both the pI and pK_a of the amino acids were used as criteria for pH selection of the sample and the BGE to further understand the focusing mechanism. The pK_a rather than the pI of the analyte was found to be the key criterion for selecting the pH of the sample and of the BGE to focus the analyte. The pH of the sample and the BGE must be

maintained at different values, one above the pK_a of the analyte and the other under the pK_a of the analyte, to obtain optimum focusing.

Chapter 5 demonstrated the application of this focusing technique in CE-PDA and CE-ESI-MS. It was found that volatile buffer systems worked for V-DIF in CE with PDA or MS detection. The optimized BGE concentration and sample matrix for focusing are different between CE-PDA and CE-MS. For different analytes, different conditions can be selected for focusing to improve the separation efficiency and thus better concentration sensitivity. Chapter 6 showed the application of the technique in CE-ESI-MS for non-aromatic amino acids. It was found that both pK_1 and pK_2 of the analytes could be used as criteria for the selection of the BGE and the sample pH in V-DIF and either positive or negative ion mode could be chosen in CE-MS. However, velocity-difference induced focusing was limited in the negative ion mode for the analytes such as Asp and Glu. Different ion modes with V-DIF should be chosen based on the analysis of the charge state changes of the analytes. Optimum focusing is achieved when the charge state changes cause abrupt changes in the analyte velocities.

The last section demonstrated the effect of more than one capillary in a continuous electrophoretic purification (CEP) system for CE preparative operation. Multiple capillary systems were found to provide better purification efficiency due to the increased number of paths for the analyte in the inlet vial to migrate to the collection vial. Multi channel microfluid devices may be used in the CEP systems to significantly improve the purification efficiency.

Future work should concentrate on the application of this focusing technique to real samples in pharmaceutical and clinical research. The proposed mechanism and the discussion of the conditions should be useful in establishing practical methods for real sample analysis.

The mechanism of the unexpectedly high purification yield of the two-capillary system needs to be further investigated. The investigation should focus on monitoring the pH in the small vial. The application of the purification method with multiple capillary systems should be expanded after the mechanism is investigated.